UNIVERSITÀ DELLA CALABRIA

University of Calabria

Chemistry and Chemical Technologies (CTC)

Ph.D Course

Science and Engineering of Environment, Structure and Energy

Cycle XXXI

Thesis title:

"Innovative Composite Membranes for Advanced Applications"

SDD

CHIM/06 Organic Chemistry

Coordinator: *Prof. Salvatore Critelli* _____

Supervisor: *Prof. Bartolo Gabriele* _____ *(Firma)*

Ph.D. Candidate: *Giuseppe Grasso* _____ *(Firma)*

Innovative composite membranes for advanced applications

Contents

Abstract

Presented thesis work is mainly focused on coatings preparation, their potentiality and applications in membrane science: from water desalination to antibiofouling membranes, to gas separation. In fact, coating preparation represents an useful and versatile technique which allows a fine control of membrane properties and performance such as chemical or physical resistance, durability, etc. One of major drawbacks is represented by production costs, which can become important in scale-up operations. Therefore, although several type and methodologies for coating preparation are known and reported in literature, a lack of cheap, efficient and scale-up adaptable coating methods made their different preparation methods of particular interest.

The results presented herein, concern the preparation of three different coating methods whose applications are briefly summarized below:

- ***Chapter 2: Development of PVDF-f-Graphene Thin Film Composite Membrane for Membrane Distillation***

  Chapter 2 reports a novel method for TFC membrane fabrication, using graphene layer coated on chemically-functionalized PVDF. PVDF is hydrophobic polymer whose properties are well suited for those applications in which hydrophobicity is needed such as Membrane Distillation. In order to increase adhesion between PVDF and graphene, we co-polymerized PVDF with a suitable monomer bearing aromatic part, using a procedure which involves 2 steps reaction: introduction of double bonds on polymer backbone by basic treatment followed by its reaction with monomer through radical reaction. Membranes have been prepared using functionalized PVDF polymer (PVDF-f) and tested on Direct Contact Membrane Distillation (DCMD) apparatus at first. Subsequently tests were conducted using PVDF-f-Graphene composite membrane, using graphene synthetized using Chemical Vapor Deposition (CVD) method. Created membranes were analyzed and their chemical, physical and morphological properties were investigated. Membranes made using PVDF-f polymer exhibited good flux and salt rejection (up to 99.9 %), whereas graphene association to PVDF-f membranes leads to lower water flux but higher rejection and durability (up to 99.99 %).

- ***Chapter 3: Synthesis of polymerizable Acriloyloxyalkyltriethyl Ammonium salts surfactants and their antibacterial activity***

In chapter 3 a simple and innovative synthetic strategy for Acryloyloxyalkiltriethyl ammonium salts surfactants (AATEABs) starting from cheap and easily available chemicals is discussed. Herein reported surfactants can be used as coating for membranes to whom they confer high anti biofouling properties. Synthetic procedure was first optimized in order to work avoiding prohibitive conditions such as Inert atmosphere or high temperature and then applied to the synthesis of surfactants bearing a different alkyl-chain length. Antibacterial activity evaluation, has been done performing several tests against Gram +\- and yeast strains; results confirmed that AATEABs bearing C11 (AUTEAB) and C12 (ADTEAB) alkyl chain possess highest activity which is remarkable high for ADTEAB. AATEABs may find applications as polymerizable coatings for watr-treatment membranes (commercial or not) to be used in Pressure-Driven Membrane Processes or in any other membrane-based system in which antifouling properties may play an important role.

- ***Chapter 4: Thin Film Composite Membrane fabrication for gas separation: Defect control and bench-scale demonstration***

Fourth chapter of this thesis work, concerns the preparation of TFC membranes to be used for CO_2/N_2 separation, on the relationship between TFC membrane material and membrane properties and the role of the protective layer in determining the amount of defects, which is a crucial aspect for all the gas separation-related processes. We report a simple and efficient procedure which can also be applied to for defect controlling during scale-up process and which is not valid for CO_2 separation membranes only. Results demonstrate a correlation between the properties of protective layer and separation performances: in particular, the possibility to apply a coating film on commercial membrane permits the creation of membranes in which the amount of defect is dramatically reduced. Another crucial aspect discussed in chapter 4 concerns the thickness of protective layer used for defect control: in fact, whereas the presence of protective layer plays an important role defect-free membrane creation process, its thickness impacts on separation operation. With our method, the preparation of membranes with very thin protective layer (0.1 µm or below) is possible.

Sommario

Il Lavoro di tesi discusso, è incentrato sui coating: la loro importanza, i metodi preparativi e le

potenzialità applicative nel campo delle membrane: dalla dissalazione di acque alla funzionalizzazione di membrane al fine di marcarne le proprietà antifouling per processi "PDMP" (Pressure-Driven Membrane Processes) quali RO, UF, MF, all' approntamento di membrane che permettano di separare miscele di gas come CO_2/N_2 . In effetti, l'applicazione di un coating ad una membrana anche commerciale, rappresenta un metodo molto efficace per conferire ad essa delle caratteristiche che prima non aveva, come resistenza chimica o meccanica, selettività nei confronti di una determinata specie o durabilità nei processi a cui la membrana è sottoposta. Tuttavia, questa tecnologia che solo oggi sta assumendo un importante rilievo che supera il mero ambito accademico, risente ancora di alcuni problemi e limitazioni come ad esempio la difficoltà nel passare dalla produzione in laboratorio a quella su larga scala, sia in termini di costi, che in termini di riproducibilità del processo. Per tali ragioni metodi semplici, economici, scalabili ed innovativi possono diventare di particolare interesse.I risultati presentati in questo lavoro di tesi, riguardano tre tipologie differenti di coating finalizzati ad altrettanti campi applicativi, trattati dettagliatamente nei singoli capitoli e brevemente riassunti di seguito:

- ***Capitolo 2: Sviluppo di membrane ibride PVDF-Grafene per processi di distillazione a membrana***

  In questo capitolo viene descritto un nuovo ed innovativo metodo per la preparazione di membrane ibride PVDF-Grafene, in cui un layer del materiale 2D viene applicato come coating su una membrana non commerciale di PVDF preventivamente modificato. Infatti, allo scopo di massimizzare l'adesione polimero-grafene mediante il fenomeno del pi-stacking il PVDF è stato trattato chimicamente. Il processo prevede due stadi: nel primo stadio vengono introdotti dei doppi legami sulla catena polimerica, mentre nel secondo si ha la loro polimerizzazione con un opportuno monomero formato da una parte polimerizzabile e da un'altra aromatica, che interagirà col grafene. Il grafene è invece stato sintetizzato utilizzando la metodologia del " Chemical Vapor Deposition" (CVD). Allo scopo di appurare eventuali differenze, sono state preparate tre diverse membrane utilizzando identiche condizioni preparative ma polimeri diversi: PVDF non funzionalizzato, PVDF funzionalizzato e Membrana composita di PVDF funzionalizzato con grafene. Le membrane ottenute sono inoltre state analizzate con diverse tecniche allo scopo di valutarne la composizione chimica e le proprietà meccaniche e topologiche.

  I risultati hanno dimostrato che le membrane create a partire dal polimero funzionalizzato esibiscono un bon flusso di vapore ed una alta reiezione salina fino al 99.9%, che aumenta

nel caso della membrana composita polimero-grafene insieme alla durabilità della stessa, sacrificando però parte del flusso di vapore.

- ***Capitolo 3: Sintesi di sali polimerizzabili di Acriloilalcossialchiltrietil ammonio e relativa attività antibatterica***

  Nel terzo capitolo viene discussa una nuova procedura per la sintesi di sali di Alchiloilossialchiltrietilammonio Bromuro (AATEABs), una particolare classe di surfactanti polimerizzabili ad elevata attività antibatterica, a partire da precursori poco costosi e facilmente disponibili sul mercato. Tali molecole, presentano una porzione acrilica che si presta ad essere polimerizzata e che può quindi essere impiegata per la creazione di coating applicabili a membrane, non necessariamente commerciali, destinate a processi di PDMP (Pressure-Driven Membrane Processes) come RO, UF, MF, etc. Tali membrane rivestite con AATEABs, oltre a guadagnare proprietà idrofiliche guadagnano anche marcate attività antibatteriche ed antifouling. L'attenzione è rivolta da una parte all'approntamento di una opportuna strategia sintetica ed alla sua ottimizzazione, che permetta di evitare di lavorare in condizioni proibitive come atmosfera inerte e\o alte temperature, mantenendo rese sintetiche comunque alte, mentre dall'altra è stata rivolta all' estensione del processo stesso a diverse molecole in cui è stata cambiata la lunghezza della porzione alchilica, purtuttavia appartenenti alla classe AATEABs. L'attività biologica di tali molecole, è stata valutata attraverso alcuni test effettuati nei confronti di Gram+, Gram- e lieviti ed è risultata essere particolarmente alta in due delle molecole sintetizzate: gli analoghi con catena alchilica ad 11 (AUTEAB) e 12 (ADTEAB) atomi di carbonio. In particolare, l'analogo AUTEAB rappresenta la molecola con il miglior compromesso tra costo dei reagenti ed attività biologica, mentre l' ADTEAB, sebbene più attivo, risulta essere più dispendioso a causa del costo maggiore del bromo alcol di partenza.

- ***Capitolo 4: Creazione di membrane TFC per la separazione di miscele di CO2/N2 : controllo dei difetti ed applicazione su larga scala***

  Il quarto ed ultimo capitolo affronta un'ulteriore possibile applicazione dei coating, in questo caso per membrane commerciali destinate alla separazione di gas in relazione a due punti principali: la relazione esistente tra il numero dei difetti e la qualità della separazione della

membrana da un lato, la relazione esistente tra lo spessore del coating e la permeanza del gas attraverso la membrana dall'altro. La creazione di difetti riduce drasticamente le prestazioni della membrana, ma questi, tuttavia, emergono inevitabilmente specie quando si tenta di produrre membrane su larga scala. D'altra parte, se il numero di difetti può essere ridotto aumentando lo spessore del coating, affinché la membrana possa lavorare in condizioni ottimali sono necessari coating molto sottili allo scopo di evitare il calo di permeanza. Il metodo proposto, si presta bene alle applicazioni su larga scala in quanto riduce il numero di difetti, pur permettendo la creazione di coating estremamente sottili ed omogenei.

Abbreviations list

AATEABs	*Acryloyloxyalkyltriethylammonium Bromides*
AFM	*Atomic Force Microscope*
AGMD	*Air-Gap Membrane Distillation*
AGMD	*Air Gap Membrane Distillation*
AIBN	*Azobisisobutyronitrile*
ATRP	*Atom-Transfer Radical Polymerization*
AUTEAB	*Acryloyloxyundecyltriethylammonium bromide*
BHT	*Butylated hydroxytoluene*
CA	*Contact Angle*
CTFE	*Chloro Trifluoroethylene*
CVD	*Chemical Vapor Deposition*
DCMD	*Direct Contact Membrane Distillation*
DI	*Deionized Water*
DMF	*N,N-Dimethylformammide*
DTAB	*Dodecyltriethylammonium Bromide*
ESI-MS	*Electrospray Ionization Mass Spectrometry*
EtOH	*Ethanol*
FT-IR	*Fourier Transform- Infrared Spectroscopy*
GO	*Graphene Oxide*
GOQDs	*Graphene Oxide Quantum Dots*
HFP	*Hexafluoro propylene*
KOH	*Potassium Hydroxide*
LEP	*Liquid Entry Pressure*
NIPS	*Nonsolvent-Induced Phase Separation*
NM	*Nano Material*
NMR	*Nuclear Magnetic Resonance*
PAN	*Poly (acrylonitrile)*
PBM	*Polymerizable Bicontinuous Microemulsion*
PCTFE	*Poly(Chlorotrifluoroethylene)*
PDMP	*Pressure-Driven Membrane Processes*
PDMS	*Poly(dimethylsiloxane)*
PEGMA	*Poly(Ethylen Glicol) Methacrylate*
PES	*Poly (Ether Sulfone)*
PMMA	*Poly (methylmetacrilate)*
PQASs	*Polymerizable Quaternary Ammonium Salts*
PTFE	*Poly (Tetrafluoroethylene)*
PVDF	*Poly(Vinylidene Fluoride)*
PVDF-f	*Functionalized PVDF*
PVDF-f/GM	*PVDF-f/Graphene TFC membrane*
PVF	*Poly (Vinylfluoride)*
QASs	*Quaternary Ammonium Salts*
RAFT	*Reversible Addition–Fragmentation chain Transfer*
RO	*Reverse Osmosis*
SEM	*Scanning Electron Microscope*
TFC	*Thin Film Composite*
TFE	*Tetrafluoroethylene*

LPM	*Liter Per Minute*
MBR	*Membrane Bioreactor*
MD	*Membrane Distillation*
MeOH	*Methanol*
MF	*Microfiltration*
NF	*Nanofiltration*
UF	*Ultrafiltration*
VDF	*Vinylidene Fluoride*
VF+F8	*Vinyl Fluoride*
VMD	*Vacuum Membrane Distillation*
XPS	*X-ray Photoelectron Spectroscopy*

Chapter 1: General Introduction

1.1 Introduction and objectives

In last decades, membrane technology has assumed a central role in several separation and purification related fields, in particular for those concerning separation and purification[1-2]. This because operation performed by membranes allow to separate or purificate compounds using low energy-demand processes, avoiding harmful chemicals and operate in an easy way. Among several reasons for choosing membrane processes compared to traditional ones, the crucial point is the possibility to separate compounds which are difficult to separate in other ways or thermally and chemically sensitive ones. However, on this purpose material play an important role and its production cost may sometimes represent a drawback. Materials represent the functional part of membrane systems and their properties are often related to selectivity and separation efficiency and represent one point on which attention has been focused on. Indeed, the need of tailored materials production with specific features fit for membrane systems, is actually encouraging ongoing research on them not only by coating[3-5], but also using different polymers, using association of polymers and nanomaterials in Mixed Matrix Systems or membrane surface functionalization, perhaps the most common methods nowadays employed and which can be either chemical of physical[3-4, 6-10]. This thesis work focuses its attention on coatings and their application in membranes for different purposes:

In the first part a layer of graphene is applied on a membrane made using functionalized PVDF. Functionalization is necessary because permits to achieve better compatibility between graphene layer and polymeric membrane benefiting from pi-stacking phenomena. Chemical functionalization involves two step-reaction in which creation of double bonds on polymer chain initially occurs, followed by radical polymerization. Graphene was synthetized using CVD method and fixed on top surface of membrane made with Functionalized PVDF using laminating machine.In order to evaluate membrane properties three different membranes have been tested on Direct Contact Membrane Distillation apparatus: made by Pristine PVDF and Functionalized PVDF (with and without graphene). Also, in order to comprehend morphological, chemical and mechanical properties other studies have been done. One of major drawbacks in coating fabrication is due to costs and process scalability which sometimes borders their use only to lab-scale experimetns. In chapter 3 is reported a novel and innovative synthetic strategy for the synthesis of a new class of Polymerizable surfactanct with

Acryloyloxyalkiltriethylammonium Bromide-like structure (AATEABs), starting from simple and cheap chemicals on market. Reported strategy was then extended to different analogus molecule, that can be used as coating for membranes to which they confers hydrophilic behaviour and remarkable antibiofouling activity, due to the presence of ammonium salt. Coating with AATEABs can be used for those membranes whenever abovementioned properties are needed such as Reverse Osmosis, Micro and Ultrafiltration, etc. Antimicrobial activity has been evaluated through biological tests performed on Gram +\- and yeast strains and resulted to be highest in those analogus bearing C_{11} and C_{12} alkyl chain length. An innovative coating method which allows creation of ultra thin coating on membranes for CO_2/N_2, is discussed in chapter 4: is well known that in the case of gas separation membranes, the priority is to reduce as much as possible the presence of defects which can prejudice the separation process. The difficult which limits their use for scaled-up systems is that it results really hard to obtain an uniform and extremely thin coating. Our attention is therefore applied on one hand to defect control and on another hand to the thickness of dense selective layer. Furthermore, the whole procedure, results to be really simple and easily scalable. Thesis outline is summarized in *Figure 1.1.1*

Thesis outline

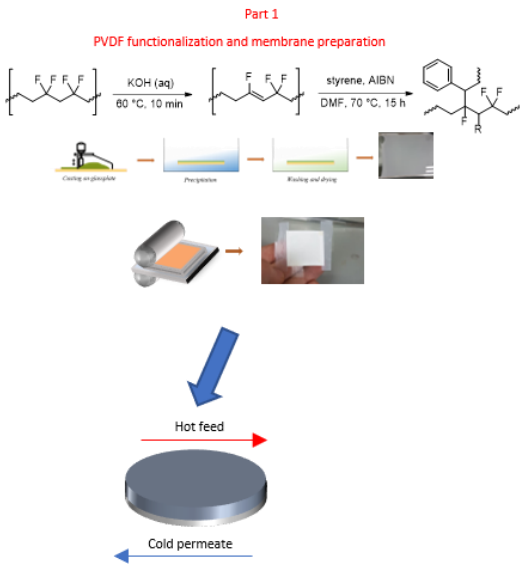

PVDF-graphene TFC membrane

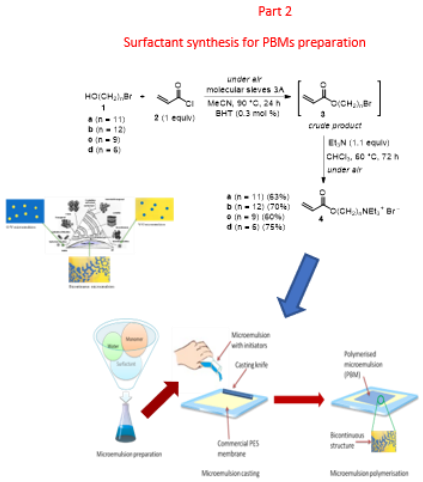

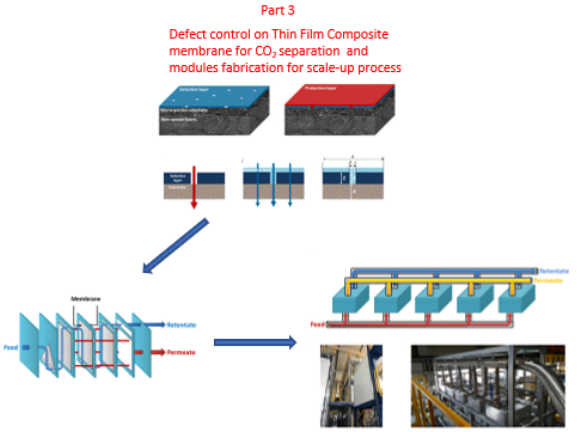

Figure 1.1.1

1.2 Fluoropolymers and membrane science

In membrane science, fluoropolymers represent one of election materials because of their outstanding properties which can be ascribed to C-F bond, its polarizability and its strength. For membrane technologies fluoropolymers are ideal candidates since they possess very interesting features such as chemical inertness and stability, mechanical strength and insulating properties. As reported in literature by Ameduri et al[11] fluoropolymer are actually employed in several fields, from automotive industries to medical applications. *Table 1.2.1* reports some of most common use of fluoropolymers.

Industry/ Application area	*Key Properties*	*Typical uses*	*Typical used Fluoropolymers*
Chemical/petrochemical industry	Chemical Resistance, Mechanical Properties,Thermal stability, cryogenic Properties	Gaskets, vessel liners, pumps, valve and pipe liners, tubings, coatings, expantion joints/bellows, heat exchanger	PTFE, PFA/MFA, ETFE,ECTFE, FEP,FKM, FFKM,TFE-P
Electrical(electronic industry	Low Dielectric Constant High Volume/Surface Resistivity High Dielectric Breakdown Voltage Flame Resistance, Thermal stability Low refractive indices	Wire and cable Insulation, connectors, optical fibres, printed circuit boards	FEP, PTFE, PFA, MFA ETFE, ECTFE PCTFE amorphous FP
Automotive/aircraft industry	Low Coefficient of Friction Good Mechanical Properties Cryogenic Properties, Chemical Resistance Low permeation properties	Seals, O-Rings, hoses in automotive power steering, transmissions, and airconditioning, bearings, sensors fuel management systems.	FKM, PTFE FFKM TH
Coatings	Thermal/Weather Stability Low Surface Energy Chemical Resistance	Cookware coatings, coatings of metal surfaces, powder coatings	PTFE PVDF, ETFE FEVE, PFA
Medical	Low Surface Energy, Stability, Purity Excellent Mechanical Properties Chemical Resistance	Cardiovascular grafts, heart patches, ligament replacement packaging films for medical products	PTFE, PCTFE
General Architecture/Fabric/Film applications	Excellent Weatherability Flame Resistance Transparency Low Surface Energy Barrier properties	Coated fabrics and films for buildings/roofs, front/backside films for solar applications	ETFE, PTFE, PVDF PCTFE, PVF, THV
Polymer additives	Low coefficient of Friction Flame Resistance Abrasion resistance Antistick properties	Polyolefin processing to avoid surface defects and for faster processing. Additives for inks, coatings, lubricants, anti-dripping agents	THV, FKM PVDF, PTFE
Semiconductor Industry	Chemical Resistance High Purity Antiadhesion, Insulation, barrier properties Thermal Stability	Process surfaces wafer carriers tubing, valves, pumps and fittings, storage tanks	PFA, ECTFE PCTE, PTFE amorphous FP
Energy conversion/ storage	Chemical/thermal resistance ion-transportation high weatherability high transparency corrosion resistance	Binder for electrodes, separators, ion-selective membranes, gaskets, membranereinforments, films for photovoltaics coatings for wind mill blades	PVDF, Fluoroionomers (PFSA) , THV, ETFE ECTFE, PTFE, FEP PVF

Ameduri et al 2018 DOI: 10.1002/chem.201802708

Table 1.2.1

In last years a lot of efforts have been done in order to get new and versatile fluoropolymers with improved features. Indeed, most of fluoropolymers actually used are synthetized starting from fluoroalkenes: *Figure 1.2.1* report a brief summary of them with respective starting materials:

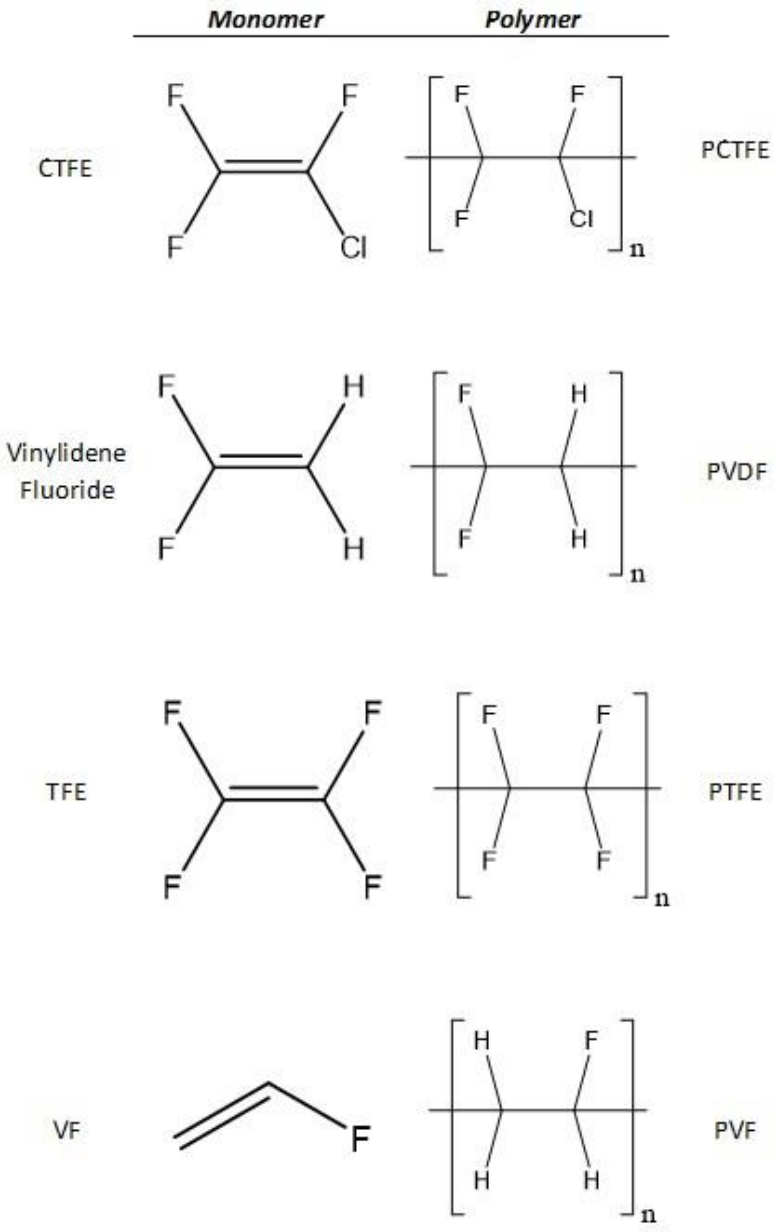

Figure 1.2.1

Among the fluorinated polymers, PVDF, HCTFE, PTFE are perhaps the ones largely used in water purification technology because of their chemical properties and in gas separation as porous support layer. Furthermore, their relatively low cost permits the use even for large-scale production of membranes.

1.3 Polymer functionalization

In membrane preparation, polymer functionalization allows a fine control at very level of the process. Indeed, functionalization can be done on polymer either before or after the membrane has been prepared. PVDF is one of most used fluorinated polymer which suits well to functionalization[5, 12-14]. In literature so many functionalization works have been done in order to create a material well tailored for specific needs. Some examples are reported in *Table 1.3*.1

	Functionalization type	***Used for***
Run1[8]	Defluorination/sulphonation functionalization.	MF
Run2[3]	PEG grafting by Argon-plasma treatment	Microporous membranes with antifouling properties
Run3[4]	Preparation of PEGMA-PVDF co-polymerization by RAFT-mediated polymerization	MF
Run4[5]	Grafted PEGMA on ozone-treated PVDF porous membrane	MF
Run5[15]	PVDF/PMMA-co-PAMPS/silica nanocomposite membranes by RAFT polymerization	Proton Exchange Membranes
Run6[12]	Naproxene grafted on PVDF membrane by ATRP polymerization	Realization of molecular-imprinted polymer

Table 1.3.1

1.4 Phase Inversion and membrane preparation

Polymeric membranes can be prepared in several ways: usually, preparation method is function of final use since that using the same polymer, different preparation methods may lead to membranes with same chemical composition and different morphological properties such as membranes with dense selective layer which is a fundamental requirement in the case of gas separation or porous membrane which suits well in the case of water purification. In general, separation efficiency is given by a combination of both chemical

and morphological properties, so preparation method is extremely important. Nowadays Phase Inversion is probably the most diffused way to prepare porous membranes, among the different methods[16-21] and includes:

- TIPS (Thermally-Induced-Phase-Separation): a technique in which polymeric and homogeneous solution at high temperature is immersed in a coagulation bath composed by non-solvent.
- VIPS (Vapor-Induced-Phase-Separation): dope solution is casted and let to interact with non solvent vapor which is usually made by water or ethanol for a specific time and under controlled contidions. VIPS allows the creation of membranes with highly controlled pore size and distribution by controlling vapor time exposure, relative humidity and temperature.
- NIPS (Nonsolvent-Induced-Phase-Separation): The polymer is dissolved in a suitable solvent and the dope solution casted on a glass plate and immersed in coagulation bath made by non-solvent which starts to exchange with solvent leading to polymer precipitation, that occurs as long as the process is complete. NIPS is very useful and powerful tool, tailored for porous membrane fabrication.

1.5 Coatings

In membrane science and related technologies[22] [23-25], coatings play a fundamental role because of the possibility to change and tune membrane features according to specific needs, without treat the material or revise the preparation process[26]. Coatings are actually used in order to overcome many drawback of physical and chemical functionalization. This because material properties such as conductivity, mechanical resistance or selectivity are due to the chemical structure which is changed during functionalization process. Therefore, when the material is functionalized this often leads to a loss of properties which might sometimes be hard to restore and consequently to a loss of performance during the operation process. In this compound the use of coating might avoid abovementioned problems since coating does not alter material properties. Furthermore, by coating it is possible to add properties, mechanical, chemical or even in terms of selectivity which are not held by starting material. Moreover, coating allows the use of sensitive materials[6] which cannot be employed in any other way. Also, coating can be applied to any type of membrane for biomedical applications, gas or liquid separation and for drug delivery systems also[7] Recently, Elimelech et al[9], reported an efficient method to fabvricate coated membranes to be used for MD application, in which pore size and distribution are finely controlled through the coating of highly porous PVDF-HFP electrospun nanofiber with pure PVDF and membranes exhibit high water flux and good rejection. Also, another interesting example concerning the use of coating in membrane systems, is discussed by Wessling et al[10]: a coating made by hydrogel was applied to hollow fibers and by application of electrical power it was possible to tune the selectivity of the system. In the last decade, due the huge diffusion of 2D materials and their production with

cheaper costs, the possibilities were widely enlarged[27-34]. Nevertheless, several studies must be done yet in order to comprehend how to maximize the synergy between plastics and 2D materials.

Chapter 1 references

1. Fontananova, E. D. a. E., Membrane Technology and sustainable growth. *Chemical Engineering Research and Design* **2004,** *82*, 1557-1562.
2. Van der Bruggen, B.; Curcio, E.; Drioli, E., Process intensification in the textile industry: the role of membrane technology. *J Environ Manage* **2004,** *73* (3), 267-74.
3. Peng Wang , K. L. T., E.T. Kang , K.G. Neoh Plasma-induced immobilization of poly(ethylene glycol) onto poly(vinylidene fluoride) microporous membrane. *Journal of membrane science* **2002,** *195*, 103-114.
4. Yiwang Chen, L. Y., Weihong Yu, E. T. Kang,* and K. G. Neoh, Poly(vinylidene fluoride) with Grafted Poly(ethylene glycol) Side Chains via the RAFT-Mediated Process and Pore Size Control of the Copolymer Membranes. *Macromolecules* **2003,** *36*, 9451-9457.
5. Yung Chang, Y.-J. S., Ruoh-Chyu Ruaan, Akon Higuchi ,; Wen-Yih Chen , J.-Y. L., Preparation of poly(vinylidene fluoride) microfiltration membrane with uniform surface-copolymerized poly(ethylene glycol) methacrylate and improvement of blood compatibility. *Journal of Membrane Science* **2008,** *309*, 165-174.
6. Ulbricht, M., Advanced functional polymer membranes. *Polymer* **2006,** *47*, 2217-2262.
7. Fang, R. H.; Kroll, A. V.; Gao, W.; Zhang, L., Cell Membrane Coating Nanotechnology. *Adv Mater* **2018,** *30* (23), e1706759.
8. Man Jae Han, G. N. B. B., Bumsuk Jung Effect of surface charge on hydrophilically modified poly(vinylidene fluoride)

membrane for microfiltration. *Desalination* **2011,** *270*, 76-83.
9. Shaulsky, E.; Nejati, S.; Boo, C.; Perreault, F.; Osuji, C. O.; Elimelech, M., Post-fabrication modification of electrospun nanofiber mats with polymer coating for membrane distillation applications. *Journal of Membrane Science* **2017,** *530*, 158-165.
10. Lohaus, T.; de Wit, P.; Kather, M.; Menne, D.; Benes, N. E.; Pich, A.; Wessling, M., Tunable permeability and selectivity: Heatable inorganic porous hollow fiber membrane with a thermo-responsive microgel coating. *Journal of Membrane Science* **2017,** *539*, 451-457.
11. Ameduri, B., Fluoropolymers: The Right Material for the Right Applications. *Chemistry* **2018**.
12. Bing, N. C.; Tian, Z.; Zhu, L. P.; Jin, H. Y.; Wang, L. L.; Wang, L. J., Controlled Grafting of S-Naproxen Imprinted Layer on PVDF Microporous Membrane by ATRP. *Advanced Materials Research* **2010,** *148-149*, 1026-1030.
13. Liao, Y.; Wang, R.; Fane, A. G., Engineering superhydrophobic surface on poly(vinylidene fluoride) nanofiber membranes for direct contact membrane distillation. *Journal of Membrane Science* **2013,** *440*, 77-87.
14. Razmjou, A.; Arifin, E.; Dong, G.; Mansouri, J.; Chen, V., Superhydrophobic modification of TiO2 nanocomposite PVDF membranes for applications in membrane distillation. *Journal of Membrane Science* **2012,** *415-416*, 850-863.
15. Ahmadian-Alam, L.; Kheirmand, M.; Mahdavi, H., Preparation, characterization and properties of PVDF-g-PAMPS/PMMA-co-PAMPS/silica nanoparticle as a new proton exchange nanocomposite membrane. *Chemical Engineering Journal* **2016,** *284*, 1035-1048.
16. P. Bernardo, E. D., and G. Golemme, Membrane Gas Separation: A Review/State of the Art. *Industrial & Engineering Chemistry Research* **2009,** *48*, 4638-4663.
17. P. van de Witte, P. J. D., J.W.A. van den Berg, J. Feijen Phase separtion processes in polymer solutios in relation to membrane formation. *Journal of Membrane Science* **1996,** *117*, 1-31.

18. Zhaoliang Cui, Naser Tavajohi Hassankiadeh, Suk Young Lee, Jong Myung Lee, Kyung Taek Woo, Aldo Sanguineti, Vincenzo Arcella, Young Moo Lee, Enrico Drioli Poly(vinylidene fluoride) membrane preparation with an environmental diluent via thermally induced phase separation. *Journal of Membrane science* **2013,** *444*, 223-36.
19. Z. H. LI, Q. Z. X., P. ZHANG, H. P. ZHANG, Y. P. WU, and T. VAN REE, Porous nanocomposite polymer electrolyte prepared by a non-solvent induced phase separation process. *Functional Materials Letters* **2008,** *1* (2), 139-143.
20. Han-han Lin, Y.-h. T., Tian-yin Liu, Hideto Matsuyama, Xiao-lin Wang, Understanding the thermally induced pha...ion process via a Maxwellâ•fiStefan model. *Journal of Membrane Science* **2016,** *507*, 143-153.
21. V.P. Khare, A. R. G., W.B. Krantz Vapor-induced phase separation—effect of the humid air exposure step on membrane morphology Part I. Insights from mathematical modeling. *Journal of Membrane Science* **2005,** *258*, 140-156.
22. Shenvi, S. S.; Isloor, A. M.; Ismail, A. F., A review on RO membrane technology: Developments and challenges. *Desalination* **2015,** *368*, 10-26.
23. Mehdizadeh, H., Membrane desalination plants from an energy–exergy viewpoint. *Desalination* **2006,** *191* (1-3), 200-209.
24. Deowan, S. A.; Galiano, F.; Hoinkis, J.; Johnson, D.; Altinkaya, S. A.; Gabriele, B.; Hilal, N.; Drioli, E.; Figoli, A., Novel low-fouling membrane bioreactor (MBR) for industrial wastewater treatment. *Journal of Membrane Science* **2016,** *510*, 524-532.
25. Galiano, F.; Friha, I.; Deowan, S. A.; Hoinkis, J.; Xiaoyun, Y.; Johnson, D.; Mancuso, R.; Hilal, N.; Gabriele, B.; Sayadi, S.; Figoli, A., Novel low-fouling membranes from lab to pilot application in textile wastewater treatment. *J Colloid Interface Sci* **2018,** *515*, 208-220.
26. Figoli, A.; Ursino, C.; Galiano, F.; Di Nicolò, E.; Campanelli, P.; Carnevale, M. C.; Criscuoli, A., Innovative hydrophobic coating of perfluoropolyether (PFPE) on commercial hydrophilic membranes for DCMD application. *Journal of Membrane Science* **2017,** *522*, 192-201.
27. Homaeigohar, S.; Elbahri, M., Graphene membranes for water desalination. *NPG Asia Materials* **2017,** *9* (8), e427.
28. Pierleoni, D.; Xia, Z. Y.; Christian, M.; Ligi, S.; Minelli, M.; Morandi, V.; Doghieri, F.; Palermo, V., Graphene-based coatings on polymer films for gas barrier applications. *Carbon* **2016,** *96*, 503-512.
29. Liu, G.; Jin, W.; Xu, N., Graphene-based membranes. *Chem Soc Rev* **2015,** *44* (15), 5016-30.
30. Yang, Y.; Zhao, R. Q.; Zhang, T. F.; Zhao, K.; Xiao, P. S.; Ma, Y. F.; Ajayan, P. M.; Shi, G. Q.; Chen, Y. S., Graphene-Based Standalone Solar Energy Converter for Water Desalination and Purification. *Acs Nano* **2018,** *12* (1), 829-835.
31. Intrchom, W.; Roy, S.; Humoud, M. S.; Mitra, S., Immobilization of Graphene Oxide on the Permeate Side of a Membrane Distillation Membrane to Enhance Flux. *Membranes (Basel)* **2018,** *8* (3).
32. Humplik, T.; Lee, J.; O'Hern, S. C.; Fellman, B. A.; Baig, M. A.; Hassan, S. F.; Atieh, M. A.; Rahman, F.; Laoui, T.; Karnik, R.; Wang, E. N., Nanostructured materials for water desalination. *Nanotechnology* **2011,** *22* (29), 292001.
33. Novoselov, K. S.; Fal'ko, V. I.; Colombo, L.; Gellert, P. R.; Schwab, M. G.; Kim, K., A roadmap for graphene. *Nature* **2012,** *490* (7419), 192-200.
34. Hosseini, S. M.; Madaeni, S. S., The Role of Nanomaterials in Water Desalination: Nanocomposite Electrodialysis Ion-Exchange Membranes. **2017,** *48*, 291-303.

Chapter 2

Developement of PVDF-Graphene Thin Film Composite membranes for Direct Contact Membrane Distillation

2.1 Chapter Summary

A simple and efficient method for the preparation of PVDF-Graphene TFC membranes is herein discussed. In order to enhance adhesion between polymer and graphene, PVDF has been functionalized (PVDF-f) with suitable molecule, using a procedure involving two reactions: basic treatment that leads to partial defluorination and formation of double bonds, followed by radical polymerization with suitable molecule bearing aromatic ring(s). PVDF-f was used to fabricate membranes which have been tested before association with Graphene layer, which has been synthetized using CVD method under appropriate conditions and used as coating on PVDF-f membranes (PVDF-f-GM). All produced membranes were analyzed in order to deeply investigate chemical and morphological properties, using most common analysis techniques. All membranes have been tested on Direct Contact Membrane Distillation apparatus with interesting results: PVDF-f membranes produces a good water flux and excellent salt rejection up to 99.9 % whereas 2D material effect in the case of PVDF-f-GM, causes a partial reduction in terms of flux on one hand and enhanced salt rejection up to 99.99 % on the other hand; also, we observed an improved membrane lasting and mechanical resistance.

2.2 Introduction

Water treatment and water-related issues are nowadays assuming remarkable importance and will become of fundamental importance in the next future; due to higher clean water demands and population growth, especially in densely populated countries such as India or China, water treatment technologies are becoming fundamental matters of discussion which claim particular consideration[1-2].Therefore, worldwide demand of water is met by novel strategies whose purpose is to preserve and recycle wastewater in order to face the problem. On this purpose, an important role is played by membrane technology which represent a steady and reliable technique that is actually enforced for different scopes including water treatment because of its enormous advantages, as well as the possibility to treat municipal and industrial wastewater either[3-5]. In fact,

membrane technology is a common and appreciated way owing to its outstanding properties in terms of environmental impact, process scalability and flexibility and energy requirements. In the framework of water shortage and reuse issue, desalination is going to be one of the dominant methods for fresh water production starting from brackish ground water, wastewater or seawater; this is of remarkable importance since in nations such as Kwait or Qatar 100% demand of water is fulfilled by desalination techniques based on membrane technology[6]. Desalination aims to produce pure water which can be used for humans, for commercial purpose or on industrial plants in salt removal occurs; actually, thermal distillation, the most common technique used for desalination, has one biggest disadvantage among all, which is represented by high energy demands[7-10].In water desalination, the biggest achievement is to reach process efficiency as high as possible, combined with use of sustainable and green energy sources such as solar energy[11-12]. The purpose of water desalination, is the production of fresh and clean water through the removal of minerals dissolved in it. In this framework, membrane processes role is greater day by day and despite thermal distillation is the oldest used method, its high energy demand represent a bottleneck[13]. Actually, more than 50% of worldwide desalination plants use Reverse Osmosis (RO) for fresh water production[14-15].RO can be actually considered leading technology in water desalination processes, but it suffers of important limitations such as harsh operative conditions and suffers of concentration polarization phenomena[14, 16] which decreases its efficiency. Due to these limitations, other systems like Membrane Distillation (MD) are assuming greater importance in desalination and water treatment processes owing to their undeniable advantages[17-23] in terms of efficiency, energy consumption and the absence of problems related to the concentration polarization[22]. Membrane Distillation, is a particular thermally-driven process in which water vapor passes from hot feed side through a microporous membrane and subsequently condensates on the cold permeate side. In this kind of processes, the driving force is represented by the water vapor pressure difference between feed and permeate sides. In order to maximize the process efficiency, features like material hydrophobicity, insulating properties and pore-size in the range of microfiltration are essential requirements to prevent membrane wetting without hinder the vapor passage, achieve good salt rejection and maintain the temperature difference between both membrane sides[24]. On this purpose, the lack of fully optimized materials is one of main obstacles which arrests scale up process: to overcome this drawbacks and design a tailored material with fit properties, several methods are reported in literature by scientific community: coating membrane with hydrophobic perfluorinated polymer[25], realize a blend of two different materials[26], use nanoparticles in association with polymeric material[27] or increase overall porosity degree by particular methods such as electrospinning[28]. In last years, the introduction of available nanomaterials (NMs) increased the number of possibilities in terms of new materials that can be used in MD processes in association with polymers with enormous benefits[29-34]: they can be dispersed in polymer matrix, used as coatings, grafted on membrane surface and also be functionalized for specific needs. On this purpose, graphene is one of most popular NMs and although deeper investigation is needed to fully understand its properties, it right away exhibited great properties[35].Basically, graphene is a monoatomic thick material entirely made by sp^2 carbon atom, whose properties such as

mechanical resistance, chemical inertness superconductivity attracted a lot of attention from scientific community[36], which steams from its potentiality to produce ultrathin membranes with tunable pore size and superior performances in terms of permeability and selectivity[37]. For instance, Sint et al[38]created nanopores on graphene terminated with nitrogen or hydrogen which act as ionic sieves inmolecular dynamic simulations. In particular, permeation of Li^+, K^+ and Na^+ ions is more favored for nitrogen-doped graphene, while permeation of anions species like Cl^- and Br^- is higher in the case of hydrogen-doped graphene. Ions passage through these membranes can be finely customized acting on both size and shape of nanopores and their functionalization. Herein we report a method to fabricate PVDF-Graphene (PVDF-f-GM), using graphene layer synthetized by CVD method as coating for membranes prepared using chemically-modified commercially available PVDF powder (PVDF-f). Functionalization starts with basic treatment which leads to to a partial defluorination and introduces double bonds onto polymer backbone, followed by radical co-polymerization with suitable monomer. Produced membranes have been analyzed in order to investigate their chemical and morphological properties and several Direct Contact Membrane Distillation tests have been performed on them.

2.3 Results and Discussions

2.3.1 PVDF-f Polymer preparation and characterization

As shown in Figure 2.3.1.1, PVDF-f was prepared using a procedure involving two step reaction: basic treatment of commercially available PVDF 6010 polymer powder with KOH in order to create double bonds onto the polymer chain, followed by their polymerization by radical reaction with suitable ring(s) bearing monomer.

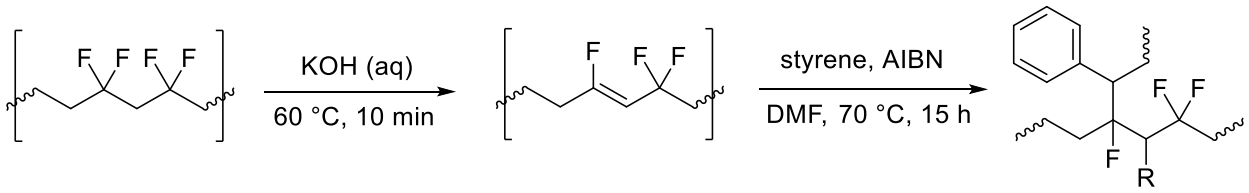

***Figure 2.3.1.1**: schematic representation of PVDF functionalization by basic treatment*

However, although membranes discussed in this work exhibit interesting properties in terms of water flux and salt rejection, polymer synthesis is the result of a series of other experiments in which we changed operative conditions and monomer that are summarized in Table 2.3.1.1 and discussed below.

Run	PVDF/monomer Ratio (wt.)	Monomer Type	Polymerization Time (h)	Polymer Synthesis	Membrane Fabrication	Flux Pure Water (LMH/bar)	Flux (Salty Water)	Rejection (%)
1	**1:1**	**Styrene**	**15**	**Yes**	**Yes**	**≈ 17**	**≈12**	**99.9**
2	1:0.5	Styrene	15	Yes	Yes	≈6.4	5.8	99.5
3	1:2	Styrene	15	Yes	No	/	/	/
4	1:1	Styrene	18	Yes	Yes	11.3	2.4	98.6
5	1:2	Styrene	18	Yes	No	/	/	/
6	1:1	Styrene	24	Yes	No	/	/	/
7	1:0.5	Styrene	24	Yes	No	/	/	/
8	1:2	Styrene	24	Yes	No	/	/	/
9	1:3	Vinyl Naphtalene	15	Yes	No	/	/	/
10	1:1.5	Vinyl Naphtalene	15	Yes	No	/	/	/
11	1:6	Vinyl Naphtalene	15	Yes	No	/	/	/

Table 2.3.1.1*l synthtetic conditions used for polymer synthesis. Reported flux values refer to a test performed using the same DCMD facility, using crossflow velocity of 1 LPM, 0,5 M NaCl solution and Feed/Permeate temperature of 70/20 °C. In the case of vinyl-naphtalene related run(s) (10-12), the amount of monomer has been calculated using an equimolar concentration with styrene.*

Main efforts were focused on the last functionalization step in which double bonds in PVDF chain are polymerized with monomer. We tried to change polymerization time and monomer amount and checked if membrane preparation was possible. We notice that during polymerization both time and monomer amount play an important role because they lead to a higher or lower functionalization degree and hence to a final polymer with different solubility in organic solvents: in fact functionalization time allows C-C bond formation between monomer and PVDF and on the other hand the chain-chain interaction that means a final higher degree of reticulation. In particular, we observed that polymer with higher degree of functionalization (Run 5-8) cannot be used for membrane preparation since no one of them exhibits solubility high enough for common solvents such DMSO, DMFor DMAc and are not suitable for membrane preparation. Vice versa, decreasing reaction time and monomer amount, both polymer and membranes can

be prepared, but membrane exhibit lower flux. Also with monomer changing (Run 9-11) though polymer functionalization occurs membranes cannot be prepared. Run1 reports optimized conditions which have been used for PVDF-f polymer preparation and hence for membrane fabrication.

2.3.2 PVDF-f polymer characterization

Characterization of the new material was accomplished by NMR analyses

Figure 2.3.2.1 a-b show ^{1}H NMR analysis performed on PVDF and PVDF-f powder respectively

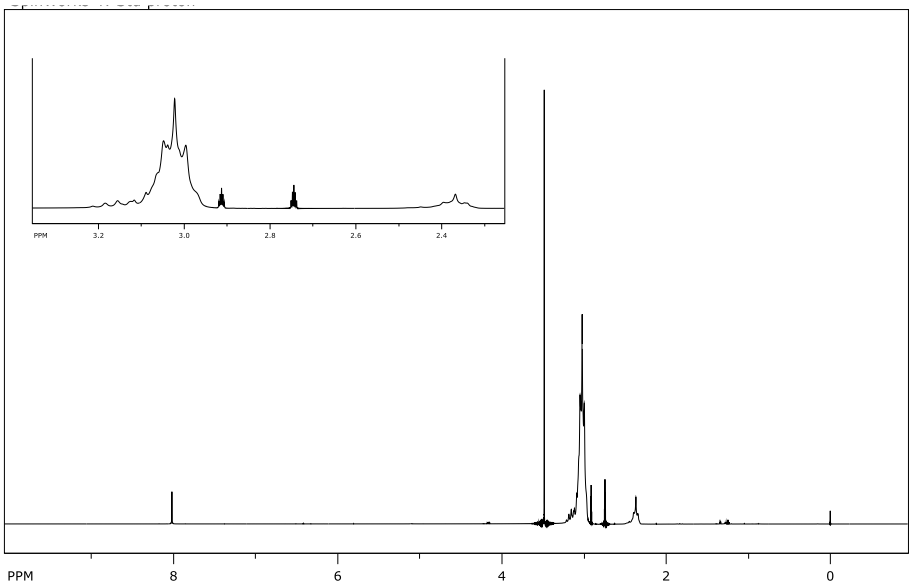

***Figure 2.3.2.1 a**: ^{1}H NMR of Pristine PVDF powder*

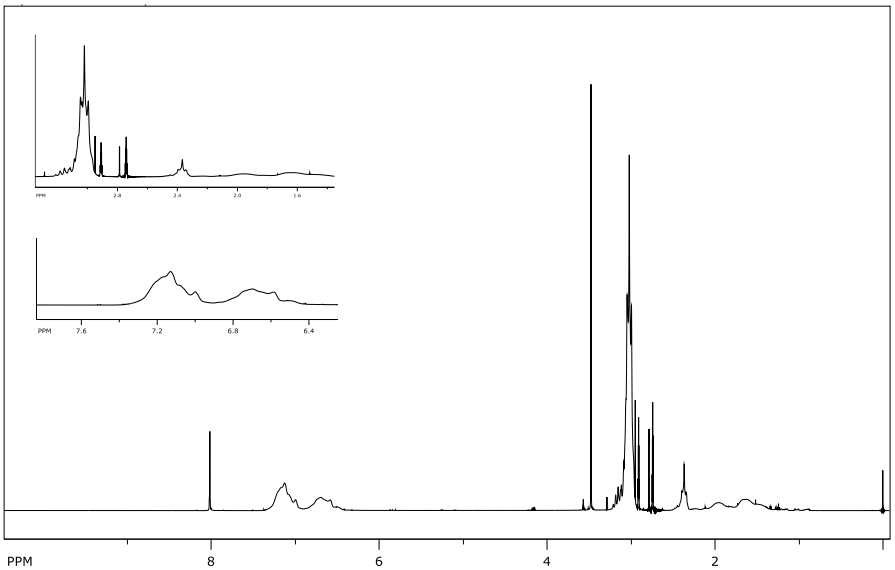

***Figure 2.3.2.1 b**: ^{1}H NMR of PVDF-f powder*

In spectrum b, it is evident the presence of signals between 6.2 and 6.7 ppm, which are typical of aromatic protons. These signals (absent in spectrum a) are therefore ascribable to the presence of phenyl rings in the material and confirm the success of the copolymerization process between PVDF and styrene. Tis is further confirmed by the signals between 1.2 and 2.1 ppm in spectrum b, which are due to the –CHPhCH$_2$- moieties.

2.3.3 Graphene Characterization by optical microscope analysis

In order to estimate the presence of defects and multilayer areas, 2x1 cm2 sample of graphene were analized after copper oxidation occurs (Figure 2.3.3.1-a) using a procedure described in the experimental part: after synthesis by CVD method, when graphene is still on the copper foil catalyst, the sample is removed from the machine and 1 cm^2 sample is gently placed on a heating plate at 120 °C for 20 min. This temperature increment causes copper oxidation, visible because of darker color in the areas not directly covered by the graphene layer owing to defects, whereas the color does not change for areas beneath graphene layer (not subjected to oxidation by O_2). Another 1 cm^2 sample is spin-coated with PMMA before copper removal by Iron nitrate (III) and Iron Chloride (III) solutions with a procedure deeply described below in the experimental part. Once dissolution occurs, the sample is placed on silicon wafer (Figure 2.3.3.1-b), PMMA is removed by dissolution in acetone and sample analyzed using optical microscope.For each sample two shots were taken at 200x and 1000x magnification (smaller and bigger picture respectively). Analysis show that some defect is visible only at high magnification degree (Figure 2.3.3.1-a) in correspondence of areas not directly covered by graphene.

in Figure 2.3.3.1-b, higher magnification picture shows that certain multi-layered areas (visible as darker blue spots) exist and the presence of residual PMMA (visible as very bright light blue area in the bottom part of image) either.

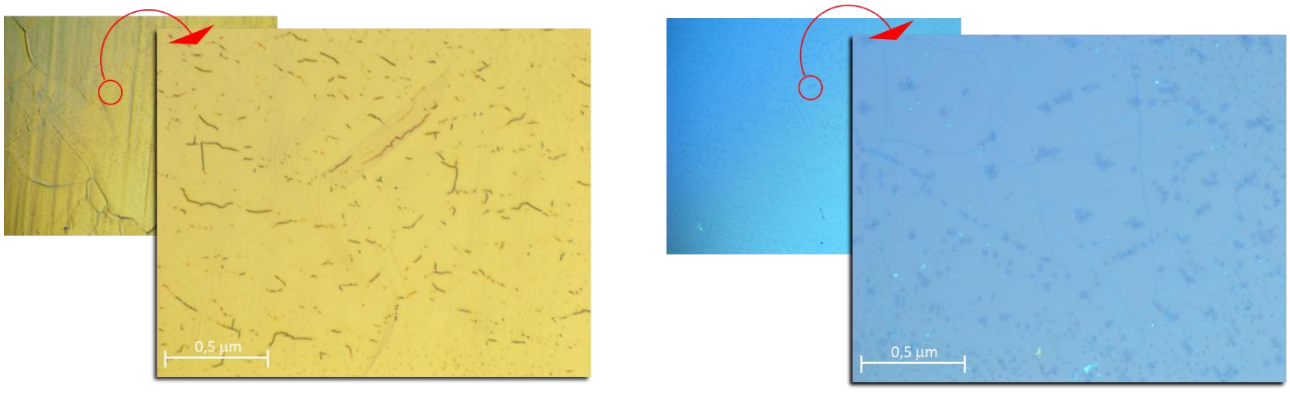

***Figure2.3.3.1-a,b**: in Picture 2.3.3.1-a after copper oxidation, optical microsope images show small darker areas which represent oxidized copper not covered by graphene layer, while Picture 2.3.3.1-b shows graphene sample on silicon wafer: darker areas represent multi layered zone while bright blue areas indicate residual PMMA polymer.*

2.3.4 Membrane Fabrication and Characterization

All the membranes were produced by phase inversion using casting thickness of 220 µm, waterbath composition was 100% water and its temperature was 19-21 °C. Once dried, membrane association with graphene is made by using laminating machine.

The whole procedure is summarized in Figure 2.3.4.1: during phase 1 the adhesion between graphene and polymer is enhanced by laminating machine, in phase 2 the catalyst solubilization occurs in order to get the final membrane (phase 3):

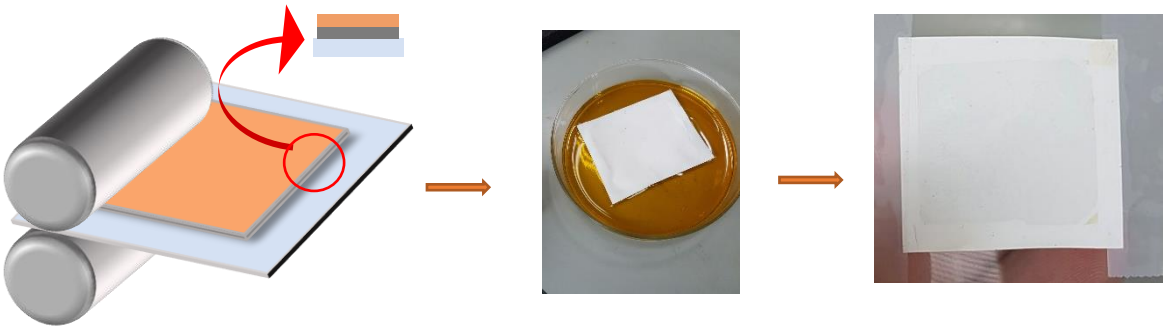

***Figure2.3.4.1**: three phases in composite membrane fabrication procedure: Lamination process (phase1), catalyst removal (phase 2) and final membrane (phase 3)*

Produced membranes have been characterized by FT-IR, SEM, AFM, XPS and Mechanical test machine.

2.3.5 FT-IR analysis

Figure 2.3.5.1 show a comparison between Pristine PVDF and PVDF-f membranes FT-IR analysis. It has been observed that the presence of phenyl rings in the case of PVDF-f is confirmed by the aromatic out-of-plane C-H bending in the 700-950 cm^{-1} region.

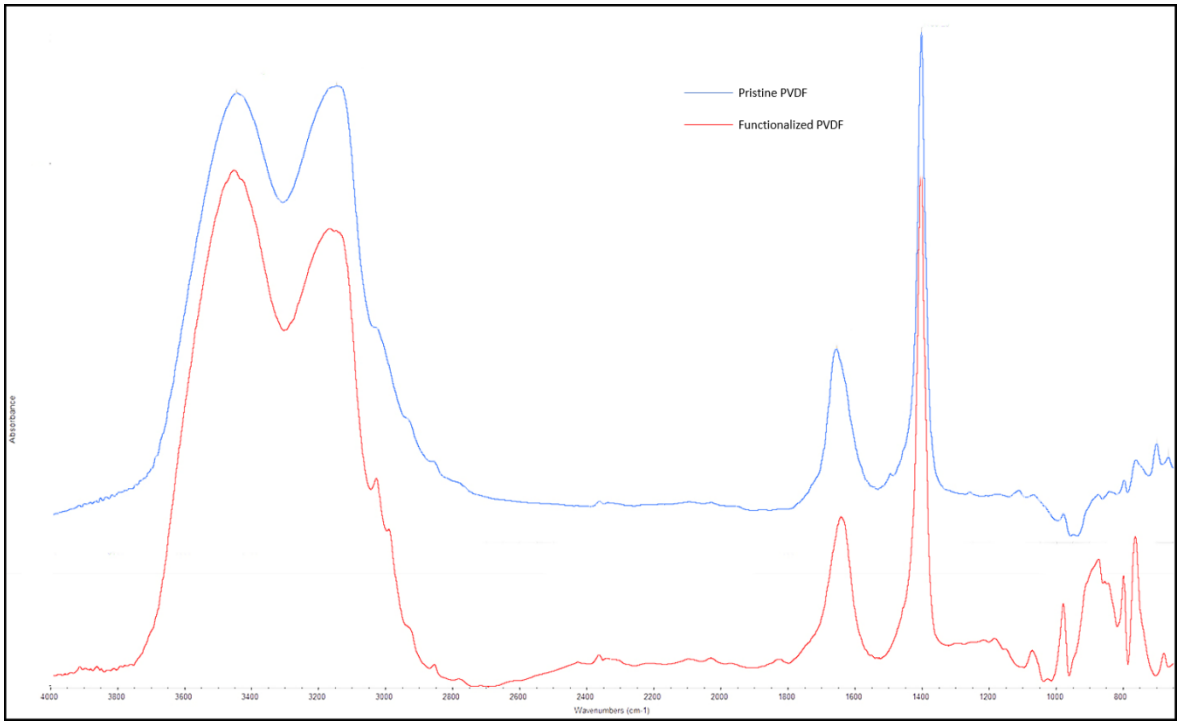

***Figure 2.3.5.1**: FT-IR spectra comparison of Pristine and Functionalized PVDF*

2.3.6 Scanning Electron Microscope (SEM) and Atomic Force Microscope (AFM) analysis

SEM and AFM representative images are shown in Figure 2.3.6.1 and Figure 2.3.6.2, respectively. In figure Figure 2.3.6.1, all the membranes show an homogeneous surface images and an asymmetric structure clearly appears in cross section pictures; it is possible to easily notice the differences between PVDF (Figure 2.3.6.1-a,b) and PVDF-f (Figure 2.3.6.1-c,d) membrane: although both membranes show hybrid structure, sponge-like area is reduced in the case of PVDF-f membrane: this indicates morphological differences which can be ascribed to functionalization procedure and can justify the difference in terms of water vapor flux exhibited in DCMD tests; also, though graphene layer is not visible in Figure 2.3.6.1-e,f, these membranes showed very similar morphological structure to PVDF-f membranes as we expected: this means that the differences in terms of flux and rejection (discussed below) can only be ascribed to graphene layer. In Figure 2.3.6.2, AFM morphological analysis shows that mean membrane roughness (Sa) increases in case of functionalized polymer (Figure 2.3.6.2-a) compared to pristine one (Figure 2.3.6.2-b). It has been calculated and resulted to be 44.65 nm in the first case and 30.98 nm in the latter one. Clearly, also in this case, roughness value differences carried by the functionalization procedure lead to a different membrane surface morphology, which can also be noticed in different contact angle value reported later in this chapter.

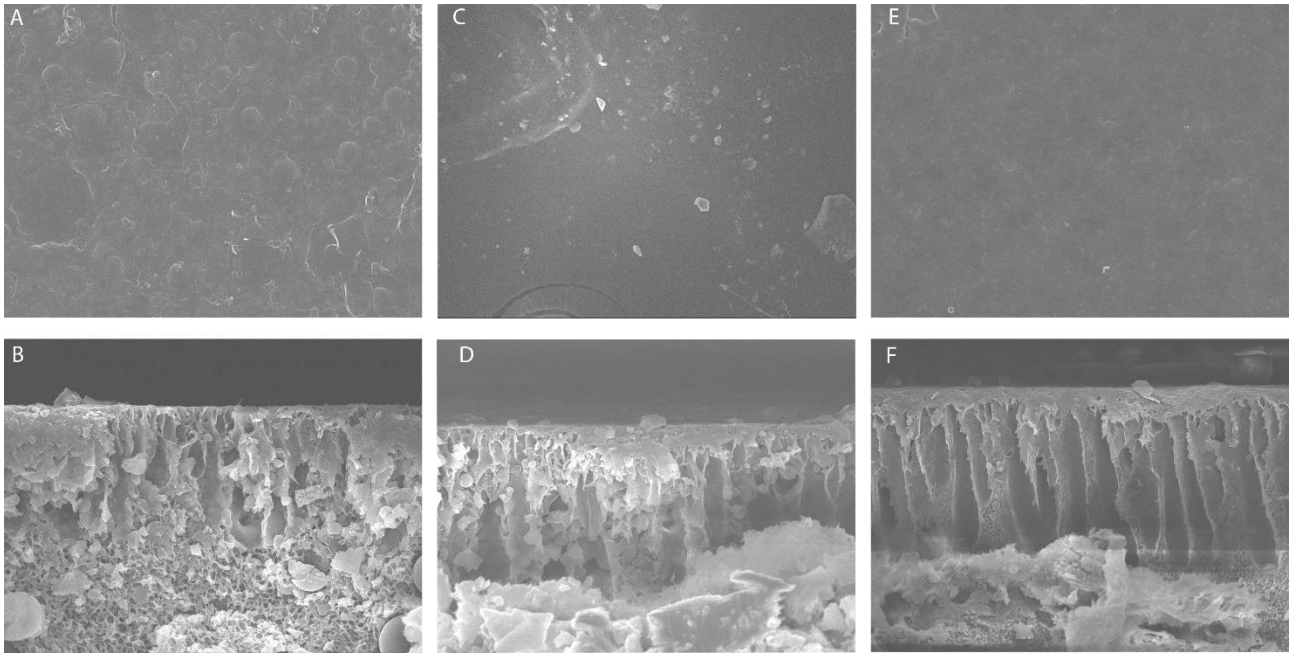

Figure 2.3.6.1 a-f*: representative SEM images of top side and cross section of pristine PVDF membrane (a,b), membrane prepared with functionalized pvdf (c,d), and PVDF-graphene composite membrane (e, f).*

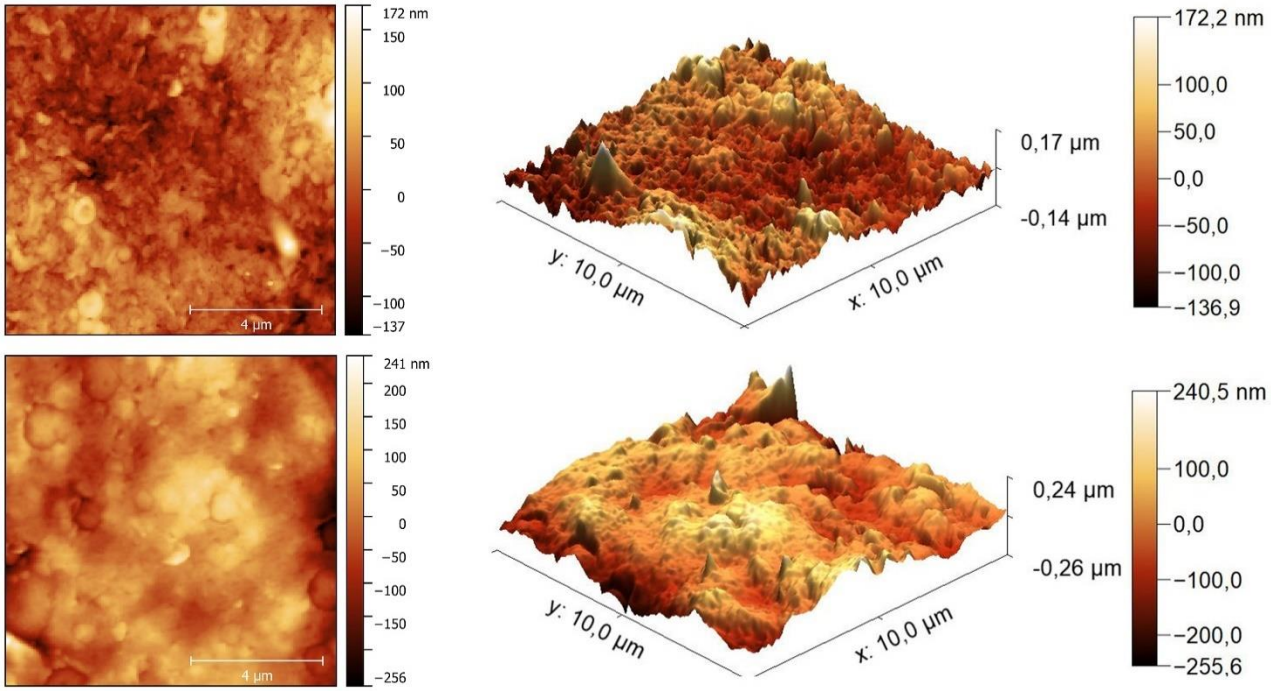

Figure 2.3.6.2 a,b*: representative AFM images of membranes prepared using pristine PVDF (a) and PVDF-f polymer (b)*

2.3.7 Contact Angle analysis

In Figure 2.3.7.1 a-e,top (a,c,e) and bottom(b,d) side contact angles for pristine (a,b), PVDF-f (c, d) and PVDF-f-GM (e) are reported. Two main considerations must be done about CA results, the first of which concerns the slight increase of values of functionalized PVDF compared to pristine one, as expected, the second is about the increment in CA value in bottom sides compared to top ones. In conclusion, low contact angle for PVDF-graphene composite membrane is reported: according to literature, observed CA values for Graphene may greatly change because they are in relation with material properties, number of layers, presence of metal catalyst, environmental air exposure time, etc[39-41]: for instance, it has been observed how graphene CA has the tendency to become greater when subject to contact with air, probably owing to its capacity to interact with small hydrocarbons as well as big difference in CA values have been found comparing graphene samples made using different catalyst. Comparing Pristine PVDF and PVDF-f membranes, an increase in CA values of the PVDF-f has been observed. This agrees both with functionalization procedure and with AFM analysis that indicates different morphological properties in terms of mean roughness. In the case of graphene, precise contact angle value is still debated question researchers are struggling with and it needs to be investigated more deeply. Furthermore, it must be noticed that CA is a measurement whose value takes into account not only chemical structure and hence hydrophilicity or hydrophobicity, but also morphological parameters such as roughness and hence the presence of cavities on the membrane surface will surely affect its value. In AFM analysis, enhanced mean roughness value of PVDF-f compared to Pristine PVDF membranes can be one of causes which justify the difference in CA values.

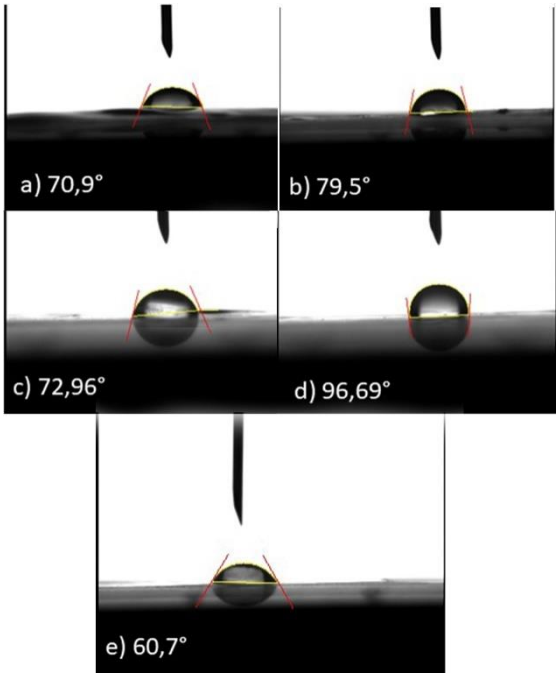

***Figure2.3.7.1 a-e**: CA value for membranes prepared using pristine PVDF (a,b), PVDF-f (c,d) and PVDF-f-GM (e)*

2.3.8 Pore size measurement

The pore size of the produced membranes is in the range of microfiltration (0.1-0.5 µm). One interesting point concerns pore forming process when phase inversion occurs. Usually pore-forming agents such as lithium chloride as well as PEG are used to control pore size and/or their distribution on final membrane. In our case, membrane prepared using pristine PVDF exhibits no flux on DCMD tests and unusual high LEP (above 5 bar) whereas membranes prepared using functionalized PVDF give good flux and very high rejection (above 99.9%) either, maintaining reasonable LEP (below 2 bar).This represents one interesting point because indicates that functionalization permits formation of membranes possessing appropriate pore size range, without using additives. Main characteristic such as Mean flow pore pressure, minimum pore diameter, bubble point pressure and bubble point pore diameter, have been estimated and reported below (Table 2.3.8.1). Pore size test performed on produced membranes, showed that a big difference in terms of pore size exists.We analized three types of membranes, made with pristine PVDF polymer, PVDF-f and PVDF-f-GM respectively. Analysis showed that in the case of pristine PVDF mean pore diameter is about 0.03 µm; this results agrees with performed experiments, since in DCMD tests no water vapor flux occurs using pristine PVDF. In the case of membranes prepared using Functionalized PVDF (PVDF-f), mean pore size is in the range of microfiltration as we expected from tests. Differently, in the case of PVDF-f/graphene TFC membranes mean pore size drastically decreases since graphene acts as barrier which partially cover membrane pores; nevertheless, despite pristine PVDF-like pore diameter and hence low measured pore size value, TFC composite membrane exhibits water flux on DCMD tests and good salt rejection (above 99.9 %). Pore-size results are summarized in Table 2.3.8.1

	Mean Flow Pore Pressure (bar)	*Mean Pore Diameter (µm)*	*Blubble point pressure (bar)*	*Bubble Point Diameter (µm)*
Pristine PVDF	*15,4*	*0,03*	*1,2*	*0,4*
PVDF-f	*3,56*	*0,13*	*1,1*	*0,4*
PVDF-f/ Graphene TFC membrane	*10,92*	*0,04*	*1,2*	*0,4*

***Table 2.3.8.1**: Pore size measurement for membranes prepared using pristine PVDF, PVDF-f and PVDF-f-GM*

2.3.9 XPS analysis

XPS analysis shown in Figure 2.3.9.1, report a comparison of C1s,O1s and F1s peaks for both pristine PVDF and PVDF-f membranes. In case of F1s spectra signals are comparable, whereas O1s signal intensity is lower in PVDF-f than pristine one. Very interesting is C1s spectra in which PVDF CF2 peak is visible at 290 eV, and two different peaks are shown at 284 and 285 eV, regarding styrene and CH2 PVDF peaks respectively. In this case, the presence of three peaks in C1s spectra, indicates that functionalization occurs and aromatic groups were successfully linked to the polymer.

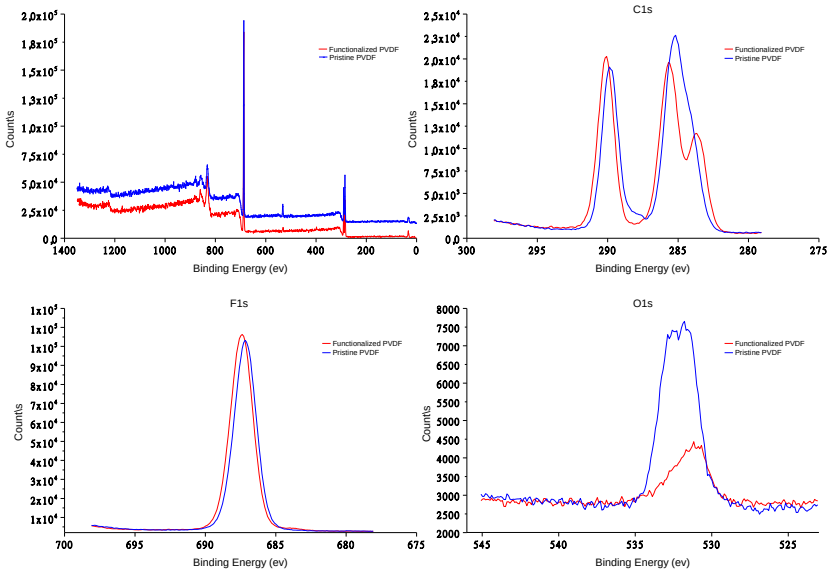

***Figure 2.3.9.1**: XPS analysis perfomed on membranes prepared using PVDF and PVDF-f polymer*

2.3.10 Mechanical Tests

Figure 2.3.10.1 reports mechanical tests performed on Pristine PVDF PVDF-f and PVDF-f-GM TFC membranes in order to evaluate their mechanical properties in terms of Young Module (E mod), tensile stress at break (Rm) and elongation stress at break (ε-Break) .Chemical functionalization somehow leads to a reduction in Emod, Rm and ε-Break values in PVDF-f membranes. However, when graphene is employed young module rises up as well as tensile stress at break and composite membrane properties are closer to pristine polymer. These composite membrane properties enhancement compared to PVDF-f membrane ones can be ascribed to graphene effect on young module and tensile stress at break. Different speech applies to elongation at

break parameter, whose values indicates that: a) functionalization procedure causes elasticity loss and b) even though 2D material is applied, the final membrane elasticity remains far less than pristine polymer.

	EMod (N/mm²)	***Rm (N/mm²)***	***ε-Break (%)***
Pristine PVDF	*208.0*	*12.9*	*140.8*
SD	*25.2*	*2.9*	*2.9*
PVDF-f	*143.3*	*3.7*	*98.8*
SD	*3.1*	*0.3*	*25.7*
PVDF-f-GM	*76.0*	*2.9*	*60.7*
SD	*12.6*	*0.1*	*0.9*

Figure 2.3.10.1*: Mechanical tests performed on Pristine PVDF, PVDF-f and PVDF-f-Gm*

2.3.11 Direct Contact Membrane Distillation (DCMD) Tests

In order to compare the properties of membranes fabricated using above described procedure, we tested pristine PVDF, PVDF-f and PVDF-f-GM membranes on the same Membrane Distillation apparatus with same operative conditions described in the experimental part. We noticed that in the case of membranes prepared using pristine PVDF polymer without pore forming agents the vapor flux across the membrane is absolutely absent, whereas PVDF-f membranes possess a certain degree of porosity perhaps owing to the functionalization treatment. However, in the case of PVDF-f membranes salt rejection remains high up to 99.9 %. In the case of PVDF-f-GM, the effect of graphene is particularly evident in terms of salt rejection which rises up to 99.99%, at the expense of vapor flux whose decrement can probably be ascribed to the " barrier effect" operated by graphene layer.

Figure 2.3.11.1-a,b,c report tests performed on membranes both with pure water (a), salty water (b) and rejection comparison for different membranes (c), using conditions in detail described in experimental part.

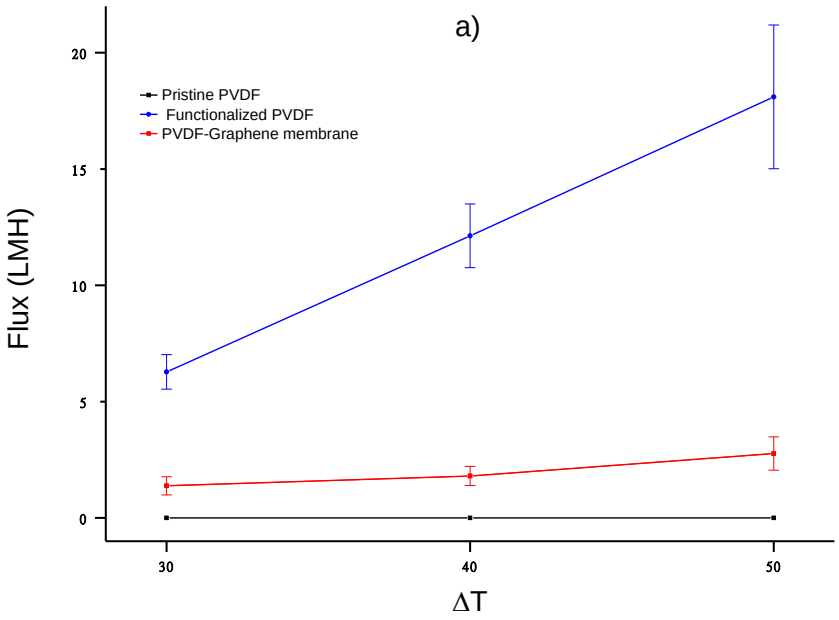

***Figure 2.3.11.1-a**: DCMD test performed using pure water*

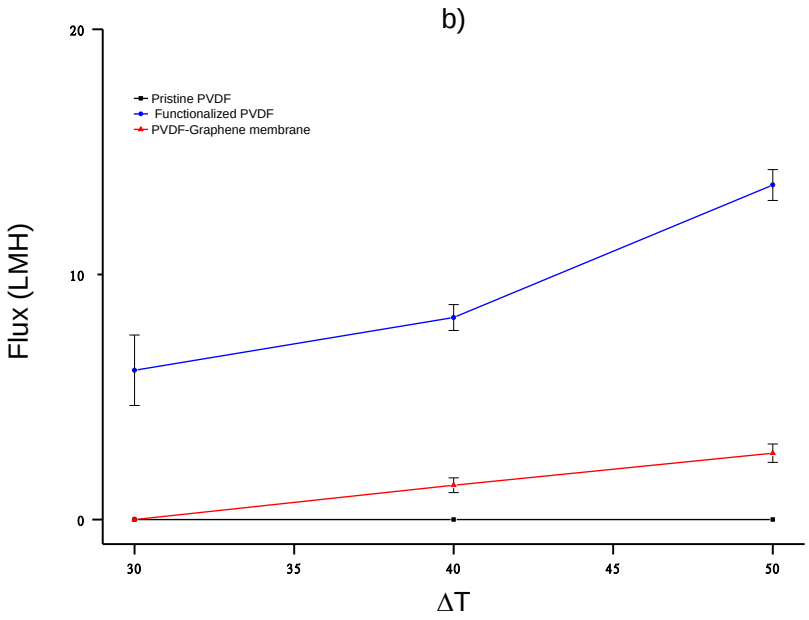

***Figure 2.3.11.1-b**: DCMD test performed using salty water*

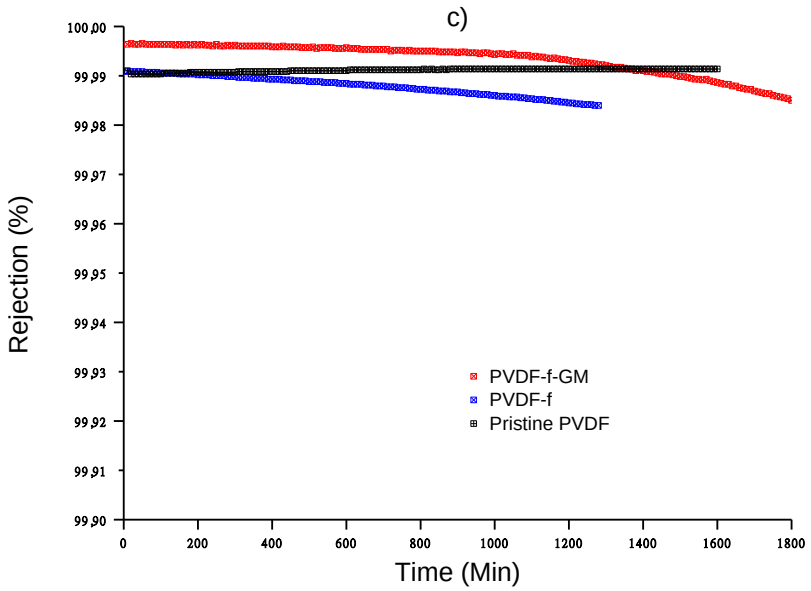

***Figure 2.3.11.1-c**: Salt rejection for the different membranes*

In literature, different works about membranes made with different types of PVDF and graphene to be used for MD applications, mostly in Air-Gap Membrane Distillation (AGMD), exist. Some of them are reported in Table 2.3.11.1 and clearly indicate that our membranes result to be competitive with other reported: in some cases they possess better salt rejection in the time (Run 4), or comparable flux with higher rejection with lower operating temperature (run 5) or even higher flux.

Membranes and differences can be ascribed to the different polymer or preparation method but also to the different type of graphene used, mostly GO or modified GO or Graphene Quantum Dots (GQDs) reported in Run(s) 5,7,4 respectively. On the other hand, another important difference concerning the way graphene is linked to membrane must be discussed: in literature, graphene and graphene-like materials are usually employed as additive during dope solution preparation or immobilized on membrane surface by vacuum filtration.

This procedure expects preventively material preparation such as chemical exfoliation of graphite, treatment with strong oxidizing chemicals in the case of GO, purification, dispersion in suitable

	Polymer	Membrane Type	Salty Concentration	Graphene	Flux Kg/(m2 h)	Rejection	Feed/Perm Temp (°C)	
1	PVDF	flat sheet	35 g\l (0,6 M)	no	1,85 Kg/(m2 h)	lower than 90 % using 10 to 15 % polymer conc.	50/20	
2	PVDF	flat sheet	pure water	no	10,37 Kg/(m2 h)	/	50/20	
1	PVDF+ NW fabric	flat sheet	35 g\l (0,6 M)	no	12,45	lower than 90 % using 10 to 15 % polymer conc.	50/20	
3	PVDF+TFE	flat sheet	17,6 g\l	no	7,2	close to 100%	55/20	
	PVDF	flat sheet	35 g/lt (0,6 M)	no	from 18 to 16 after 8h	PVDF from 99,5 to 94,6 after 8h	60/20	AGMD
	PVDF+GQDs1(0,05 wt%)	flat sheet	35 g/lt (0,6 M)	si	6	PVDF+GQD1P from 99,9% to 99,8 % after 8h	60/20	AGMD
4	PVDF+GQDs2(0,1) wt%)	flat sheet	35 g/lt (0,6 M)	si	from 13 to 8 after 8h	PVDF+GQD2P from 99,9% to 99,8 % after 8h	60/20	AGMD
	PVDF+GQDs3(0,25) wt%)	flat sheet	35 g/lt (0,6 M)	si	18	PVDF+GQD3P from 99,9% to 99,8 % after 8h	60/20	AGMD
	PVDF+GQDs4(0,5) wt%)	flat sheet	35 g/lt (0,6 M)	si	8	PVDF+GQD4P from 99,2% to 95,2 % after 8h	60/20	AGMD
	PVDF	flat sheet	35 g/lt (0,6 M)	NO	3,4	99,9	85/20	AGMD
	PVDF+GO 0,1%	flat sheet	35 g/lt (0,6 M)	si (GO)	3,8	99,7	85/21	AGMD
	PVDF+GO 0,3%	flat sheet	35 g/lt (0,6 M)	si (GO)	4,7	99,9	85/22	AGMD
5	PVDF+GO 0,5%	flat sheet	35 g/lt (0,6 M)	si (GO)	5,4	99,6	85/23	AGMD
	PVDF+ GO-APTS 0,1%	flat sheet	35 g/lt (0,6 M)	si (GO) funz	4,5	99,8	85/24	AGMD
	PVDF+GO-APTS 0,3%	flat sheet	35 g/lt (0,6 M)	si (GO) funz	6,25	99,9	85/25	AGMD
	PVDF+GO-APTS 0,5%	flat sheet	35 g/lt (0,6 M)	si (GO) funz	5,7	99,7	85/26	AGMD
6	PVDF	flat sheet	3 wt. %	NO	1	99,1	50/20	DCMD
	PVDF	flat sheet	3,5 wt. %	NO	18,2	88,5	80/15	AGMD
7	PVDF+GO-ODA M1	flat sheet	3,5	GO-ODA	13,8	96,3	80/16	AGMD
	PVDF+GO-ODA M2	flat sheet	3,5	GO-ODA	16,7	98,3	80/17	AGMD
	PVDF	flat sheet	0,5 M	no	0	100	70/20	DCMD
	PVDF-f	flat sheet	pure water	no	≈17		70/20	DCMD
This work	PVDF-f	flat sheet	0,5 M	no	≈12	99,9	70/20	DCMD
	PVDF-f/ Graphne	flat sheet	pure water	yes	≈3		70/20	DCMD
	PVDF-f/ Graphne	flat sheet	0,5 M	yes	≈3	99,99	70/20	DCMD

***Table 2.3.11.1**: literature work comparison. Run1[42],Run2[43],Run3[44],Run4[31],Run5[30], Run6[45], Run7[46]*

2.4 Experimental

2.4.1 Chemicals

PVDF 6010 (Solef, Solvay), KOH (Daejung, 1 Kg flakes, 93% purity), AIBN (Junsei,1 Kg, purity ≥ 98 %), Styrene (Sigma Aldrich, 1 lt, purity 99.9 %) and DMF (Sigma Aldrich, purity ≥ 99.8 %) have been used without further purification. For graphene synthesis, 15 micron thickness copper catalyst(Welcos, 99.9%), Nitrogen (Air Korea 99.999%), Argon (Air Korea 99.999%), Methane (Air Korea 99.999%), Hydrogen (Air Korea 99.999%) have been employed.

2.4.2 PVDF-f synthesis

The PVDF functionalization (PVDF-f) was realized on the base of one procedure present in literature[47], which involves two reactions: the first step corresponds to a basic treatment with KOH to induce the formation of double bonds in the polymeric backbone by HF elimination, while the second step is a radical copolymerization of the double bonds with styrene, as shown in Figure 2.3.1.1. Briefly, PVDF 6010 (40 g) were suspended in a KOH solution (40 g in 719.6 g of deionized water) containing absolute EtOH (0.4 g) under nitrogen atmosphere. The suspension was stirred at 60 °C for 10 min, and then a solution of PVDF (38 g) in DMF (0.456 l) was slowly added in portions, followed by styrene (38 gr) and AIBN (0.623 g). The resulting mixture was stirred at 70 °C for 15 h.

After cooling, the polymeric material was precipitated with 2.5-3 fold excess of MeOH, then filtered, washed with DI water, and dried under vacuum at 50 °C overnight in order to obtain dry PVDF powder.
Polymerization step was carried out using conditions described in Table 2.3.1.1.

2.4.3 PVDF-f characterization

PVDF-f was characterized by NMR and FT-IR spectroscopies. 1H and spectra were taken on a 600 MHz spectrometer (VNMRS 600 MHz) in DMF-d7 as the solvent, while the FT-IR spectrum was registered on a Thermo-scientific Nicolet 6700 FTIR instrument. All spectra showed the presence of the aromatic styrene rings, thus confirming the functionalization.

2.4.4 CVD-Graphene synthesis

Graphene was synthetized by CVD method, using the operative conditions summarized in Figure 2. For this purpose, high purity reagents were used: ≥ 99.999 % purity argon, hydrogen and methane and 15 micron copper catalyst.

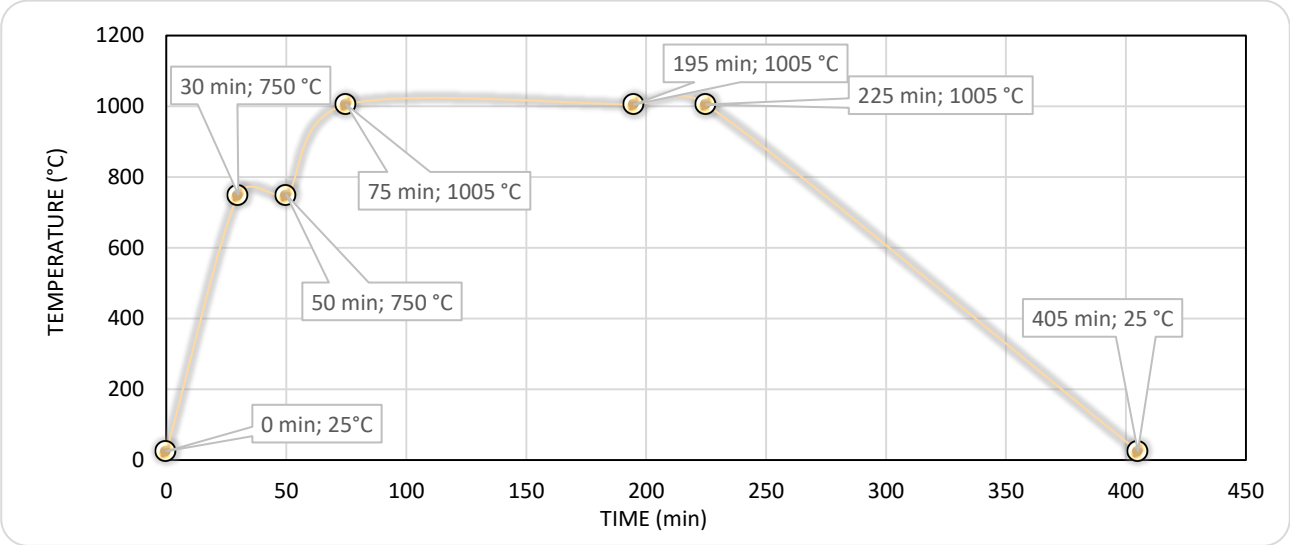

***Figure 2**: Synthetic conditions used for graphene synthesis by CVD method*

Phase 1: 30 min, Ar flux =500 sccm, P= 1.5 Torr, T to 750 °C

- *Phase 2: 20 min, H2 flux = 40 sccm, P = 1.5 Torr*
- *Phase 3: 25 min, H2 flux = 40 sccm, P = 1.5 Torr, T = from 750 to 1020 °C*
- *Phase 4: 120 min, H2 flux = 40 sccm, P = 1.5 Torr (Copper annealing phase)*
- *Phase 5: 30 min, H2 flux = 120 sccm, CH4 flux= 5 sccm P = 4.5 Torr (Graphene growth)*
- *Phase 6: 120-180 min, H2 flux = 40 sccm, P = 1.5 Torr, T = from 1020 to RT*

2.4.5 Graphene characterization by Optical Microscope

In order to evaluate graphene defects, the prepared samples were analyzed by optical microscopy.

Once the procedure is completed and graphene is still on the copper foil catalyst, the sample is removed from the machine and 1 cm^2 sample was gently placed on a heating plate at 120 °C for 20 min. This leads to oxidation of copper, which assumes a darker color in the areas not directly covered by the graphene layer owing to defects, whereas the color does not change for areas beneath graphene layer (not subjected to oxidation). Eventually. in order to evaluate presence of multilayer areas not visible unless copper removal occours, another 1 cm^2 sample was transferred on Si wafer using wet-transfer method: at first this sample was spin-coated with PMMAand placed on heating plate at 120 °C to ease adhesion between graphene and PMMA. Subsequently the catalyst was solubilized using the procedure involving iron nitrate and iron chloride

solutions below described. Now the PMMA-graphene sample is placed on SiO2 wafer and then on a heating plate again at 120 °C for 20 min in order to heat PMMA and ease wafer-graphene adhesion. The sample is now plunged into a solvent able to solubilize PMMA (we used acetone), air dried, before being observed using optical microscope

2.4.6 Membrane preparation

As it is known, usually pore forming agents are used to control pores size and their distribution as well. We noticed that preparing flat sheet membranes using Pristine PVDF without any additives addiction, these membranes exhibit low porosity degree and no water vapor flux on MD tests, whereas functionalization leads to the formation of microporous membrane without any of above-mentioned pore forming agents is employed.

2.4.6.1 Pristine PVDF and PVDF-f flat sheet membrane preparation

Flat-sheet membranes have been produced by NIPS (Nonsolvent Induced Phase Separation) technique. Dope solution was prepared using about 18% wt. polymer concentration in DMF. After stirring the solution for 12h at 60°C, the dope solution was cast on a glass support by using a casting machine (with a casting knife thickness of 220 µm) and immersed in DI water bath at a temperature of about 20°C.Once phase inversion process was completed, the membrane was first washed in ethanol bath and subsequently in the hexane bath to remove the last traces of the solvent and dried.

2.4.6.2 PVDF-f-GM fabrication

Laminating machine (Laminatoer K-Lami customized) have been used to ease adhesion between graphene and PVDF membranes (PVDF-f or Pristine PVDF) (step 1). Once process was completed, copper was still attached to graphene ad it was solubilized, using an iron chloride (III) and Iron nitrate (III) solutions as etchant (step 2). Then, the membrane was washed several times with water and air dried overnight (step 3). The laminating process steps are summarized in Figure 2.4.2.1.

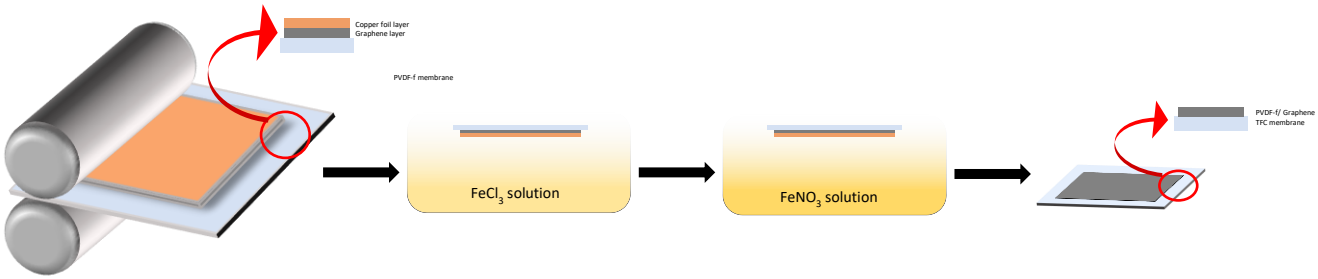

Step 1: adhesion enhancement by lamination process

Step 2: use of iron chloride and iron nitrate solution as etchant in order to solubilize copper catalyst

Step3: Final PVDF-f- GM after drying process is complete

Figure 2.4..2.1 :PVDF-f-GM preparation: At first PVDF-f and graphene adhesion is enhanced by laminating machine (**step 1**), followed by catalyst chemical etching with iron nitrate and iron chloride etchant solutions (**step 2**) in order to obtain final composite membrane (**step 3**)

2.4.7 Membrane Characterization

2.4.7.1 SEM analysis

Membrane morphology has been evaluated by SEM analysis using Nova Nano SEM instrument. Samples were preventively frozen with liquid nitrogen and cutted using a sharp small blade.

Cross-section and top surface of the produced membranes were analyzed.

2.4.7.2 XPS analysis

XPS analysis have been performed with particular attention on carbon, fluorine and oxygen atoms, in order to check the nature of bonds formed by these atoms, using a Thermo-scientific theta probe basic system.

2.4.7.3 Mechanical tests

In order to check the mechanical properties of the membranes, Young module, max strain and max stress have been evaluated using UTM- Shimadzu, AGS-J facility.

2.4.7.4 AFM Analysis

Surface roughness and morphology of membranes were estimated by mean of Atomic Force Microscope (AFM) analysis, using XE-100 machine.

2.4.8 LEP and wettability

Membrane wettability is one crucial aspects in Membrane Distillation (MD) process since it can affect its performances, in terms of rejection and thence in terms of long-term stability. In water desalination through MD processes, highly hydrophobic materials such as PTFE or PVDF and possessing high LEP are usually employed. LEP (liquid entry pressure) for a hydrophobic, dry membrane, is the pressure that must be applied so that the liquid penetrates through it. This is a fundamental parameter to consider in order to evaluate membrane efficiency, since it is comprehensive of several other factors such as hydrophobicity, geometry, pore size and distribution, surface free energy and nature of solution as well. As reported in literature, LEP can be calculated by the following equation:

LEP= (-4Bσ cosΘ)/r_max (1)

Where B is geometry-related factor (B=1 for cylindrical pores), σ is solution surface-tension, Θ is contact angle and r_max is the largest pore diameter.

2.4.9 Water flux through the membrane

Flux through membrane (J) is proportional to the vapor pressure difference between both side of membrane and can be expressed as:

$$J = C_m\,(P_{fm} - P_{pm}) \qquad (2)$$

Where P_{fm} and P_{pm} are vapor pressure in feed and permeate side respectively and C_m is membrane distillation coefficient, determined on predominant transport mechanism (mass transport or Knudsen diffusion)

2.4.10 DCMD experiments

Experiments were carried out using classical configuration of lab-scale DCMD facility already described in literature[47] Briefly, main part of system is made by two tanks (feed and permeate) which can be heated or

chilled selectively. One membrane-containing Teflon cell in which crossflow velocities can ben regulated separately for feed and permeate side, represent functional part of entire machine.
Flux across membrane is function of difference of water vapor pressure between feed and permeate side, the membrane surface (area) and can be easily estimated using weight increase of permeate solution in the time. Salt rejection has been calculated using following equation:

$R_S = (1- C_f/C_p)*100$ *(3)*

Where Cf and Cp represent salt concentrations in feed and permeate side respectively.

Flux has been calculated using the equation below:

$$F = \frac{m}{\rho_w S\,t} \quad (4)$$

where m is the difference of permeate weight in the time, ρw is the water density and S is the membrane surface area.

2.5 Chapter Conclusions

The large diffusion of nanomaterials in last years brought a lot of exploitable benefits and many possibility. In membrane science NMs use is still subjected to their production cost that can sometimes limitate their use. On the other hand, their association with polymeric materials is usually done by dispersion of NMs in polymer matrix before membrane fabrication. In this chapter a novel approach to use graphene layer as coating for a specific desalination process has been realized. The synthesis of NMs is simple and done by CVD method and its interaction with polymer is maximized by previous polymer modification with suitable molecules bearing aromatic rings. Results showed that in the case of pristine PVDF the membrane pore size is to small for a working membrane in this kind of process. PVDF-f membranes, on the other hand, work well in terms of flux and rejection either. Graphene coating application, has different effects instead: it causes a flux reduction probably because it acts as barrier; beside that it enhances the salt rejection which rises up to 99.99% and confers good mechanical properties to the membrane, which also exhibits longer lasting during the tests.

Chapter 2 references

1. Pendergast, M. M.; Hoek, E. M. V., A review of water treatment membrane nanotechnologies. *Energy & Environmental Science* **2011,** *4* (6), 1946.
2. Jayashree Dhote, S. I. a. A. C., REVIEW ON WASTEWATER TREATMENT TECHNOLOGIES. *International Journal of Engineering Research & Technology (IJERT)* **2012,** *1* (5).
3. Deowan, S. A.; Galiano, F.; Hoinkis, J.; Johnson, D.; Altinkaya, S. A.; Gabriele, B.; Hilal, N.; Drioli, E.; Figoli, A., Novel low-fouling membrane bioreactor (MBR) for industrial wastewater treatment. *Journal of Membrane Science* **2016,** *510*, 524-532.
4. Galiano, F.; Friha, I.; Deowan, S. A.; Hoinkis, J.; Xiaoyun, Y.; Johnson, D.; Mancuso, R.; Hilal, N.; Gabriele, B.; Sayadi, S.; Figoli, A., Novel low-fouling membranes from lab to pilot application in textile wastewater treatment. *J Colloid Interface Sci* **2018,** *515*, 208-220.
5. Quintana, J. B.; Weiss, S.; Reemtsma, T., Pathways and metabolites of microbial degradation of selected acidic pharmaceutical and their occurrence in municipal wastewater treated by a membrane bioreactor. *Water Res* **2005,** *39* (12), 2654-64.
6. Mehdizadeh, H., Membrane desalination plants from an energy–exergy viewpoint. *Desalination* **2006,** *191* (1-3), 200-209.
7. Ali, A.; Tufa, R. A.; Macedonio, F.; Curcio, E.; Drioli, E., Membrane technology in renewable-energy-driven desalination. *Renewable and Sustainable Energy Reviews* **2018,** *81*, 1-21.
8. Abdullah, N.; Rahman, M. A.; Dzarfan Othman, M. H.; Jaafar, J.; Ismail, A. F., Membranes and Membrane Processes. **2018**, 45-70.
9. Macedonio, F.; Drioli, E., Pressure-driven membrane operations and membrane distillation technology integration for water purification. *Desalination* **2008,** *223* (1-3), 396-409.
10. Daufin, G.; Escudier, J. P.; Carrère, H.; Bérot, S.; Fillaudeau, L.; Decloux, M., Recent and Emerging Applications of Membrane Processes in the Food and Dairy Industry. *Food and Bioproducts Processing* **2001,** *79* (2), 89-102.
11. Mohammed Rasool wtaishat, F. B., Desalination by solar powered membrane distillation systems. *Desalination* **2013,** *308*, 186-197.
12. Pandey, P. K.; Upadhyay, R., Desalination of Brackish Water using Solar Energy. *Int J Renew Energy R* **2016,** *6* (2), 350-354.
13. Goh, P. S.; Ismail, A. F.; Hilal, N., Nano-enabled membranes technology: Sustainable and revolutionary solutions for membrane desalination? *Desalination* **2016,** *380*, 100-104.
14. Su, X.; Li, W.; Palazzolo, A.; Ahmed, S., Concentration polarization and permeate flux variation in a vibration enhanced reverse osmosis membrane module. *Desalination* **2018,** *433*, 75-88.
15. Shenvi, S. S.; Isloor, A. M.; Ismail, A. F., A review on RO membrane technology: Developments and challenges. *Desalination* **2015,** *368*, 10-26.
16. Jang, E.-S.; Mickols, W.; Sujanani, R.; Helenic, A.; Dilenschneider, T. J.; Kamcev, J.; Paul, D. R.; Freeman, B. D., Influence of Concentration Polarization and Thermodynamic Non-ideality on Salt Transport in Reverse Osmosis Membranes. *Journal of Membrane Science* **2018**.
17. Janajreh, I.; Hashaikeh, R.; Hussain, M. N., Evaluation of Thermal Efficiency of Membrane Distillation under Conductive Layer Integration. *Energy Procedia* **2017,** *105*, 4935-4942.
18. Curcio, E.; Drioli, E., Membrane Distillation and Related Operations—A Review. *Separation & Purification Reviews* **2005,** *34* (1), 35-86.
19. Deshmukh, A.; Boo, C.; Karanikola, V.; Lin, S.; Straub, A. P.; Tong, T.; Warsinger, D. M.; Elimelech, M., Membrane distillation at the water-energy nexus: limits, opportunities, and challenges. *Energy & Environmental Science* **2018,** *11* (5), 1177-1196.
20. Gonzalez, D.; Amigo, J.; Suarez, F., Membrane distillation: Perspectives for sustainable and improved desalination. *Renew. Sust. Energ. Rev.* **2017,** *80*, 238-259.
21. Alobaidani, S.; Curcio, E.; Macedonio, F.; Diprofio, G.; Alhinai, H.; Drioli, E., Potential of membrane distillation in seawater desalination: Thermal efficiency, sensitivity study and cost estimation. *Journal of Membrane Science* **2008,** *323* (1), 85-98.
22. Pangarkar, B. L.; Sane, M. G.; Guddad, M., Reverse Osmosis and Membrane Distillation for Desalination of Groundwater: A Review. *ISRN Materials Science* **2011,** *2011*, 1-9.

23. Deshmukh, A.; Elimelech, M., Understanding the impact of membrane properties and transport phenomena on the energetic performance of membrane distillation desalination. *Journal of Membrane Science* **2017,** *539*, 458-474.
24. Criscuoli, A.; Carnevale, M. C., Desalination by vacuum membrane distillation: The role of cleaning on the permeate conductivity. *Desalination* **2015,** *365*, 213-219.
25. Figoli, A.; Ursino, C.; Galiano, F.; Di Nicolò, E.; Campanelli, P.; Carnevale, M. C.; Criscuoli, A., Innovative hydrophobic coating of perfluoropolyether (PFPE) on commercial hydrophilic membranes for DCMD application. *Journal of Membrane Science* **2017,** *522*, 192-201.
26. Li, L.; Hou, J. W.; Ye, Y.; Mansouri, J.; Chen, V., Composite PVA/PVDF pervaporation membrane for concentrated brine desalination: Salt rejection, membrane fouling and defect control. *Desalination* **2017,** *422*, 49-58.
27. Razmjou, A.; Arifin, E.; Dong, G.; Mansouri, J.; Chen, V., Superhydrophobic modification of TiO2 nanocomposite PVDF membranes for applications in membrane distillation. *Journal of Membrane Science* **2012,** *415-416*, 850-863.
28. Dong, Z.-Q.; Ma, X.-h.; Xu, Z.-L.; You, W.-T.; Li, F.-b., Superhydrophobic PVDF–PTFE electrospun nanofibrous membranes for desalination by vacuum membrane distillation. *Desalination* **2014,** *347*, 175-183.
29. Hou, D.; Lin, D.; Ding, C.; Wang, D.; Wang, J., Fabrication and characterization of electrospun superhydrophobic PVDF-HFP/SiNPs hybrid membrane for membrane distillation. *Separation and Purification Technology* **2017,** *189*, 82-89.
30. Leaper, S.; Abdel-Karim, A.; Faki, B.; Luque-Alled, J. M.; Alberto, M.; Vijayaraghavan, A.; Holmes, S. M.; Szekely, G.; Badawy, M. I.; Shokri, N.; Gorgojo, P., Flux-enhanced PVDF mixed matrix membranes incorporating APTS-functionalized graphene oxide for membrane distillation. *Journal of Membrane Science* **2018,** *554*, 309-323.
31. Jafari, A.; Kebria, M. R. S.; Rahimpour, A.; Bakeri, G., Graphene quantum dots modified polyvinylidenefluride (PVDF) nanofibrous membranes with enhanced performance for air Gap membrane distillation. *Chemical Engineering and Processing - Process Intensification* **2018,** *126*, 222-231.
32. Intrchom, W.; Roy, S.; Humoud, M. S.; Mitra, S., Immobilization of Graphene Oxide on the Permeate Side of a Membrane Distillation Membrane to Enhance Flux. *Membranes (Basel)* **2018,** *8* (3).
33. Ko, C.-C.; Ali, A.; Drioli, E.; Tung, K.-L.; Chen, C.-H.; Chen, Y.-R.; Macedonio, F., Performance of ceramic membrane in vacuum membrane distillation and in vacuum membrane crystallization. *Desalination* **2018,** *440*, 48-58.
34. Yang, F.; Efome, J. E.; Rana, D.; Matsuura, T.; Lan, C., Metal-Organic Frameworks Supported on Nanofiber for Desalination by Direct Contact Membrane Distillation. *ACS Appl Mater Interfaces* **2018,** *10* (13), 11251-11260.
35. Novoselov, K. S.; Fal'ko, V. I.; Colombo, L.; Gellert, P. R.; Schwab, M. G.; Kim, K., A roadmap for graphene. *Nature* **2012,** *490* (7419), 192-200.
36. Geim, A. K., Graphene: Status and Prospects. *Science* **2009,** *80* (324), 1530-1534.
37. Humplik, T.; Lee, J.; O'Hern, S. C.; Fellman, B. A.; Baig, M. A.; Hassan, S. F.; Atieh, M. A.; Rahman, F.; Laoui, T.; Karnik, R.; Wang, E. N., Nanostructured materials for water desalination. *Nanotechnology* **2011,** *22* (29), 292001.
38. K. Sint, B. W., P. Král, Selective Ion Passage through Functionalized Graphene. *Journal of American Chemical Society* **2008,** *130*, 16448-16449.
39. Li, Z.; Wang, Y.; Kozbial, A.; Shenoy, G.; Zhou, F.; McGinley, R.; Ireland, P.; Morganstein, B.; Kunkel, A.; Surwade, S. P.; Li, L.; Liu, H., Effect of airborne contaminants on the wettability of supported graphene and graphite. *Nat Mater* **2013,** *12* (10), 925-31.
40. Hong, G.; Han, Y.; Schutzius, T. M.; Wang, Y.; Pan, Y.; Hu, M.; Jie, J.; Sharma, C. S.; Muller, U.; Poulikakos, D., On the Mechanism of Hydrophilicity of Graphene. *Nano Lett* **2016,** *16* (7), 4447-53.
41. Taherian, F.; Marcon, V.; van der Vegt, N. F.; Leroy, F., What is the contact angle of water on graphene? *Langmuir* **2013,** *29* (5), 1457-65.
42. Deyin Hou, H. F., Qinliang Jiang , Jun Wanga, Xiaohui Zhang, Preparation and characterization of PVDF flat-sheet membranes for direct contact membrane distillation. *Separation & Purification Technology* **2014,** *135*, 211-222.
43. J. Phattaranawik , R. J., A.G. Fane Effect of pore size distribution and air flux on mass transport in direct contact membrane distillation. *Journal of Membrane Science* **2003,** *215*, 75-85.

44. Chunsheng Feng, B. S., Guomin Li, Yonglie Wu, Preliminary research on microporous membrane from F2.4 for membrane distillation. *Separation & Purification Technology* **2004,** *39*, 221-228.
45. Yonglie Wu, Y. K., Xiao Lin, Weihong Liu and Jiping Xu, Surface-modified hydrophilic membranes in membrane distillation. *Journal of Membrane Science* **1992,** *72*, 189-196.
46. Zahirifar, J.; Karimi-Sabet, J.; Moosavian, S. M. A.; Hadi, A.; Khadiv-Parsi, P., Fabrication of a novel octadecylamine functionalized graphene oxide/PVDF dual-layer flat sheet membrane for desalination via air gap membrane distillation. *Desalination* **2018,** *428*, 227-239.
47. Liu, J.; Shen, X.; Zhao, Y.; Chen, L., Acryloylmorpholine-Grafted PVDF Membrane with Improved Protein Fouling Resistance. *Industrial & Engineering Chemistry Research* **2013,** *52* (51), 18392-18400.

Chapter 3

Synthesis of polymerizable Acryloyloxyalkyltriethylammonium salts surfactants and their antibacterial activity

Chapter based on the article titled: " Synthesis and Antibacterial Activity of Polymerizable Acrylkoyloxyalkiltriethyl Ammonium Salts"

*(Raffaella Mancuso, Roberta Amuso, Biagio Armentano, Giuseppe Grasso, Vittoria Rago, Anna Rita Cappello, Francesco Galiano, Alberto Figoli, Giorgio De Luca, Jan Hoinkis and Bartolo Gabriele, ChemPlusChem **2017**)*

3.1 Chapter Summary

Herein, we report a novel and efficient synthetic scheme for the synthesis of polymerizable quaternary ammonium salts (PQASs), an important class of surfactants owing great antibacterial properties. PQASs and more precisely "Acryloyloxyalkyltriethylammonium bromides" (AATEABs) may be used as coating for membranes (commercial or not) used in wastewater treatment, when antibiofouling and antibacterial properties are required. Synthetic strategy we advance, involves a series of two-steps reaction which starts from commercially and easily available substrate and which is totally realized under air, avoiding inert conditions such as nitrogen atmosphere and purification by column. Biological tests performed on Gram+\- and yeast strains, revealed that antibacterial activity is higher in AATEABs bearing alkyl chain of 11 and 12 atoms.

3.2 Introduction

QAAs are a particular class of salts which are well known to own remarkable antimicrobial activity, that have extensively used for long time as disinfectant and antiseptics[1-2]. In particular, they have been used as additive in textile industries for several productions or as polymerizable co-monomers able to prevent textile washing-away[3-6]. In consideration of QAS antibacterial activity, several studies have been done in order to develop polymeric materials starting from quaternary ammonium salts or finalized to their post-functionalization[7-

[15].In this contest, the work herein reported is of particular relevance in the framework of membrane with antifouling feature development, already reported in literature[16], in which commercial polyethersulfone (PES) membranes were functionalized by coating with antimicrobial film, which properties make the membrane able to prevent growth of microorganism and hence increase membrane lifetime; on that purpose a particular PQAS, acryloyloxyalkyltriethylammonium bromide (AUTEAB), has been used as co-monomer in an in-situ radical polymerization of PBM (Polymerizable Bicontinuous Microemulsion) containing AUTEAB as co monomer. Tests performed on membrane bioreactors (MBR) confirmed its activity and promotion as possible candidate for large scale operation. In this chapter, a novel and efficient strategy for synthesis of acryloyloxyalkyltriethylammonium bromide salts (AATEABs) with 6, 9, 11 and 12 carbon alkyl chain is reported discussed: AATEABs synthetic strategy has been optimized and conducted under air, avoiding inert atmosphere and purification of crude product. Our strategy results thus particularly appropriate and suitable for any scale-up process and industrial application. In order to evaluate AATEABs antimicrobial activity, several test have been conducted on Gram+\- bacterias and yeast strains.

3.3 Results and discussion

Basically, our synthetic strategy for the synthesis of AATEABs is based on two step reaction which consists in an esterification of readily available ω-bromoalkanol with acryloyl chloride in presence of molecular sieves, followed by quaternization step with triethylamine. The whole synthetic process is summarized in Scheme 3.3.1.

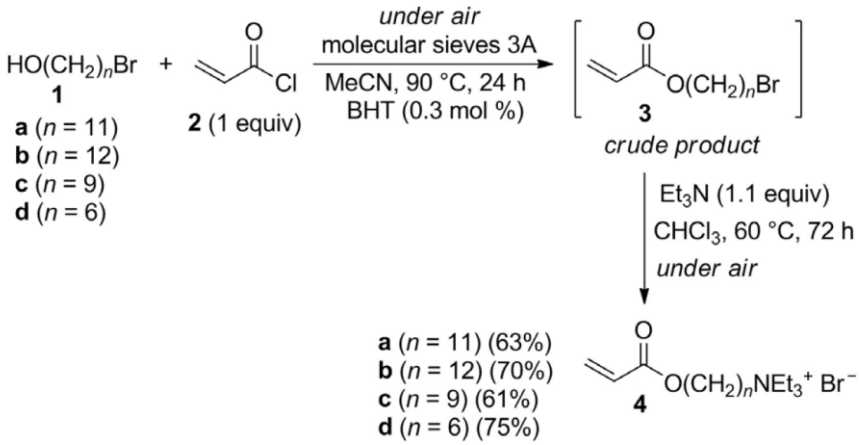

***Scheme 3.3.1**: Acryloyloxyalkyltriethylammonium bromides (AATEABs, **4a-d**) synthetic scheme, starting from bromoalkanols **1a-d**, easily available on the market.*

*Initially, the work has been focused on the optimization of both esterification and quaternization step in order to avoid the use of prohibitive and costly conditions such as inert atmosphere, time and use of expensive chemicals for the purification of crude product **3**. The final optimized conditions which lead to the synthesis of crude product **3**, expect the use of CH_3CN as solvent, 1:1 molar ratio of Acryloyl chloride **2** with respect to bromoalkanol **1**, using a small amount of BHT (dibuthylhydroxytoluene) as radical scavenger, in the presence of 3Å molecular sieves powder at 90 °C for 24 hours. The intermediate **3** obtained from first step, was used without purification by chromatographic or any other methods for the next step which consists in quaternization by reaction of **3** with triethylamine, using a 1.1:1 molar ratio with respect bromoalkanol **1**, using $CHCl_3$ at 60 °C for 72 hours. The product **4a-d**, were obtained with a good purity >96% by ^1H NMR analysis and high yield over two steps (61-75% basing on bromoalkanols **1a-d**), by precipitation and washing operationusing diethyl ether. In order to extend the procedure to other AATEABs analogues with shorter alkyl chain, we tried to extend the procedure to the synthesis of **4e-f**, as summarized in Scheme 3.3.2.*

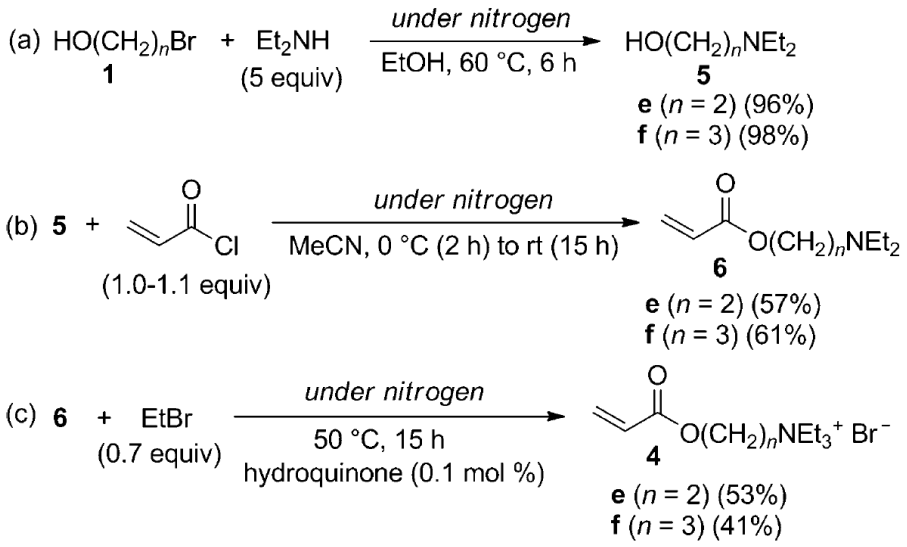

***Scheme 3.3.2**: Generalization procedure for the synthesis of AATEABs analogues **4e-f**, starting from 2-bromoethanol **1e** and 2-bromopropanol **1f**.*

*However, the synthetic strategy for **4e-f** required a change of synthetic strategy since they cannot be obtained with high yield and satisfactory purity using the same condition used in the case of **4a-d**. To prepare the**4e-f** derivates, we adopted the strategy summarized in Scheme 3.3.2 which involves three steps reaction: reaction of bromoethanol **1e** or bromopropanol **1f** with high excess of diethylamine to give 2-(dimethylamino)ethanol and 3-(diethylamino)propanol **5e** and **5f** respectively, followed by their esterification with acryloylchloride **2** to give 2-(diethylamino)ethylacrylate **6e** and 3-(diethylamino)propylacrylate **6f**; quaternization of **6e-f** with low molar amount of Ethylbromide to afford **4e-f** represents the final step. In this case the low molar amount of EtBr is important because it eases purification process. The evaluation of antimicrobial activity of AATEABs*

4a-f *has been done by tests against two Gram positive strains (Staphylococcus aureus and Streptococcus pyogenes), three Gram negative strains (Escherichia coli, Klebisiella pneumoniae and Pseudomonas aeruginosa) and two yeast strains (Saccharomyces cervisae and Candida albicans). Among all AATEABs tested,* ***4a,b*** *(C_{11} and C_{12} alkyl chain respectively) exhibited the highest activity against Gram positive bacteria and yeast strains, with a* ***4b/4a*** *activity ratio of 4/1 (inhibition resulted to be 40-50% at 128 µg ml^{-1} in the case of* ***4a*** *and 50-60% at 32 µg ml^{-1} in the case of* ***4b****), whereas activity against Gram negative strains resulted to be significantly reduced (30-40% at 512 µg ml^{-1} for* ***4a*** *and 40-50% at 256 µg ml^{-1} for* ***4b****). Besides,* ***4d*** *(C_6 alkyl chain) exhibited activity only against Gram positive strains, resulting therefore inactive against Saccharmomyces Cervisae and Candida albicans, despite the use of high concentration. Contrariwise, product* ***4c*** *(C_9 alkyl chain) exhibited remarkable activity agains Candida albicans, a type of yeast strain (40% at 128 µg ml^{-1}) without exhibiting any activity against Gram positive or negative. AATEABs with shorter alkyl chain* ***4e-f*** *(C_2 and C_3 respectively) resulted to be totally inactive against any bacterial or yeast strains. Comparison term for AATEABs activity, is the use of non-polymerizable quaternary ammonium salt: DTAB (Dodecyltrimethylammonium bromide) with Kirby-Bauer method[17].Briefly, Bacteria or yeast strain on which AATEABs were tested, can be grouped into three main categories, based on size of diffusion zones diameter: Resistant, intermediate and sensitive. DTAB activity resulted to be comparable to AATEABs* ***4a,b*** *(C_{11} and C_{12} respectively): against Gram positive strains, But it is higher in the case of Gram negative strains. Different speech must be done concerning the activity against yeast strains: in general, DTAB and* ***4b*** *(C_{12} chain) have comparable activity, while* ***4a*** *resulted to be less active than* ***4b*** *and DTAB.*

3.4 AATEABs Characterization

Characterization of AATEABs was accomplished by NMR, Mass spectroscopy, Melting point and IR analysis

3.4.1 ^{1}H and ^{13}C NMR analysis

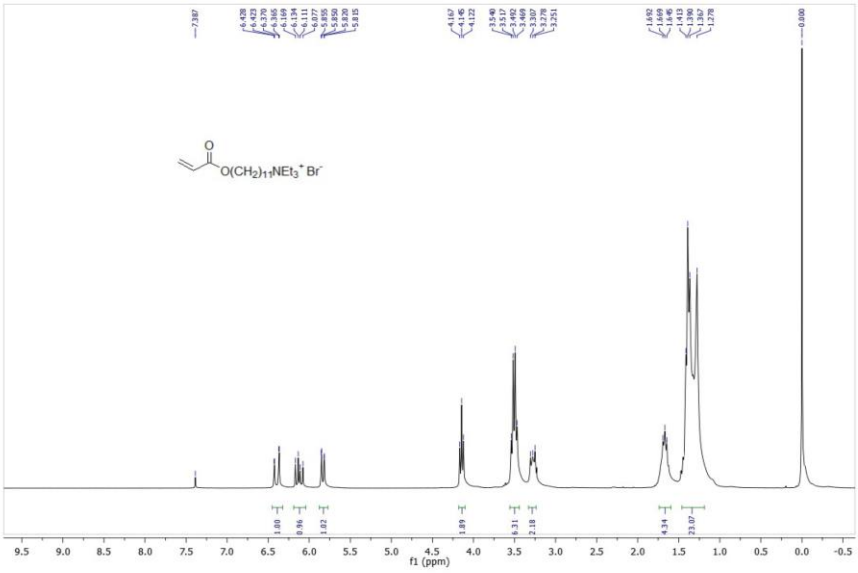

Figure 3.4.1.1*^{1}H NMR Spectra for Acryloyloxyundecyltriethylammonium bromide (**4a**):(300 MHz, CDCl3): δ = 6.39 [distorted dd, J = 17.3, 1.5, 1 H, OC(O)CH=CHH], 6.12 (distorted dd, J = 17.3, 10.3, 1 H, OC(O)CH=CHH), 5.84 [distorted dd, J = 10.4, 1.6, 1 H, OC(O)CH=CHH], 4.14 [t, J = 6.7, 2 H, C(O)OCH2], 3.51 [q, J = 7.1, 6 H, 3 N(CH2CH3)3], 3.34-3.22 [m, 2 H, NCH2(CH2)10O], 1.79-1.59 [m, 4 H, NCH2CH2(CH2)7CH2CH2O], 1.48-1.15 [m, 23 H, 14 H of NCH2CH2(CH2)7CH2CH2O + 9 H of N(CH2CH3)3]; 13C NMR (75 MHz, CDCl3): δ = 166.4, 130.5, 128.7, 64.7, 57.5, 53.5, 29.37, 29.34, 29.32, 29.15, 29.13, 28.6, 26.5, 25.9, 22.1, 8.1*

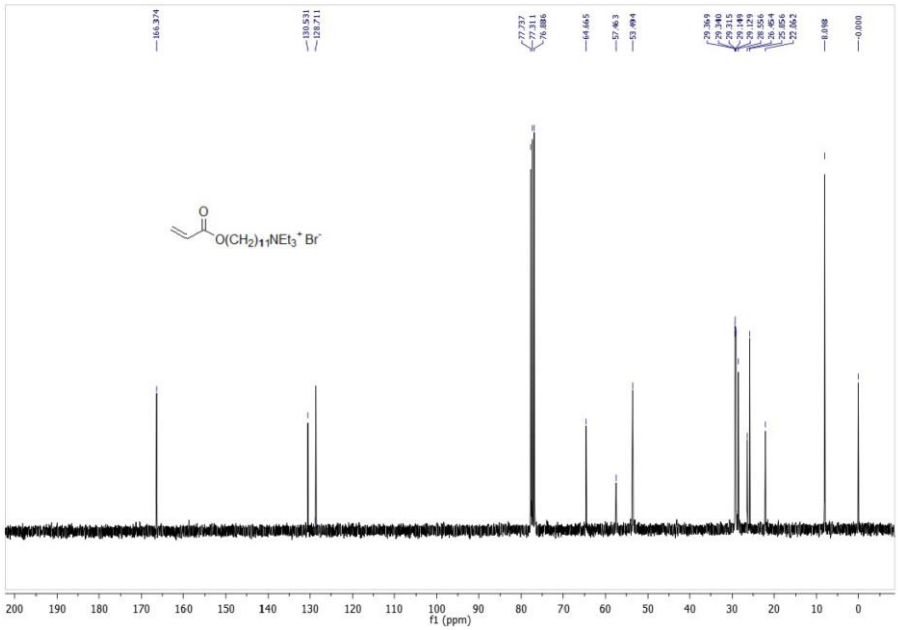

Figure 3.4.1.2*^{13}C NMR Spectra for Acryloyloxyundecyltriethylammonium bromide (**4a**): (75 MHz, CDCl3): δ = 166.4, 130.5, 128.7, 64.7, 57.5, 53.5, 29.37, 29.34, 29.32, 29.15, 29.13, 28.6, 26.5, 25.9, 22.1, 8.1*

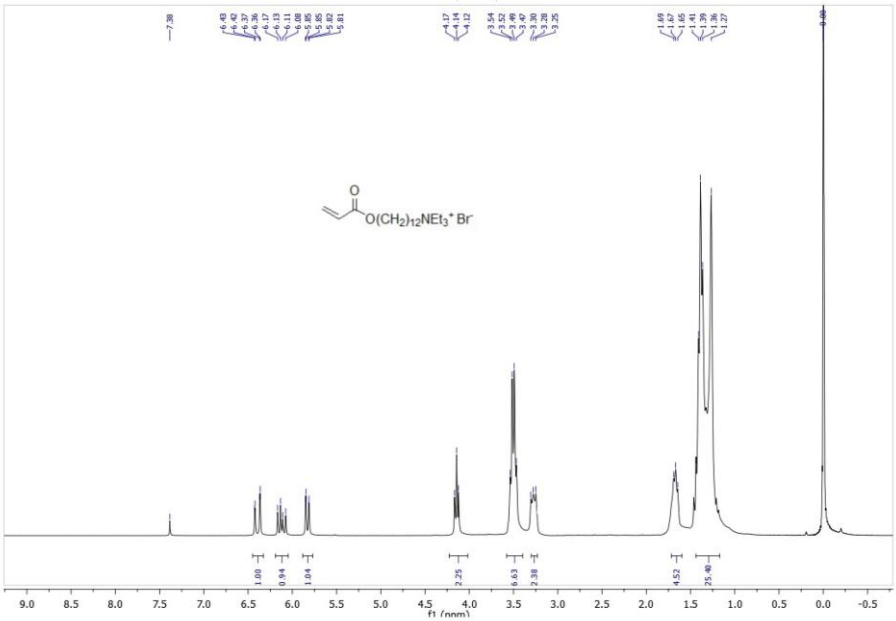

Figure 3.4.1.3 *^{1}H NMR Spectra for Acryloyloxydodecyltriethylammonium bromide (**4b**): (300 MHz, CDCl3): δ = 6.39 [distorted dd, J = 17.3, 1.5, 1 H, OC(O)CH=CHH], 6.12 [distorted dd, J = 7.4, 10.4, 1 H, OC(O)CH=CHH], 5.83 [distorted dd, J = 10.4, 1.6, 1 H, OC(O)CH=CHH], 4.14 [t, J = 6.8, 2 H, C(O)OCH2], 3.50 [q, J = 6.9, 6 H, 3 N(CH2CH3)3], 3.34-3.22 [m, 2 H, NCH2(CH2)11O], 1.77-1.60 [m, 4 H, NCH2CH2(CH2)8CH2CH2O], 1.48-1.15 [m, 25 H, 16 H of NCH2CH2(CH2)8CH2CH2O + 9 H of N(CH2CH3)3]*

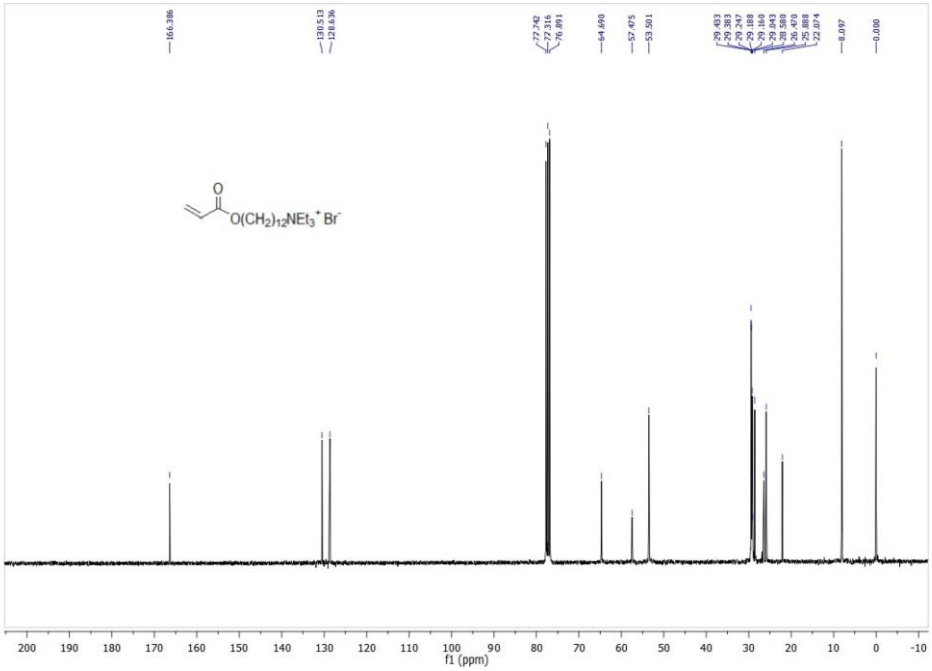

Figure 3.4.1.4 *^{13}C NMR Spectra for Acryloyloxydodecyltriethylammonium bromide (**4b**): (75 MHz, CDCl3): δ =166.4, 130.5, 128.6, 64.7, 57.5, 53.5, 29.43, 29.38, 29.25, 29.19,29.16, 29.04, 28.6, 26.5, 25.9, 22.1, 8.1*

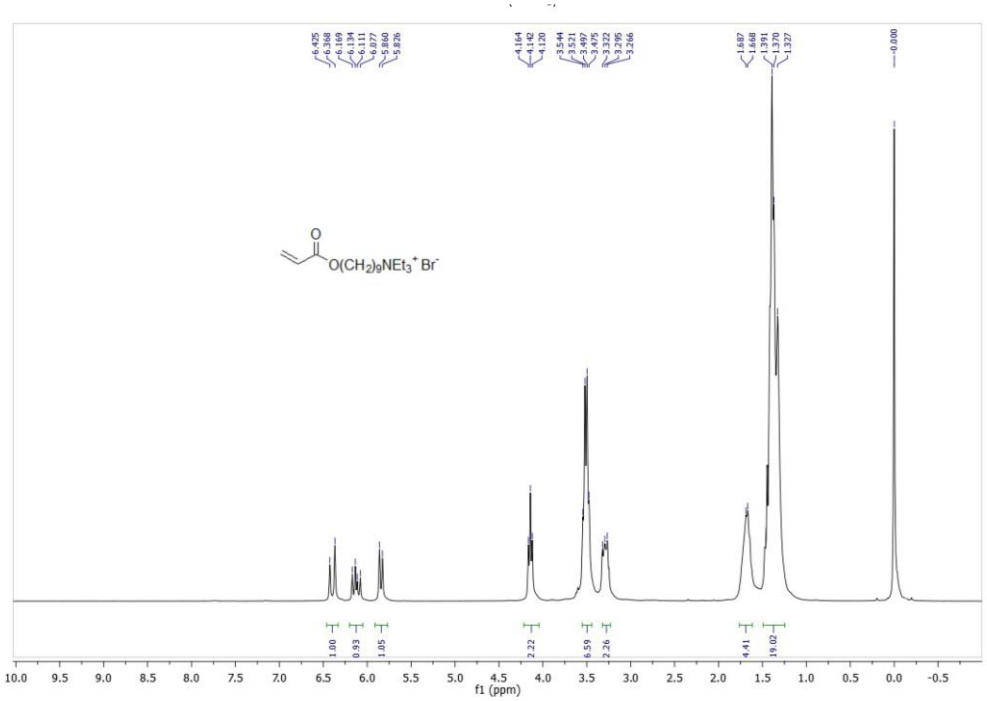

Figure 3.4.1.5 *[1]H NMR Spectra for Acryloyloxynonyltriethylammonium bromide (**4c**): (300 MHz, CDCl3): δ = 6.39 [distorted dd, J = 17.3, 1.5, 1 H, OC(O)CH=CHH], 6.12 (distorted dd, J = 17.3, 10.3, 1 H, OC(O)CH=CHH], 5.84 [distorted dd, J = 10.4, 2.0, 1 H, OC(O)CH=CHH], 4.14 [t, J = 6.7, 2 H, C(O)OCH2], 3.50 [q, J =7.3, 6 H, 3 N(CH2CH3)3], 3.34-3.24 [m, 2 H, NCH2(CH2)8O], 1.78-1.60 [m, 4 H, NCH2CH2(CH2)5CH2CH2O], 1.49-1.24 [m, 19 H, 10 H of NCH2CH2(CH2)5CH2CH2O + 9 H of N(CH2CH3)3]*

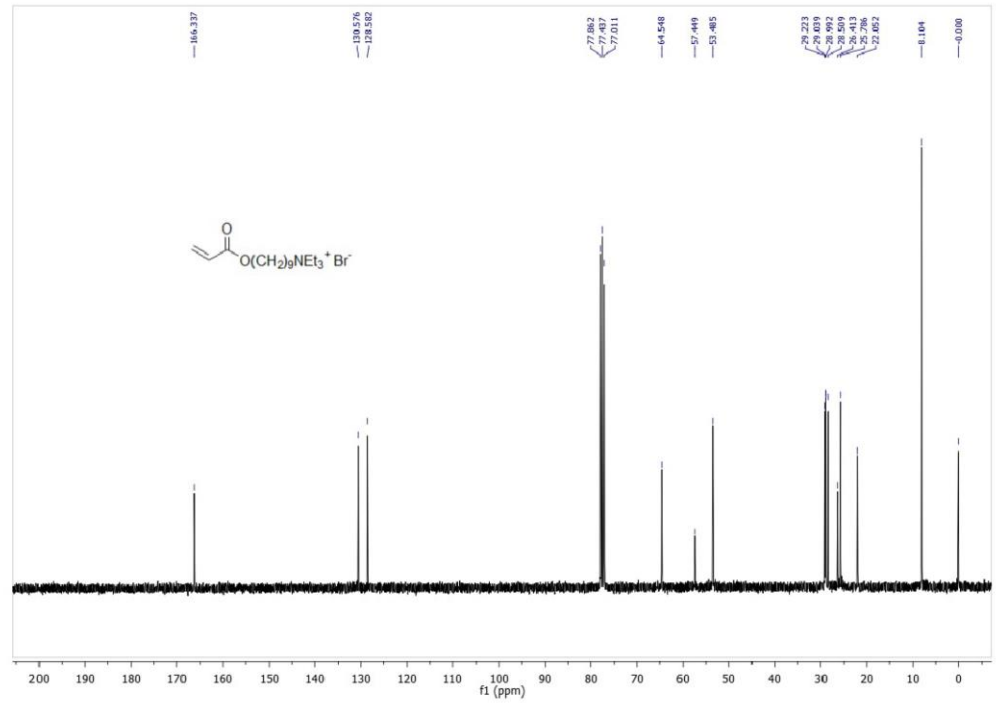

Figure 3.4.1.6 *[13]C NMR Spectra for Acryloyloxynonyltriethylammonium bromide (**4c**): (75 MHz, CDCl3): δ =166.3, 130.6, 128.6, 64.6, 57.4, 53.5, 29.2, 29.0, 28.99, 28,5, 26.4, 25.8, 22.0, 8.1*

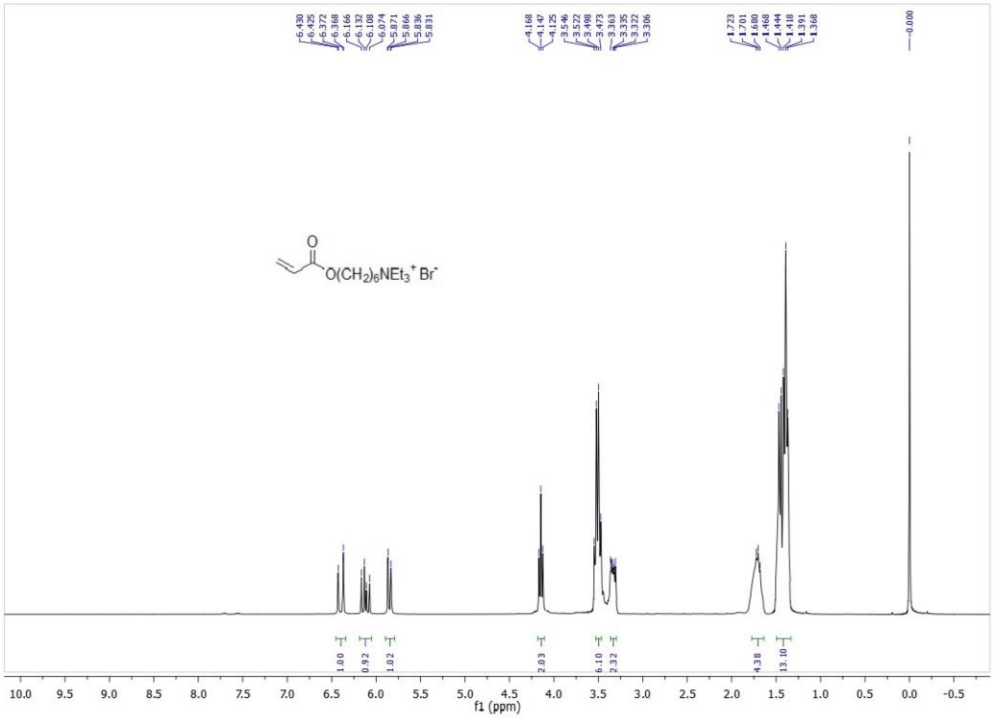

Figure 3.4.1.7 *^{1}H NMR Spectra for Acryloyloxyhexyltriethylammonium bromide (**4d**): (300 MHz, CDCl3) δ = 6.40 [distorted dd, J = 17.3, 1.5, 1 H, OC(O)CH=CHH], 6.12 (distorted dd, J = 17.3, 10.3, 1 H, OC(O)CH=CHH], 5.85 [distorted dd, J = 10.4, 1.4, 1 H, OC(O)CH=CHH], 4.15 [t, J = 6.5, 2 H, C(O)OCH2], 3.51 [q, J = 7.3, 6 H, 3 N(CH2CH3)3], 3.40-3.28 [m, 2 H, NCH2(CH2)5O], 1.83-1.64 [m, 4 H, NCH2CH2(CH2)2CH2CH2O], 1.54-1.31 [m, 13 H, 4 H of NCH2CH2(CH2)2CH2CH2O + 9 H of N(CH2CH3)3]*

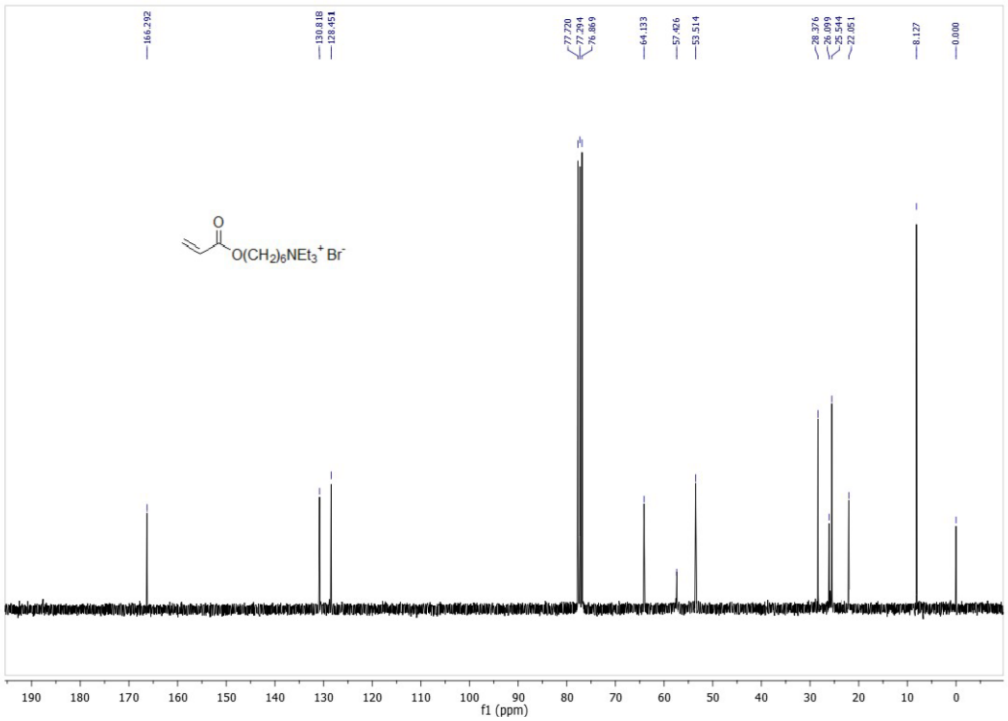

Figure 3.4.1.8 *^{13}C NMR Spectra for Acryloyloxyhexyltriethylammonium bromide (**4d**): (75 MHz, CDCl3): δ = 166.3, 130.8, 128.4, 64.1, 57.4, 53.5, 28.4, 26.1, 25.5, 22.0, 8.1*

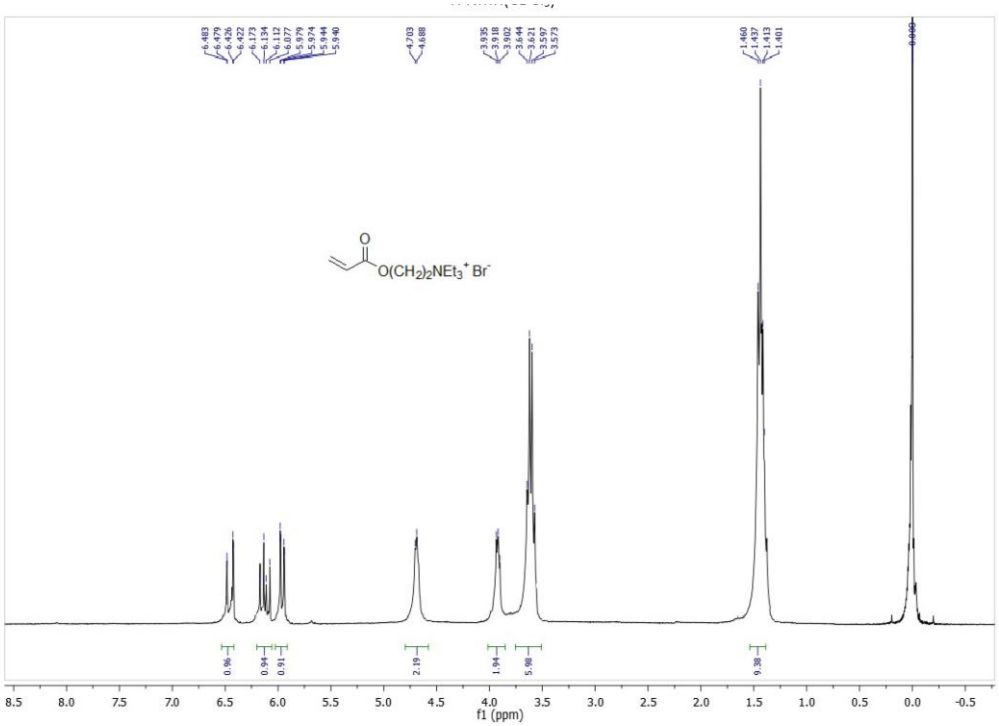

Figure 3.4.1.9 *^{1}H NMR Spectra for Acryloyloxyethyltriethylammonium bromide (**4e**) (300 MHz, CDCl3): δ = 6.46 [distorted dd, J = 17.2, 1.2, 1 H, OC(O)CH=CHH], 6.12 [distorted dd, J = 17.2, 10.4, 1 H, OC(O)CH=CHH], 5.96 [distorted dd, J = 10.4, 1.2, 1 H, OC(O)CH=CHH], 4.80-4.59 (m, 2 H, C(O)OCH2), 4.01-3.86 (m, 2 H, NCH2), 3.76-3.48 [m, 6 H, 3 NCH2], 1.60-1.31 [m, 9 H, N(CH2CH3)2];*

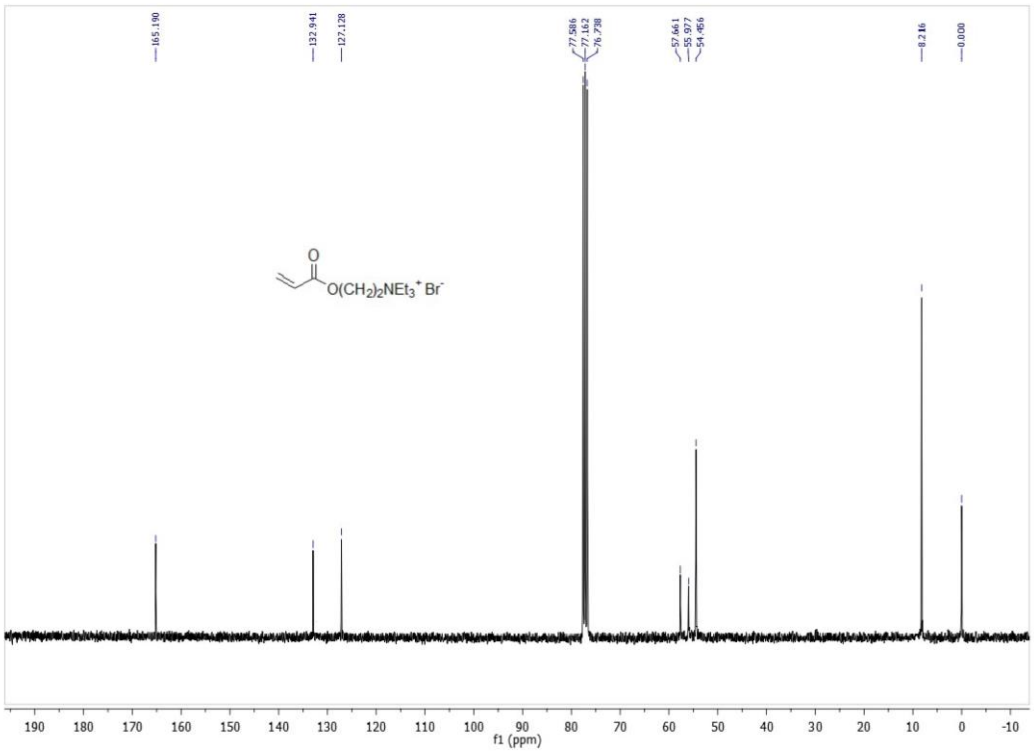

Figure 3.4.1.10 *^{13}C NMR Spectra for Acryloyloxyethyltriethylammonium bromide (**4e**) (75 MHz, CDCl3): δ =165.2, 132.9, 127.1, 57.7, 56.0, 54.5, 8.2*

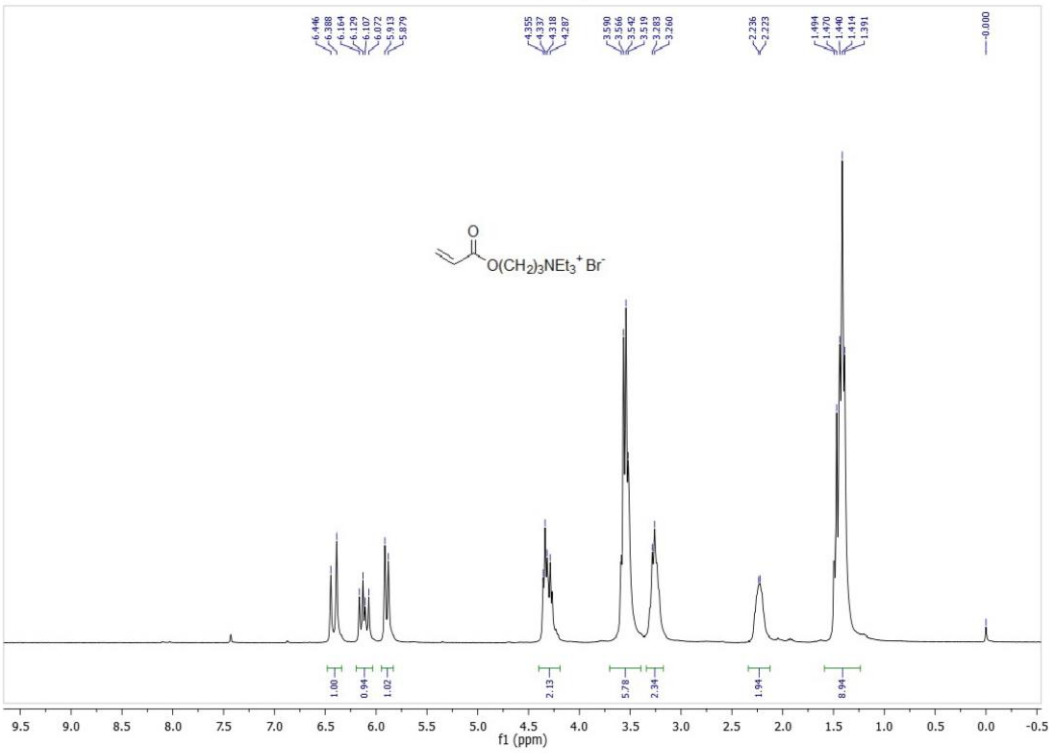

Figure 3.4.1.11 *^{1}H NMR Spectra for Acryloyloxypropyltriethylammonium bromide (**4f**) (300 MHz, CDCl3): δ = 6.25 [d dist, J = 17.1, 1 H, OC(O)CH=CHH], 5.95 [distorted dd, J = 17.1, 10.4, 1 H, OC(O)CH=CHH], 5.73 [distorted d, J = 10.4, 1 H, OC(O)CH=CHH], 4.26-4.02 (m, 2 H, C(O)OCH2), 3.52-3.23 [m, 6 H, 3 NCH2], 3.20-2.96 (m, 2 H, NCH2), 2.24-1.95 (m, 2 H, C(O)OCH2CH2CH2N), 1.42-1.09 [m, 9 H, N(CH2CH3)3]*

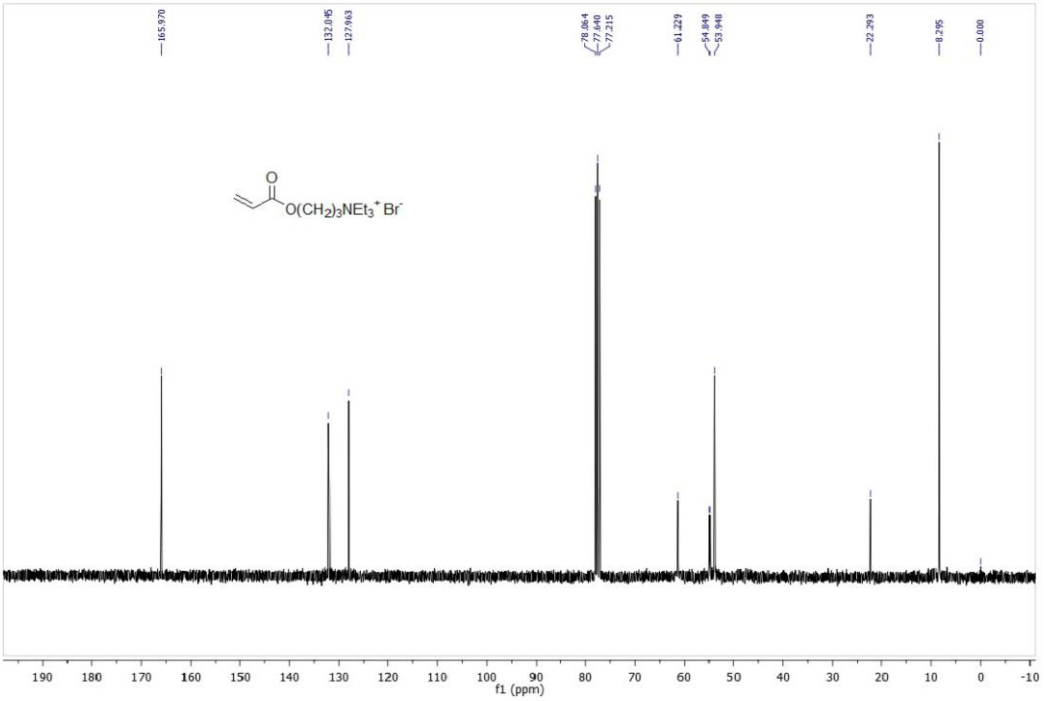

Figure 3.4.1.12 *^{13}C NMR Spectra for Acryloyloxypropyltriethylammonium bromide (**4f**) (75 MHz, CDCl3): δ =166.0, 132.0, 128.0, 61.2, 54.8, 53.9, 22.3, 8.3*

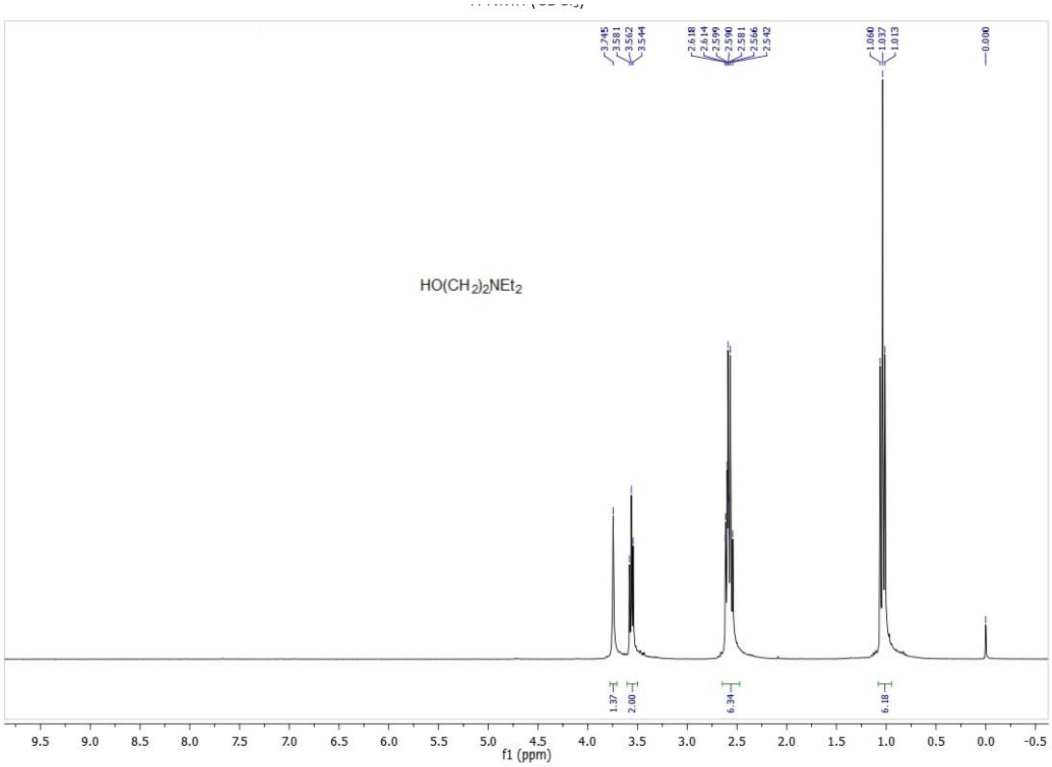

Figure 3.4.1.13 *^{1}H NMR Spectra for 2-Dimethylamino ethanol (**5e**) (300 MHz, CDCl3): δ = 3.74 (s, br, 1 H, OH), 3.56 (t, J = 5.5, 2 H, HOCH2), 2.63-2.52 [m, 6 H, 3 NCH2], 1.04 [t, J = 7.1, 6 H, N(CH2CH3)2]*

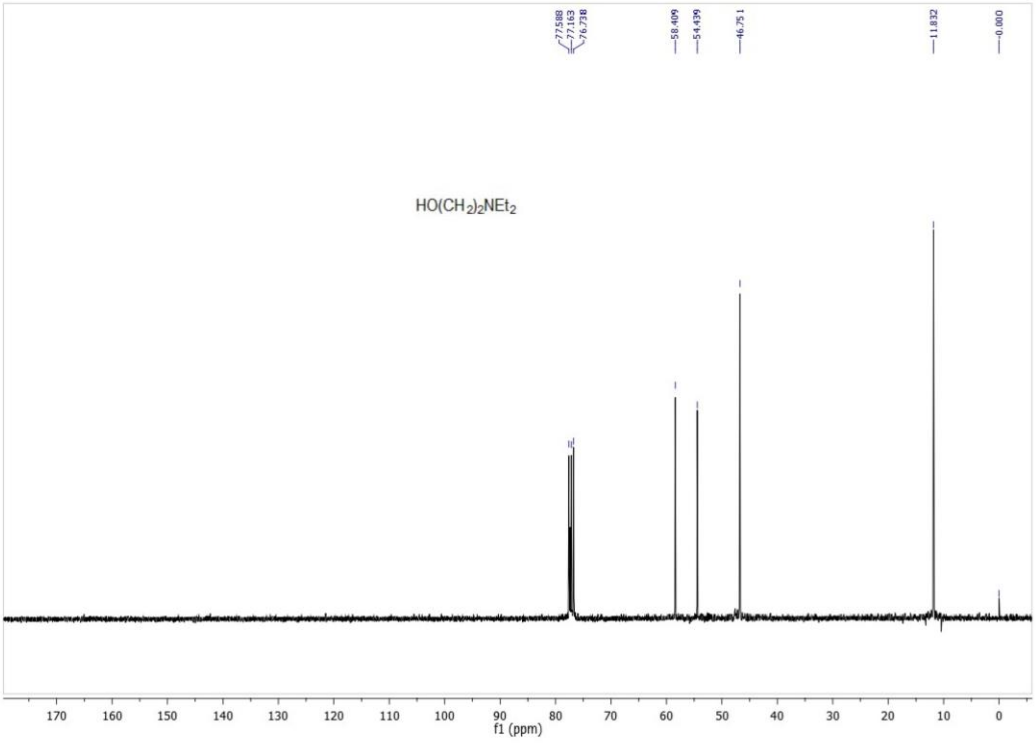

Figure 3.4.1.14 *^{13}C NMR Spectra for 2-Dimethylamino ethanol (**5e**) (75 MHz, CDCl3): δ = 58.4, 54.4, 46.8, 11.81*

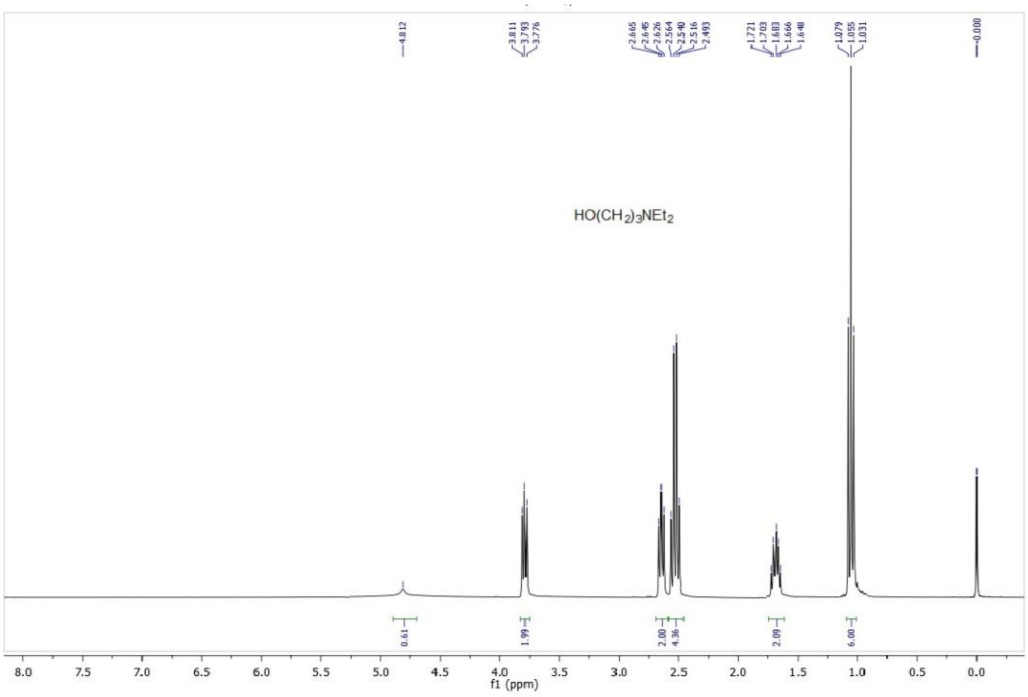

Figure 3.4.1.15 *^{1}H NMR Spectra for 3-Diethylamino propan-1-ol (**5f**) (300 MHz, CDCl3): δ = 4.81 (s, br, 1 H, OH), 3.79 (t, J = 5.4, 2 H, HOCH2), 2.65 (t, J = 5.4, 2*
H, NCH2), 2.53 [q, J = 7.1, 4 H, 2 NCH2], 1.74-1.63 (m, 2 H, HOCH2CH2CH2N), 1.06 [t, J = 7.1, 6 H, N(CH2CH3)2]

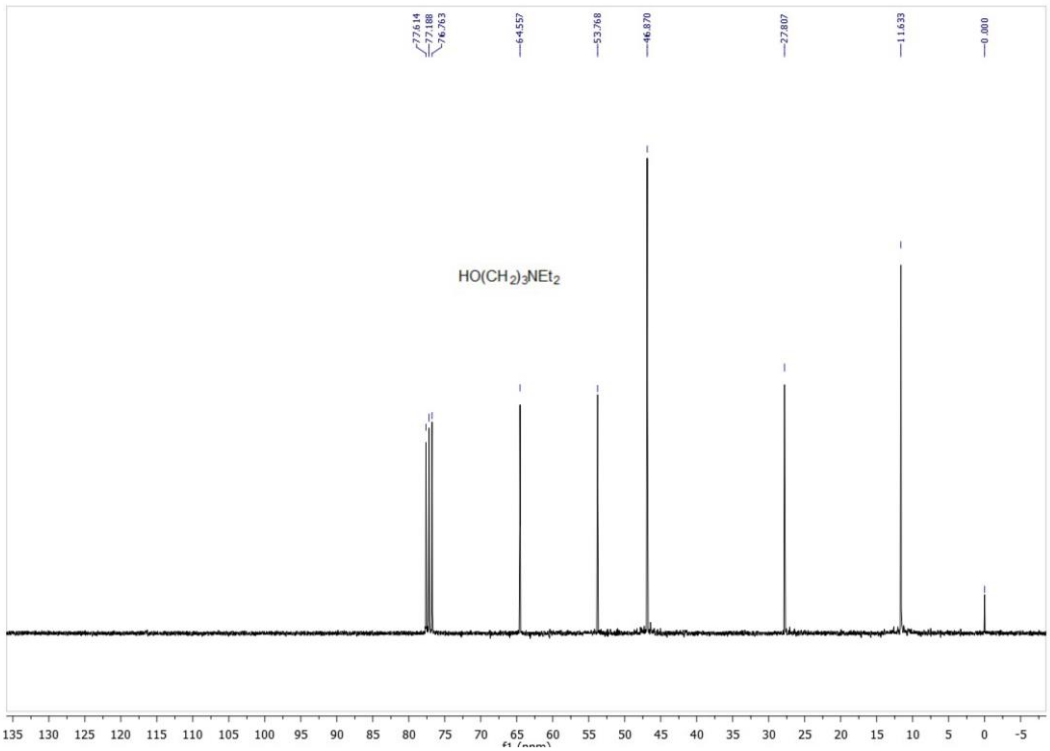

Figure 3.4.1.16 *^{13}C NMR Spectra for 3-Diethylamino propan-1-ol (**5f**) (75 MHz, CDCl3): δ =64.6, 53.8, 46.9, 27.8, 11.6*

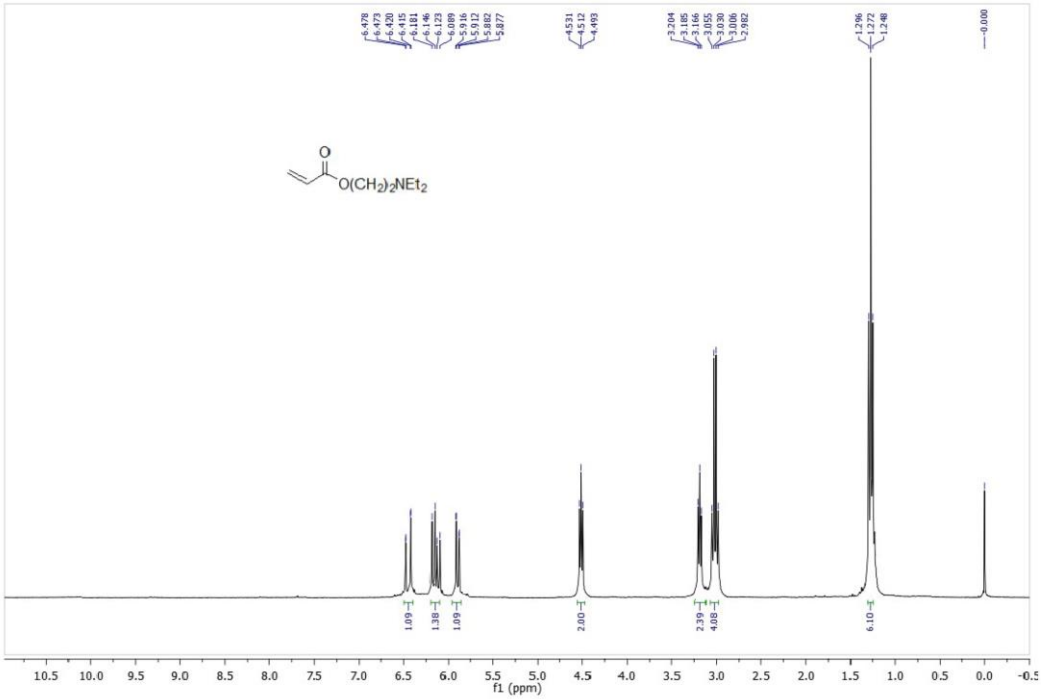

Figure 3.4.1.17 *^{1}H NMR Spectra for (2-Diethylamino)ethyl acrylate (**6e**) (300 MHz, CDCl3): δ =6.42 [distorted dd, J = 17.3, 1.4, 1 H, OC(O)CH=CHH], 6.14 [distorted dd, J = 17.3,*
10.4, 1 H, OC(O)CH=CHH], 5.90 [distorted dd, J = 10.4, 1.4, 1 H, OC(O)CH=CHH], 4.51 (t, J = 5.6, 2 H, C(O)OCH2), 3.18 (t, J = 5.6, 2 H, NCH2), 3.02 [q, J = 7.3, 4 H, 2 NCH2], 1.04 [t, J = 14.0, 6 H, N(CH2CH3)2]

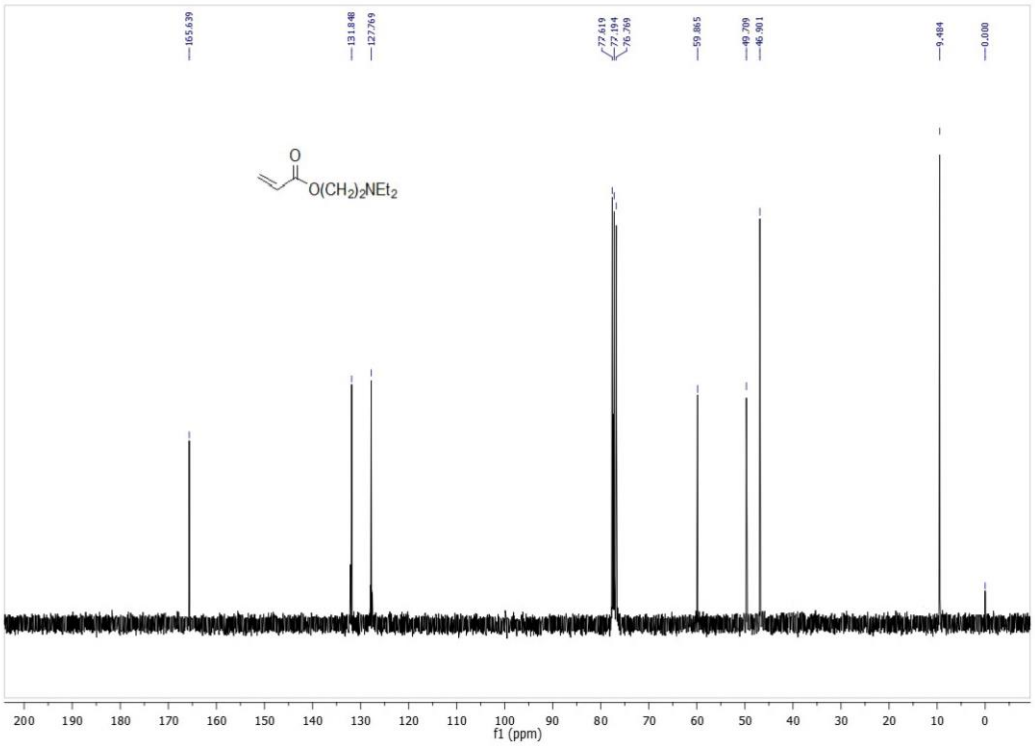

Figure 3.4.1.18 *^{13}C NMR Spectra for 3-Diethylamino propan-1-ol (**6e**) (75 MHz, CDCl3): δ = 165.6, 131.8, 127.8, 59.9, 49.4, 46.9, 9.5*

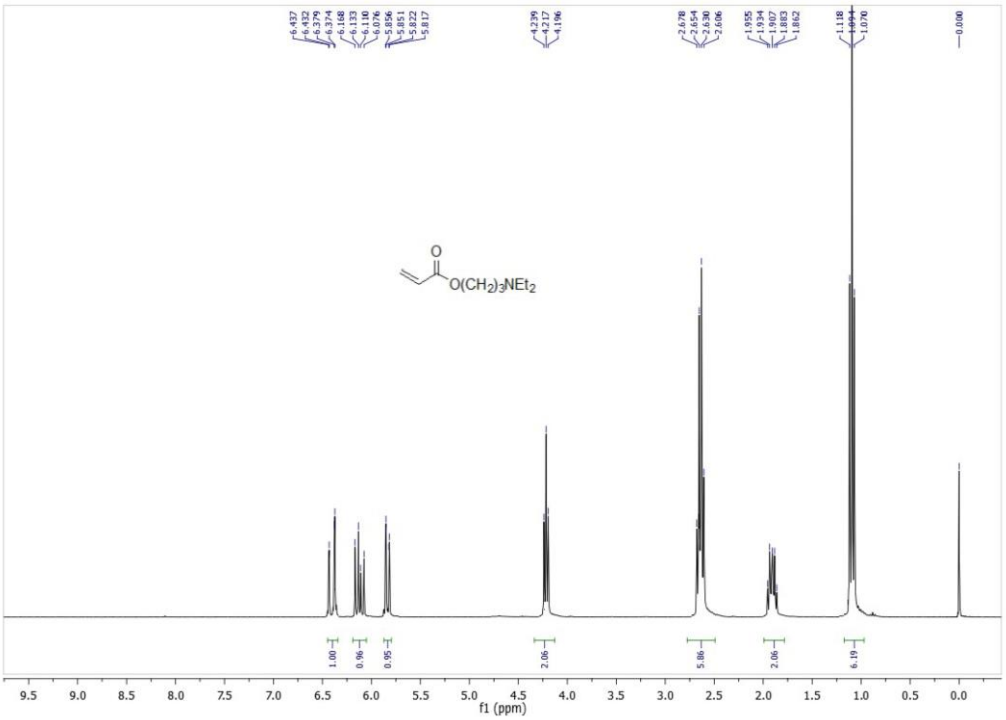

Figure 3.4.1.19 *^{1}H NMR Spectra for (3-Diethylamino)propyl acrylate (**6f**) (300 MHz, CDCl3): δ = 6.40 [distorted dd, J = 17.3, 1.5, 1 H, OC(O)CH=CHH], 6.12 [distorted dd, J = 17.3, 10.4, 1 H, OC(O)CH=CHH], 5.83 [distorted dd, J = 10.4, 1.5, 1 H, OC(O)CH=CHH], 4.21 (t, J = 6.4, 2 H, C(O)OCH2), 2.71-2.58 [m, 6 H, 3 NCH2], 1.97-1.84 (m, 2 H, C(O)OCH2CH2CH2N), 1.09 [t, J =7.2, 6 H, N(CH2CH3)2]*

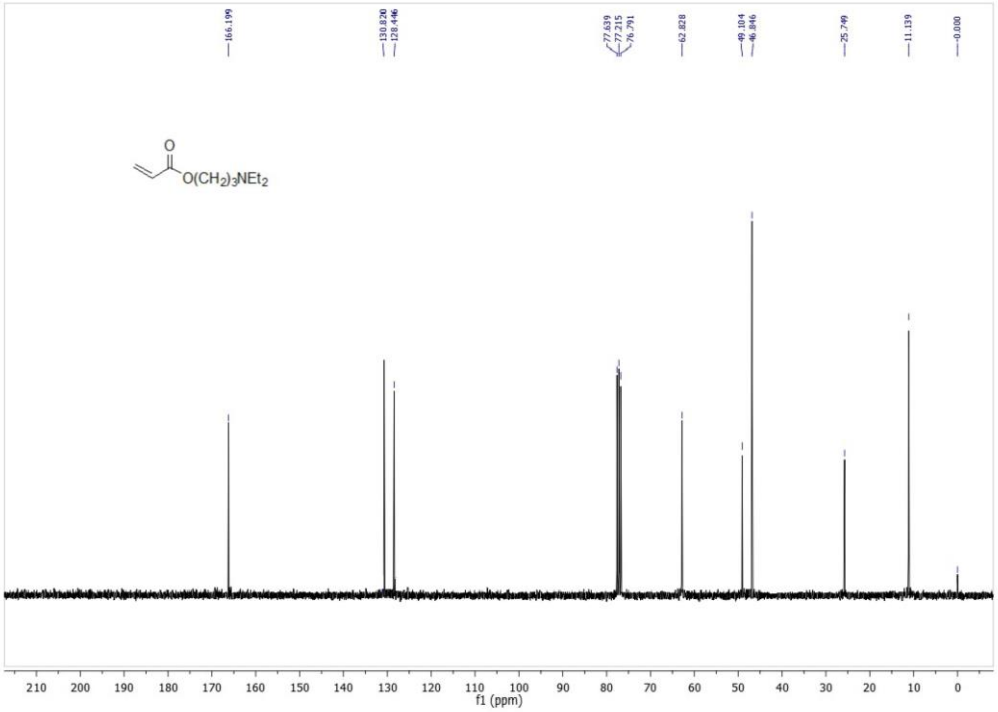

Figure 3.4.1.20 *^{13}C NMR Spectra for (3-Diethylamino)propyl acrylate (**6f**) (75 MHz, CDCl3): δ = 166.2, 130.7, 128.4, 62.8, 49.1, 46.8, 25.7, 11.1*

3.4.2 IR analysis

- *Acryloyloxyundecyltriethylammonium bromide (**4a**)*
    - *IR (KBr): v = 3432 (s, br), 2978 (w), 2929 (m), 2853 (m), 1721 (s), 1631 (w), 1477 (m), 1456 (w), 1408 (m), 1296 (m), 1204 (s), 1028 (w), 986 (m), 811 (m) cm^{-1};*

- *Acryloyloxydodecyltriethylammonium bromide (**4b**)*
    - *IR (KBr): v = 3429 (s, br), 2926 (m), 2854 (m), 1721 (s), 1635 (w),1466 (w), 1408 (m), 1234 (w), 1193 (m), 1059 (w), 986 (w), 812 (w) cm^{-1}*

- *Acryloyloxynonyltriethylammonium bromide (**4c**)*
    - *IR (KBr): v = 3421 (s, br), 2930 (w), 2856 (s), 1719 (s), 1634 (m), 1408 (m), 1275 (m), 1197 (m), 1059 (m), 986 (w), 885 (w) cm^{-1}*

- *Acryloyloxyhexyltriethylammonium bromide (**4d**)*
    - *IR (Film): v = 3435 (s, br), 2947 (m), 2864 (w), 1712 (s), 1636 (m), 1488 (m), 1409 (m), 1386 (m), 1296 (m), 1207 (w), 1060 (m), 1009 (m), 772 (w) cm^{-1}*

- *Acryloyloxyethyltriethylammonium bromide (**4e**)*
    - *IR (Film): v = 3426 (m, br), 2980 (m), 2652 (m), 1727 (s), 1636 (m), 1510 (w), 1463 (m), 1410 (m), 1267 (s), 1190 (s), 1063 (m), 986 (m), 856 (w) cm^{-1}*

- *Acryloyloxypropyltriethylammonium bromide (**4f**)*
    - *IR (Film): v = 3426 (s, br), 2987 (w), 1714 (m), 1636 (m), 1488 (w), 1412 (m), 1299 (m), 1207 (m), 1065 (s), 986 (w) cm^{-1}*

- *2-Dimethylamino ethanol (**5e**)*
    - *IR (Film): v = 3419 (s), 2975 (w), 2850 (w), 1644 (m), 1470 (w), 1387 (w), 1197 (w),1038 (m), 623 (m) cm^{-1}*

- *3-Diethylamino propan-1-ol (**5f**)*
    - *IR (Film): v = 3380 (s, br), 2971 (s), 2876 (m), 2824 (m), 1654 (m), 1470 (m), 1384 (m), 1294 (w), 1196 (w), 1060 (m), 937 (w), 771 (w, br) cm^{-1}*

- *(2-Diethylamino)ethyl acrylate (**6e**)*
    - *IR (film): v = 3424 (s), 2979 (m, br), 1726 (s), 1636 (m), 1568 (w),1353 (w), 1269 (m), 1191 (m), 987 (w), 810 (w) cm^{-1}*

- *(3-Diethylamino)propyl acrylate (**6f**)*
    - *IR (Film): v = 3424 (s, br), 2971 (m), 2799 (w), 2659 (w), 1724 (s), 1637 (s), 1473 (m), 1409 (s), 1296 (s), 1198 (s), 1061 (w), 986 (m), 819 (w) cm^{-1}*

3.4.3 Melting point evaluation

- *Acryloyloxyundecyltriethylammonium bromide (**4a**): Colorless solid, mp = 40-41°C*
- *Acryloyloxydodecyltriethylammonium bromide (**4b**): Colorless solid, mp = 65-67 °C*
- *Acryloyloxynonyltriethylammonium bromide (**4c**): Colorless solid, mp = 28-29 °C*
- *Acryloyloxyhexyltriethylammonium bromide (**4d**): Colorless gummy low-melting solid*
- *Acryloyloxyethyltriethylammonium bromide (**4e**): Yellow oil*
- *Acryloyloxypropyltriethylammonium bromide (**4f**): Brown oil*
- *2-Dimethylamino ethanol (**5e**): Yellowish oil*
- *3-Diethylamino propan-1-ol (**5f**): Yellowish oil*
- *(2-Diethylamino)ethyl acrylate (**6e**): Yellow oil*
- *(3-Diethylamino)propyl acrylate (**6f**): Brown oil*

3.4.4 MS analysis and TIC determination

- *Acryloyloxyundecyltriethylammonium bromide (**4a**):*
    - *MS (ESI+, direct infusion): m/z = 326.31*
    - *Anal. calcd for $C_{20}H_{39}BrNO_2$ (405.43): C, 59.25; H, 9.70; Br, 19.71; N, 3.45; found C, 59.28; H, 9.68; Br, 19.72; N, 3.48*
- *Acryloyloxydodecyltriethylammonium bromide (**4b**):*
    - *MS (ESI+, direct infusion): 340.32*
    - *Anal. calcd for $C_{21}H_{41}BrNO_2$ (419.46): C, 60.13; H, 9.85; Br, 19.05; N, 3.34; found C, 60.15; H, 9.89; Br, 19.08; N, 3.31*
- *Acryloyloxynonyltriethylammonium bromide (**4c**):*
    - *MS (ESI+, direct infusion): 298.27*
    - *Anal. calcd for $C_{18}H_{35}BrNO_2$ (377.38): C, 57.29; H, 9.35; Br, 21.17; N, 3.71; found C, 57.32; H, 9.33; Br, 21.20; N, 3.70*
- *Acryloyloxyhexyltriethylammonium bromide (**4d**):*
    - *MS (ESI+, direct infusion): 256.23*

- *Anal. calcd for $C_{15}H_{30}BrNO_2$ (336.31): C, 53.57; H, 8.99; Br, 23.76; N, 4.16; found C, 53.55; H, 8.97; Br, 23.79; N, 4.13.*

- *Acryloyloxyethyltriethylammonium bromide (**4e**):*
  - *MS (ESI+, direct infusion): 200.17*
  - *Anal. calcd for $C_{11}H_{22}BrNO_2$ (280.20): C, 47.15; H, 7.91; Br, 28.52; N, 5.00; found C, 47.17; H, 7.89; Br, 28.50; N, 5.01*
- *Acryloyloxypropyltriethylammonium bromide (**4f**):*
  - *MS (ESI+, direct infusion): 214.18*
  - *Anal. calcd for $C_{12}H_{23}BrNO_2$ (293.22): C, 49.15; H, 7.91; Br, 27.25; N, 4.78; found C, 49.13; H, 7.88; Br, 27.27; N, 4.80.*
- *2-Dimethylamino ethanol (**5e**):*
  - *GC-MS: 117 (1) [M+], 115 (11), 100 (7), 87 (7), 86 (100), 73 (7), 72 (7), 59 (5), 58 (40), 56 (4), 44 (12), 43 (8), 42 (5)*
  - *Anal. calcd for $C_4H_{11}NO$ (89.14): C, 53.90; H, 12.44; N, 15.71; found C, 53.93; H, 12.41; N, 15.74*
- *3-Diethylamino propan-1-ol (**5f**):*
  - *GC-MS: 131 (16) [M+], 116 (5), 87 (7), 86 (100), 72 (43), 58 (29), 56 (7), 44 (8), 42 (9)*
  - *Anal. calcd for $C_7H_{17}NO$ (131.22): C, 64.07; H, 13.06; N, 10.67; found C, 64.05; H, 13.03; N, 10.69*
- *(2-Diethylamino)ethyl acrylate (**6e**):*
  - *GC-MS: 171 (1) [M+], 100 (4), 99 (21), 87 (7), 86 (100), 58 (16), 56 (5), 55 (12), 44 (3), 42 (4)*
  - *Anal. calcd for $C_9H_{17}NO_2$ (171.24): C, 63.13; H, 10.01; N, 8.18; found C, 63.10; H, 10.02; N, 8.16.*
- *(3-Diethylamino)propyl acrylate (**6f**):*
  - *GC-MS: 185 (12) [M+], 170 (12), 113 (26), 98 (4), 87 (9), 86 (100), 85 (7), 72 (19), 58 (17), 56 (7), 55 (22), 44 (5), 42 (8), 41 (5);*
  - *Anal. calcd for $C_{10}H_{19}NO_2$ (185.26): C, 64.83; H, 10.34; N, 7.56; found C, 64.81; H, 10.32; N, 7.53.*

3.5 Experimental part

3.5.1 Chemicals and apparatus

CH_3CN (purity ≥99.9%) was purchased from Hypersolv and was distilled over 4Å molecular sieves which have been previously activated. CH_3Cl (purity 99.0-99.4 %) was purchased from Sigma-Aldrich and was freshly distilled over activated 4Å sieves before use. Et_2O (purity ≥ 99.9%) stabilized with BHT (Diisobuthylhydroxytoluene, 1 ppm) as stabilizer, was purchased from Sigma-Aldrich and used without

further purification. EtOH (purity 99.8 %) was purchased from Panreac and used without further purification. Cyclohexane (purity ≥ 99.8 %) was purchased from Panrec and used as it was.

6-Bromo-1-Hexanol (purity > 95%), 9-bromo-1-nonanol (purity > 95%), 11-bromo-1-undecanol (purity > 98%), 12-bromo-1-dodecanol (purity > 98%) and 2-bromoethanol (purity ≥ 95 %), were purchased from TCI Europe and used without further purification. 3-Bromo-1-propanol was purchased from Fluorochem (purity 97%) and used as received. BHT (purity 99%) was purchase from Fluka and used as received. Acryloyl chloride (stabilized with 400 ppm phenothiazine; purity 97%), triethylamine (purity 99%), diethylamine (purity 98%), ethyl bromide (purity 98%), and hydroquinone (purity 99%) were purchased from Sigma–Aldrich and used as received. NaHCO3 (purity 98–100%) was purchased from Panreac and used as received. Na2SO4 (purity 99.2%) was purchased from Analar and used without purification. Molecular sieves 4Å (pellets, 1.6 mm diameter) were purchased from Sigma–Aldrich and activated by oven at 3008 °C for 4 h. Molecular sieves 3Å (powder) were purchased from Alfa Aesar and activated in an oven at 3008C for 4 h.

All reactions were analyzed by TLC on silica gel 60F254 (Merck) and by GLC by using a Shimadzu GC-2010 gas chromatograph and capillary columns with polymethylsilicone +5% phenylsilicone (HP-5) as the stationary phase. Evaporation refers to the removal of solvent under reduced pressure. Melting points are uncorrected. ^{1}H *NMR and* ^{13}C *NMR spectra were recorded at 258C with a Bruker DPX Avance 300 Spectrometer in* $CDCl_3$ *solutions at 300 and 75 MHz, respectively, with* Me_4Si *as internal standard. Chemical shifts (d) and coupling constants (J) are given in ppm and in Hz, respectively. IR spectra were taken with a JASCO FT-IR 4200 spectrometer. Mass spectra were obtained by using a Shimadzu QP2010 GC-MS apparatus at 70 eV ionization voltage and by electrospray ionization mass spectrometry (ESI-MS) by using an Agilent 6540 UHD accurate-mass Q-TOF spectrometer equipped with a Dual AJS ESI source working in positive mode. N2 was employed as the desolvation gas at 3008C and a flow rate of 8 Lmin1. The nebulizer was set to 45 psig. The Sheat gas temperature was set at 4008C and a flow of 12 Lmin1. A potential of 3.5 kV was used on the capillary for positive ion mode. The fragmentor was set to 175 V. MS spectra were recorded in the 150–1000 m/z range. The HPLC system was an Agilent 1260 Infinity. A reversed-phase C18 column (ZORBAX Extended-C18 2.150 mm, 1.8 mm) with a Phenomenex C18 security guard column (4 mm x 3 mm) were used. The flow-rate was 0.4 mLmin1 and the column temperature was set to 30°C. The eluents were formic acid/water (0.1:99.9, v/v; phase A) and formic acid/acetonitrile (0.1:99.9, v/v; phase B). The following gradient was employed: 0–10 min, linear gradient from 5% to 95% B; 10–15 min, washing and reconditioning of the column to 5% B. Injection volume was 10 mL. The eluate was monitored through MS TIC. Microanalyses were conducted using a Thermo-Fischer Elemental Analyzer Flash 2000.*

3.5.2 Synthesis of Acryloyloxyalkyltriethylammonium bromides (AATEABs) 4a-d

3.5.2.1 First step: Synthesis of bromoalkyl acrylate 3a-d by esterification of bromoalkanols 1a-d with acryloyl chloride 2

*BHT (13.9 10^{-3} g, 6.3·10^{-5} mol, for **1a**; 2.6 10^{-3} g, 12·10^{-3}mol, for **1b**; 3.7 g, 17·10^{-3} mmol, for **1c**; 3.8·10^{-3} g, 17·10^{-3}mol for **1d**), followed by acryloyl chloride (dropwise; 1.62·10^{-3} L, 1.80 g, 19.9·10^{-3} mol, for **1a**; 310·10^{-3} L, 344·10^{-3}g, 3.8·10^{-3} mol, for **1b**; 430·10^{-3} L, 480·10^{-3} g, 5.3·10^{-3} mol, for **1c**; 450·10^{-3} L, 500·10^{-3} g, 5.5·10^{-3} mol, for **1d**), and activated sieves 3Å (10 g for **1a**, 1.9 g for **1b**, 2.7 g for **1c**, 2.8 g for **1d**) were added to a stirred solution of the ω-bromoalkan-1-ol (11-bromo-1-undecanol **1a**: 5.0 g, 19.9·10^{-3} mol; 12-bromo-1-dodecanol **1b**: 1.0 g, 3.8·10^{-3} mol; 9-bromo-1-nonanol **1c**: 1.1 g, 5.3·10^{-3} mol; 6-bromo-1-hexanol **1d**: 1.0 g, 5.5·10^{-3} mol) in anhydrous CH_3CN (100·10^{-3} L for **1a**; 19.1·10^{-3} L for **1b**; 26.6·10^{-3} L for **1c**; 27.7·10^{-3} L for **1d**), which was maintained at room temperature in a Schlenk flask. The flask was sealed, and the mixture maintained under stirring for 24 hours at 90 °C. After cooling down, in order to remove molecular sieves the mixture was filtered and subsequently the solvent was evaporated. The intermediate products **3a–d** thus obtained were allowed to react in the next step as such without purification.*

3.5.2.2 Second step: quaternization of ω-bromoalkyl acrylate 3a-d with triethylamine

*Triethylamine (3.06·10^{-3} L, 2.22 g, 21.9·10^{-3} mol, for **3a**; 580·10^{-3} L, 423·10^{-3} g, 4.18·10^{-3} mol, for **3b**; 810·10^{-3} L, 590·10^{-3} g, 5.83·10^{-3} mol, for **3c**; 840·10^{-3} L, 613·10^{-3} g, 6.05·10^{-3} mol, for **3d**) was added dropwise to a solution of the intermediate ω-bromoalkyl acrylate **3** derived from the first step in anhydrous $CHCl_3$ (9.6·10^{-3} L for **3a**; 2.0·10^{-3} L for **3b**; 2.6·10^{-3} L for **3c**; 2.7·10^{-3} L for **3d**), at room temperature in a Schlenk flask. The flask was sealed, and the mixture stirred at 60 °C for 72 h. After cooling down, Et_2O (75·10^{-3} L for **3a**; 15·10^{-3} L for **3b**; 20·10^{-3} L for **3c** and **3d**) was added dropwise to the solution which was maintained under stirring for 10 min. Formation of white precipitate occurs, followed by its filtration and further washing process with diethyl ether, to give the pure acryloxyalkyltriethylammonium bromide (AATEAB): acryloyloxyundecyltriethylammonium bromide (AUTEAB, **4a**) was a colorless solid (m.p.= 40–41 °C; yield: 5.10 g, 63% based on starting **1a**); acryloyloxydodecyltriethylammonium bromide (**4b**) was a colorless solid (m.p.= 65–67 °C; yield: 1.11 g, 70% based on starting **1b**); acryloyloxynonyltriethylammonium bromide (**4c**) was a colorless solid (m.p.= 25–26 °C; yield: 1.22 g, 61% based on starting **1c**); acryloyloxyhexyltriethylammonium bromide (**4d**) was a colorless gummy lowmelting solid (yield: 1.39 g, 751% based on starting **1d**).*

3.5.3 Synthesis of Acryloyloxyalkyltriethylammonium bromides (AATEABs) 4e and 4f

3.5.2.1 First step: Reaction of Et_2NH with ω-bromoalkanols 1e and 1f

*Et_2NH ($4.1\cdot10^{-3}$ L, 2.91 g, $39.8\cdot10^{-3}$ mol for **1e**; $7.4\cdot10^{-3}$ L, 5.25 g, $71.6\cdot10^{-3}$ mol, for **1f**) was added dropwise to a solution of 2-bromoethanol **1e** (1.0 g, $8.0\cdot10^{-3}$ mol) or 3-bromo-1-propanol **1f** (2.0 g, $14.4\cdot10^{-3}$ mol) in EtOH ($14.5\cdot10^{-3}$ L for **1e**; $26.0\cdot10^{-3}$ L for **1f**), which was maintained under nitrogen with stirring. The reaction mixture was heated at 60 °C for 6 h. After cooling down, CH_2Cl_2 ($30\cdot10^{-3}$ L for **1e**; $54\cdot10^{-3}$ L for **1f**) was added, and the mixture was washed with a 5% w/w solution of $NaHCO_3$ ($310\cdot10^{-3}$ L for **1e**; $320\cdot10^{-3}$ L for **1f**) followed by water ($5\cdot10^{-3}$ L for **1e**; $10\cdot10^{-3}$ L for **1f**). The phases were separated, and the organic phase dried over Na_2SO_4. After filtration and elimination of the solvent by distillation at atmospheric pressure, the products were obtained as yellowish oils [2-(dimethylamino)ethanol **5e**: $688\cdot10^{-3}$ g, 96%; 3-(dimethylamino)propanol **5f**: 1.85 g, 98%].*

3.5.3.2 Second step: Synthesis of (diethylamino)alkyl acrylate 6e-f by esterification of 2-(diethylamino)alkanols 5e-f with acryloyl chloride 2

*Acryloyl chloride **2** ($626\cdot10^{-6}$ L, $697\cdot10^{-3}$ g, $7.7\cdot10^{-3}$mol for **5e**; $1.15\cdot10^{-3}$ L, 1.28 g, $14.1\cdot10^{-3}$ mol for **5f**) was added dropwise to a solution of the 2-(diethylamino)alkanols [2-(diethylamino)ethanol **5e**: $688\cdot10^{-3}$ g, $7.7\cdot10^{-3}$ mol; 3-(diethylamino)propanol **5f**: 1.85 g, $14.1\cdot10^{-3}$ mol] in anhydrous CH_3CN ($7.7\cdot10^{-3}$ L for **5e**; $14.1\cdot10^{-3}$ L for **5f**) at 0 °C under nitrogen with stirring. The solution was maintained at 0 °C for 2 h and then stirred for 15 h at room temperature. The reaction mixture was then treated with a 5% w/w $NaHCO_3$ solution ($50\cdot10^{-3}$ L for **5e**; $90\cdot10^{-3}$ L for **5f**) and finally extracted with CH_2Cl**2** ($710\cdot10^{-3}$ L for **5e**; $720\cdot10^{-3}$ L for **5f**). After phase separation, the organic layer was dried over Na_2SO_4. After filtration and elimination of the solvent by distillation at atmospheric pressure, the products were obtained as yellowish oils [(2-diethylamino)ethyl acrylate **6e**: $750\cdot10^{-3}$ g, 57%; (3-diethylamino)propyl acrylate **6f**: 1.6 g, 61%)].*

3.5.3 .3 Third step: Quaternization of (diethylamino)alkyl acrylate 6e-f with EtBr

*The 2-(diethylamino)alkyl acrylate (**6e**: $750\cdot10^{-3}$ g, $4.38\cdot10^{-3}$ mol; **6f**: 1.6 g, $8.64\cdot10^{-3}$ mol) was allowed to react with pure EtBr ($2.2\cdot10^{-4}$ L, $318\cdot10^{-3}$ g, $2.92\cdot10^{-3}$ mol, for **6e**; $0.43\cdot10^{-3}$ L, $628\cdot10^{-3}$ g, $5.76\cdot10^{-3}$ mol, for **6f**) in the presence of hydroquinone ($1\cdot10^{-3}$ g, $9.11\cdot10^{-3}$ mol, for **6e**; $2\cdot10^{-3}$ g, $1.8\cdot10^{-5}$ mol, for **6f**) at 50 °C for 15 h. The*

*crude product was purified after several washings under stirring with cyclohexane (10 x ($15 \cdot 10^{-3}$ L)) followed by drying under vacuum for 24–30 h. The products appear as tarry yellow oils (acryloyloxyethyltriethylammonium bromide **4e**: $650 \cdot 10^{-3}$ g, yield 53%; acryloyloxypropyltriethylammonium bromide **4f**: 1.1 g, 43%).*

3.6 Chapter conclusions

*An efficient, simple and cheap approach for the synthesis of an important class of Polymerizable Quaternary Ammonium Salts (PQAS), precisely Acryloyloxyalkyltriethylammonium bromides (AATEABs) is in here discussed. AATEABs obtained bear variable alkyl chain and represent useful and efficient starting materials which can be used by themselves or as polymerizable coating on commercial membranes to whom AATEABs confer remarkable antibiofouling activity. Also, our synthetic approach can be easily applied either to lab or large scale productions of membranes for water treatment. Optimized conditions in this procedure, allow to work under air, avoiding harsh conditions and chromatographic purification and starting from chemicals which are cheap and easily available on market. AATEABs **4a-d** with longer alkyl chain (C_6, C_9, C_{11}, C_{12}) synthesis consists in two steps reaction: Esterification of commercially available ω-bromoalkan-1-ols **1a-d** with acryloyl chloride **2** in the presence of 3Å molecular sieves powder, followed by quaternization reaction of (bromoalkyl)acrylate intermediate **3** with triethylamine. Anyhow, this synthetic strategy revealed to be not successful for the synthesis of AATEABs **4e-f** bearing shorter alkyl chain (C_2, C_3 respectively) for whose synthesis approach needed to be partially changed. Newly AATEABs **4e-f** were obtained using a sequence of three steps reaction: Reaction of bromoalkan-1-ols with diethylamine, followed by estherification with acryloyl chloride **2** and quaternization with EtBr. In order to evaluate antimicrobial activity, AATEABs **4a-f** have been tested against Gram positive, Gram negative and yeast strains. Among AATEABs **4a-f**, **4a** (C_{11} alkyl chain) and **4b** (C_{12} alkyl chain) possess highest antibacterial activity against bacteria and yeast strains, except for Pseudomonas aeruginosa. Analogous speech can be done for **4c** (C_9 alkyl chain) against Saccharomyces cervisiae and Candida albicans. AATEABs **4b** and **4a** resulted to be the most active derivate, especially against Staphylococcus aureus and Streptococcus pyogenes. In particular, **4b** acrivity is approximately four times higher than **4a**, with a MIC value of 64μg mL^{-1}.Finally, we can conclude that AATEABs obtained with novel, cheap and easily scalable approach, represent an important class of polymerizable molecules which can be used in several fields, such as biomedical, textile or water treatment. In particular, these molecules fits well for those applications in which an antibiofouling features are needed.*

Chapter 3 references

1. Russel, G. M. a. A. D., Antiseptics and Disinfectants: Activity, Action, and Resistance. *Clinical Microbiology Reviews* **1999,** *12* (1), 147-179.
2. Tischer, M.; Pradel, G.; Ohlsen, K.; Holzgrabe, U., Quaternary ammonium salts and their antimicrobial potential: targets or nonspecific interactions? *ChemMedChem* **2012,** *7* (1), 22-31.
3. Simoncic, B.; Tomsic, B., Structures of Novel Antimicrobial Agents for Textiles - A Review. *Textile Research Journal* **2010,** *80* (16), 1721-1737.
4. Bhowmick, S.; Mohanty, S.; Koul, V., Fabrication of transparent quaternized PVA/silver nanocomposite hydrogel and its evaluation as an antimicrobial patch for wound care systems. *J Mater Sci Mater Med* **2016,** *27* (11), 160.
5. Morais, D. S.; Guedes, R. M.; Lopes, M. A., Antimicrobial Approaches for Textiles: From Research to Market. *Materials (Basel)* **2016,** *9* (6).
6. Shahid-ul-Islam, S.-u.-I.; Butola, B. S.; Mohammad, F., Silver nanomaterials as future colorants and potential antimicrobial agents for natural and synthetic textile materials. *Rsc Adv* **2016,** *6* (50), 44232-44247.
7. Yao, C.; Li, X.; Neoh, K. G.; Shi, Z.; Kang, E. T., Surface modification and antibacterial activity of electrospun polyurethane fibrous membranes with quaternary ammonium moieties. *Journal of Membrane Science* **2008,** *320* (1-2), 259-267.
8. Yao, C.; Li, X.-s.; Neoh, K. G.; Shi, Z.-l.; Kang, E. T., Antibacterial poly(D,L-lactide) (PDLLA) fibrous membranes modified with quaternary ammonium moieties. *Chinese Journal of Polymer Science* **2010,** *28* (4), 581-588.
9. Yagci, M. B.; Bolca, S.; Heuts, J. P. A.; Ming, W.; de With, G., Self-stratifying antimicrobial polyurethane coatings. *Progress in Organic Coatings* **2011,** *72* (3), 305-314.
10. Siedenbiedel, F.; Tiller, J. C., Antimicrobial Polymers in Solution and on Surfaces: Overview and Functional Principles. *Polymers* **2012,** *4* (1), 46-71.
11. Xue, Y.; Xiao, H.; Zhang, Y., Antimicrobial polymeric materials with quaternary ammonium and phosphonium salts. *Int J Mol Sci* **2015,** *16* (2), 3626-55.
12. Santos, M. R. E.; Fonseca, A. C.; Mendonca, P. V.; Branco, R.; Serra, A. C.; Morais, P. V.; Coelho, J. F. J., Recent Developments in Antimicrobial Polymers: A Review. *Materials (Basel)* **2016,** *9* (7).
13. Muñoz-Bonilla, A.; Cerrada, M. L.; Fernández-García, M., CHAPTER 1. Introduction to Antimicrobial Polymeric Materials. **2013**, 1-21.
14. Muñoz-Bonilla, A.; Fernández-García, M., Polymeric materials with antimicrobial activity. *Progress in Polymer Science* **2012,** *37* (2), 281-339.
15. Sherrington, D. J. a. D. C., Novel polymerizable mono- and divalent quaternary ammonium cationic surfactants: I. Synthesis, structural characterization and homopolymerization. *Polymer* **1996,** *37* (8), 1453-1462.
16. Galiano, F.; Figoli, A.; Deowan, S. A.; Johnson, D.; Altinkaya, S. A.; Veltri, L.; De Luca, G.; Mancuso, R.; Hilal, N.; Gabriele, B.; Hoinkis, J., A step forward to a more efficient wastewater treatment by membrane surface modification via polymerizable bicontinuous microemulsion. *Journal of Membrane Science* **2015,** *482*, 103-114.
17. A. W. Bauer, W. M. M. K., J. C. Sherris and M. Turck, Antibiotic suceptibility testing by a standardized disk method. *The American Journal of Clinical Pathology* **1966,** *45* (4).

Chapter 4

Novel method for the preparation of Thin Film Composite membranes for gas separation and defects control by protective layer coating

Chapter based on the article tiled: " Defect control for Large-Scale Thin-Film Composite membrane and its Bench-Scale demonstration"

*(Myung Jin Yoo, Jun yeok Lee, Seung Yeon Yoo, Jee Yeon Oh, Jong Min Roh, Giuseppe Grasso, Jung Hyun Lee, Da Hun Lee, Woong Jin Oh, Jeong-Gu Yeo, Hoon Cho, Ho Bum Park, Journal of Membrane Science **2018**)*

4.1 Chapter Summary

Membrane technology for gas separation, started diffusion in In late '70s. Mainly, research efforts have been focused on production of suitable materials, in particular with regard to one critical point for carbon dioxide separation processes which is represented by the trade-off between selectivity and permeability, nowadays known as " Robeson upper bound".In membrane technologies and in particular in TFC membranes, material and membrane properties are different and separate aspects, but their relation plays a fundamental role which must be taken into account in order to understand how the membrane work and eventually change material. Actually, among the studies made on membrane processes and different type of technologies for different purposes, few materials and TFC membrane l for CO_2/N_2 separation have been successfully commercialized since the difficult to prepare very thin selective layer, essential condition for optimal separation because selective layer thickness affects CO_2 permeance.However, another problem is represented by defects presence, in particular for large scale production. In fact, creation of defect-free membrane is very hard to achieve, but defects presence can alter gas transport properties.In this chapter effect of defects is theoretically analyzed and a novel method for TFC membrane preparation which can also be applied for large scale production is presented.

4.2 Introduction

Nowadays several technologies for CO_2 capture from mixed gas are known, such as adsorption or absorption[1-5], loop-cycle combustion[6-8], membranes[9-11] or Gas hydrates and cryogenic distillation[12-17]. Despite the large amount of technologies, due to low demands in terms of energy, lower cost production and their simplicity and and performances, membrane[11] are actually considered the most attractive and promising method which is supplanting the absorption technology, widely used for more than 60 years. Although in literature there is a large amount of studies concerning several materials and respective CO_2 separation properties, they are mainly focused on thick film membranes or single gas membranes or lab-scale membranes[18-23]. Indeed, when scale-up process is needed, in addiction to thin layer, membrane design plays a key role and must be considered. Main issues are therefore represented by the difference between lab and industrial scale membranes, in particular for data reliability, because producing several square meter membrane is different from making few square centimeters sample. However, ultimate challenge for membrane research is represented by the application at industrial level, which is often neglected by academia but that is equally important. In fact in literature, not many work concerning industrial scale application of working membranes have been done[24-25], probably because of difficulties concerning the defect control and preparation of defect-free membranes in large scale. One of most challenging goals for CO_2 separation technology is the competitiveness with absorption methods; on this purpose, exceptional high permeance level is required and hence thickness must be reduced avoiding defects. In 2016, Roussanly et al. investigated membrane properties in postcombustion CO_2 capture in coal-fired plants and estimated that considering Robenson upper bound limit, selective layer thickness should be maintained under 0.1 micron, in order to be competitive with absorbtion technology. Optimal results can be achieved iwith a thickness lower than 50 nm[26], but if we consider that lower thickness may also lead to a higher defect ratio, we understand why membrane performances estimation is usually calculated using theoretical approaches[26-28]. In order to control defects during membrane fabrication process, one way is the insertion of Polydimethylsiloxane (PDMS) gutter layer on porous support, immediately beneath the dense selective layer: although this method has been widely used, it is not compatible with high permeance CO_2 separation systems. In fact, in 2015 Kattula et al. found that introduction of gutter layer in Thin Film Composite membranes, might significantly reduce permeance and selective either. They estimated that in order to prevent selectivity decrease, the relative permeability of gutter layer to the selective layer should ben 5-10 or higher[29]. Permeance for PDMS gutter layer has been measured and reported to be between 2000 and 6000 GPU, not sufficient for high permeance membranes considering model study[9, 30-34] reported. 1 GPU is 10−6 cm3(STP)/cm^2 s cmHg and preparation of PDMS gutter layer is a tricky procedure which expect a pre-soaking step followed by crosslink process. Alternatively,

another method consists on creation of protective layer which can help to prevent defects during membrane fabrication and hence to avoid selectivity decrease; moreover, protective-layer method can also be applied to large scale module fabrication. Though its use is well known in literature, protective layer effect has never been used to study its impact on membrane performances. This chapter reports a theoretical approach finalized to comprehend the impact of protective layer on the defect control and hence on membrane performance. In particular, selective layer leads to a great reduction of defects amount with only slight decrease of selectivity; coverage ratio can be controlled basing on layer thickness and this method can be applied to both lab-scale and bench-scale CO_2/N_2 separation membrane module system, in which protective layer method can find one possible application.

4.3 Results and discussion

4.3.1 TFC membrane and role of protective layer

Controlling defects during membrane preparation process, plays a fundamental role and can hardly affect membrane performances in terms of selectivity and permeability. In fact, small number and tiny defects are enough to compromise membrane separation process. There are several way in which defects can be generated and different causes can lead to their formation: environmental such as micro dust and low instrumentation accuracy, but also the preparation process, material type and structural configuration of membrane can generate imperfections. Usually, TFC preparation approach for industrial membranes consists in a substrate whose role is to provide mechanical strength, beneath selective layer which represents the real " barrer" in which separation occurs. In order to maximize efficiency, TFC membranes combine a low mass transport resistance possessed by porous substrate with a thin selective layer, but sometimes large pore size and highly porous substrate for reduced mass transport resistance can generate defects in selective layer, in particular for thinnest one, because of selective layer penetration into porous matrix as reported in Figure 4.3.1.1 a

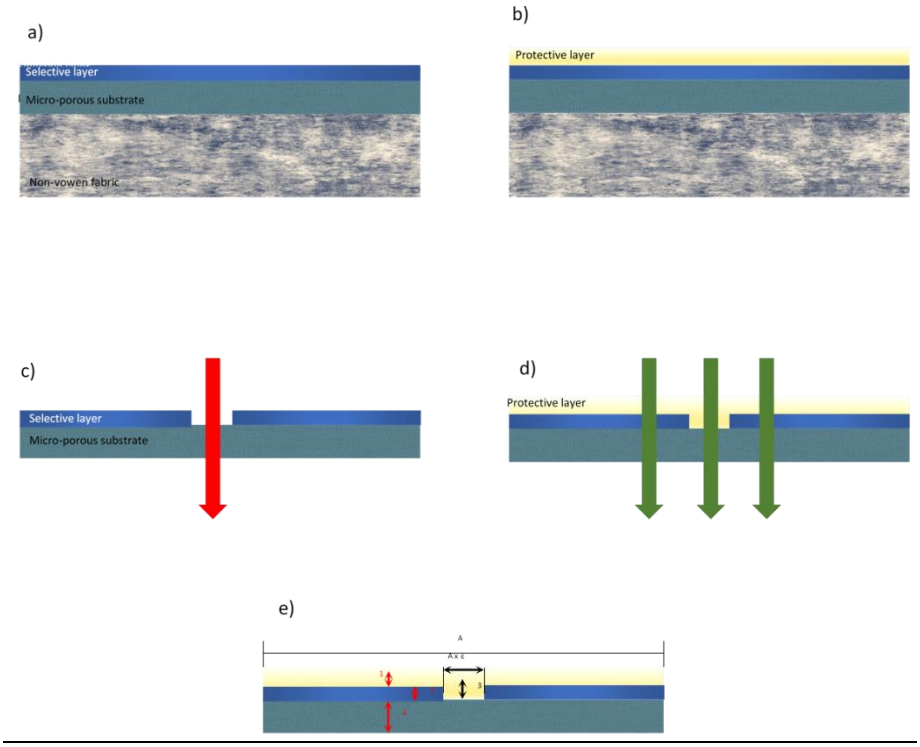

Figure 4.3.1.1 Representation of TFC membrane without protective layer (a), with protective layer (b), gas transport and defect-containing membrane (c), effect of protective layer coating on defective membrane (d) and layers resistance in a TFC membrane

In industrial scale, sometimes gutter layer is used and placed between porous and selective layer, however the best option remains the the protective layer, as meant in Figure 4.3.1.1 b. Defects can affect mass transport in membrane process and confer a neglectable mass transport resistance and lead to a selectivity loss, as showed in picture Figure 4.3.1.1 c. Selective layer, causes increase in mass transport resistance on one hand, and on the other hand enhances selectivity lost because of defects, as showed in picture Figure 4.3.1.1d

4.3.2 Estimation of gas transport properties on defective TFC membranes coated with protective layer.

Through the use of selective layer, it is possible to maintain membrane selectivity even for those membranes containing defects: however, due to this approach a permeance loss may occur because protective layer may also offer resistance in TFC membranes and decrease membrane permeance. It is possible to estimate protective layer properties depending on defects ratio and material properties: a deeper investigation and systematic study in order to comprehend how protective layer works, is therefore important. We tried to mathematically estimate the effect and protective layer effectiveness in a TFC membrane with some defects, using a resistance model which helped us to have one idea about transport properties. Henis and Tripodi proposed a mathematical approach which explains the transport in TFC membranes[35], used as starting point

for more complicated and improved models used in literature[36-41]. The model we used, takes into account porosity, pore penetration, thickness and permeability of each layer. Transport areas can be divided in different areas, as showed in Figure 4.3.1.1 e:

- *Protective layer*
- *Selective layer*
- *Defective layer filled with protective layer*
- *Substrate*

We must do also consider that:

- *Protective layer is homogeneous and non-porous*
- *Selective layer is homogeneous, non porous, excluding defective areas*
- *No pressure lost in region 3 (region 2 and 3 have same pressure)*
- *No pore penetration into substrate matrix*
- *The depth of defective area in region 3 is the same as thickness of selective layer*

Based on these assumptions, resistance can be expressed as:

$$R_1 = \frac{l_1}{P_1 A} \quad (2)$$

$$R_2 = \frac{l_2}{P_2 A(1-\varepsilon)} \quad (3)$$

$$R_3 = \frac{l_2}{P_1 A^{\varepsilon}} \quad (4)$$

$$R_4 = \frac{l_4}{P_4 A} \quad (5)$$

where R_i ,l_i , and Pi are the resistance, thickness, and permeability of each region (i), respectively. A is the membrane area and ε is the defect ratio. The total resistance (RT) and membrane permeance (JT) can be expressed as:

$$R_T = R_1 + \frac{1}{\frac{1}{R_2}+\frac{1}{R_3}} + R_4 \quad (6)$$

$$\frac{J}{J_T} = \frac{1}{J_1} + \frac{1}{J_2 + J_3} + \frac{1}{J_4} \quad (7)$$

$$J_T = \frac{1}{\frac{l_1}{P_1} + \frac{1}{\frac{P_2(1-\varepsilon)}{l_2} + \frac{P_1 \varepsilon}{l_2}} + \frac{1}{J_4}} \quad (8)$$

where Ji is the permeance of each region (i). Thus, it is possible to calculate the permeance of a defective membrane coated by protective layer, using the protective layer thickness (l_1), protective layer permeability (P_1), selective layer thickness (l_2), selective layer permeability (P_2), defect ratio (ε), and substrate permeance (J_4).

4.3.3 Calculation of optimized properties of protective layer, by mathematical method.

For theoretical membrane performance calculations, we used abovementioned equations and our material in order to elucidate the effect of protective layer on defective membrane as correlation with defect ratio. CO2 permeability of selective layer was set at 110 barrer (1 barrer = 10−10 cm3 (STP) cm/cm2 s cmHg), CO2/N2 selectivity of selecrive layer was fixed at 72.6, thickness was 90 nm and substrate permeance was fixed at 130k GPU for CO2 and 150k GPU for N2. In Figure 4.3.3.1a, differences depending on protective layer existence as function of defect ratio are reported (CO2 permeability: 3900 barrer, thickness: 0.1 micron): then protective layer does not exist, we observe decrease of selectivity from a 10-4% defect ratio; in 0.01% of defect ratio, we lost over 50 % of selectivity, but in membrane with same defect ratio, selectivity rises up to 90 % if we use protective layer. This data indicates that selective layer is very helpful in recovering membrane properties subsequently to defects creation. Theoretically, coverage operated by protective layer can be enhanced when resistance of protective layer increases; as discussed before, choosing proper protective layer material is fundamental in order to maximize separation performance, since protective layer has its own permeability, its own selectivity and offers its own resistance to mass transport: this is summarized in Figure 4.3.3.1b-d which shows effect of overall performances based on selective layer properties. In particular, Figure 4.3.3.1b shows that permeability is fundamental feature for a selective layer, but when defect ratio increases, protective layer with lower permeance is preferred. Figure 4.3.3.1c shows that membrane with 5000 barrer protective layer on a selective layer with 0.015% defect ratio maintain a selectivity of 90 %, while 0.15 % defect ratio can be covered by 500 barrer protective layer for the same selectivity. Figure 4.3.3.1d shows effects of protective layer selectivity on membrane overall selectivity and indicates the importance of properly design selective layer.

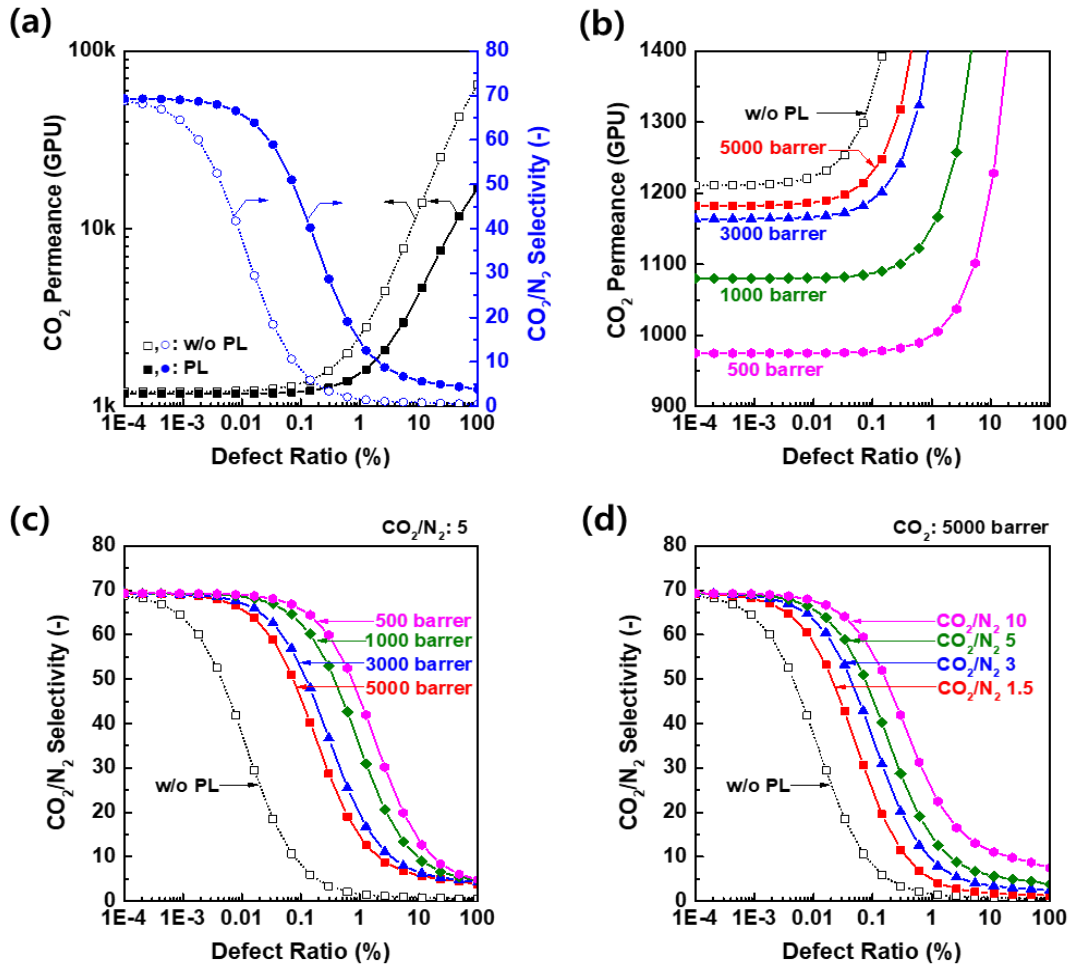

Figure 4.3.3.1 a-d *Theoretical approach on membrane performance determination, basing on protective layer properties: Effect of protective layer in defective TFC membrane (a), CO_2 permeance (b) and CO_2/N_2 selectivity(c) as function of protective layer permeability and CO2/N2 selectivity as function of protective layer selectivity (d) .*

Another important aspect to be considered is protective layer thickness: picture 3.4.3.2 a-d show how it can affect membrane performances as function of defect ratio. CO_2 permeability was fixed at 5000 barrer with CO_2/N_2 selectivity of 5 in Figure 4.3.3.2 a-b, whereas permeability was fixed at 1000 barrer with a selectivity of 5 in picture Figure 4.3.3.2 c-d. Lower Permeability protective layer affects the transport resistance depending on thickness (Figure 4.3.3.2 c-d) . Figure 4.3.3.2 b shows that 5000 barrer protective layer with 0.3 micron thickness can easily cover a membrane with 0.035 % defects, maintaining 90 % selectivity, whereas 1000 barrer protective layer with 0.3 micron thickness can cover 0.22 % defective membrane, with selectivity of 90 %

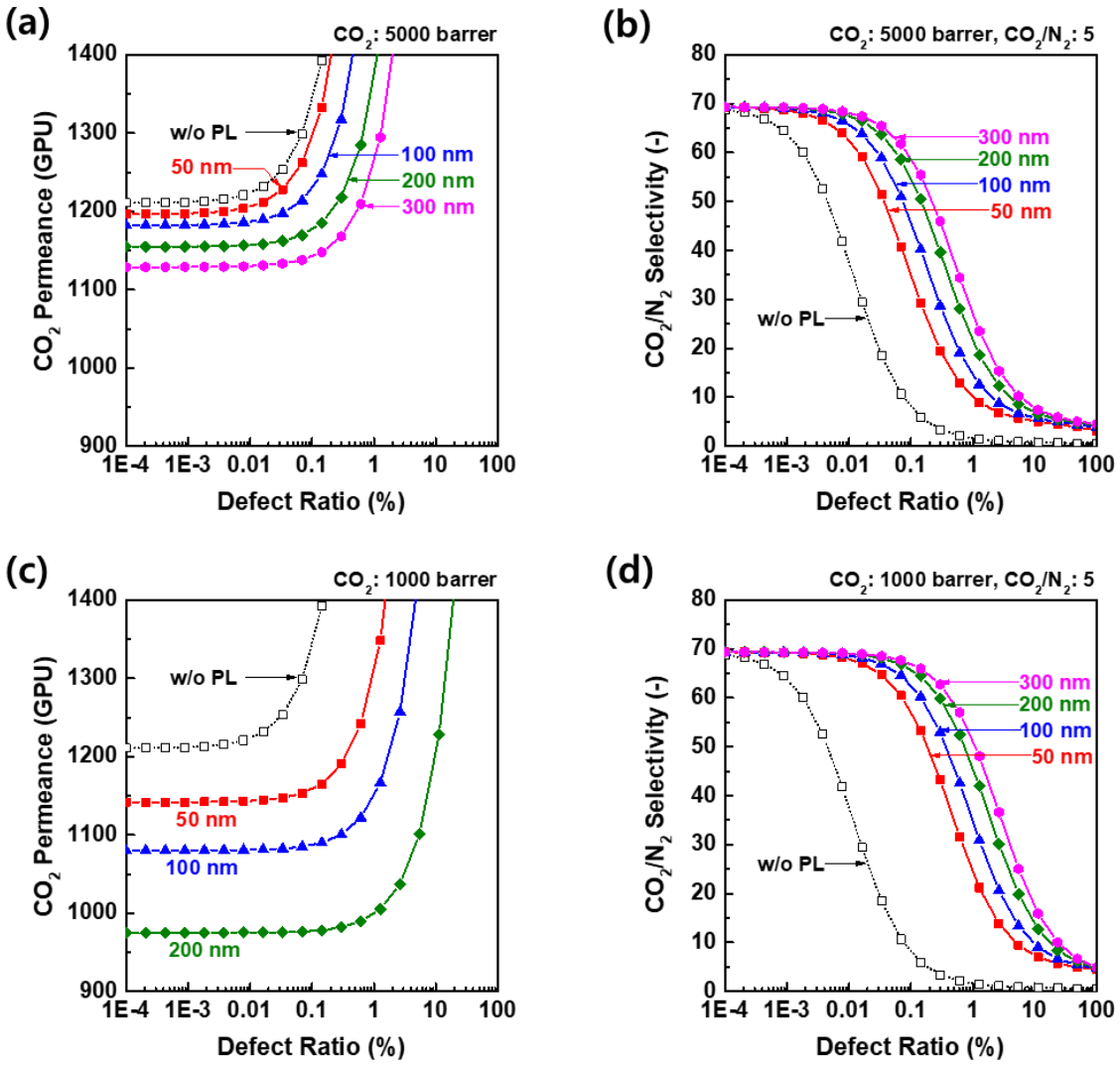

Figure 4.3.3.2 a-d membrane performances depending on protective layer properties. (a,c) CO_2 permeance as function of protective layer thickness : CO_2 5000 barrer (a), CO_2 1000 barrer (c). CO_2/N_2 selectivity as function of layer thickness (b, d). CO_2 5000 barrer and CO_2/N_2 5 (b), CO_2 1000 barrer and CO_2/N_2 5 (d)

It clearly appears how the protective layer is deeply related to membrane performance. Protective layer thickness and properties must thus carefully determined according to defect ratio, in order to maximize its effectiveness and avoid performance loss.

4.3.4 Protective layer coated membranes: preparation and gas transport measurement and bench-scale tests.

Preparation and gas transport test have been performed on produced membranes, in order to check reliability of layer coating effectiveness on defective membranes. In Figure 4.3.4.1a-d SEM images of pristine porous

and coated membranes are reported. When selective layer is applied on porous substrate (a), defect formation may occurs (b) and can easily solved by coating with protective layer (c). Cross section image (d) show that 60 nm protective layer thickness was realized, while selective layer is only 90 nm.

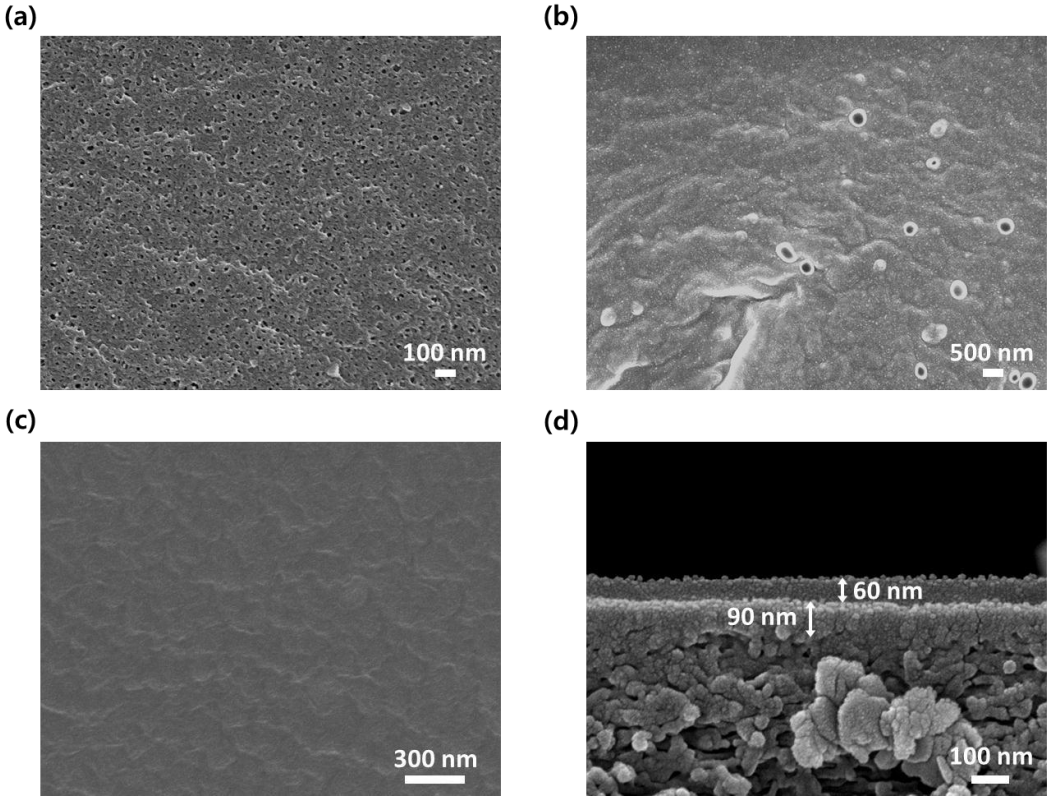

Figure4.3.4.1a-d Representative SEM images of prepared membrane: coating-free pristine support (a), selective layer application and defect formation (b), protective layer coating helps to recover membrane properties (c) and cross section of produced membranes confirms that coating occurs (d)

For our membranes, gas transport properties are summarized in Figure 4.3.4.2a-b. For measurement, feed pressure was fixed to 2 bar and permeate side was exposed to ambient air. Mixed gas conditions were used (14 mol. % of CO_2 and 86 mol. % of N_2), CO2 permeance was about 1200 GPU with a selectivity of 51.5 at stage cut of 0.2%. The stage cut is fundamental in order to define gas transport properties under mixed gas conditions: it is defined as fraction of permeate flow rate compared to the feed flow rate, due to the polarization in concentration; mixed gas transport properties come close to pure gas transport properties as the stage cut decreased to suppress concentration polarization. Figure 4.3.4.2 also show that CO_2 permeance level depends on stage cut ,whereas N_2 remains almost unchanged; this indicates that selectivity, higher at low stage cut, can be ascribed to higher CO_2 permeance. In Figure 4.3.4.2 b a comparison between experimental data and model calculation is reported. Dot lines represent theoretical gas transport properties without coating layer, whereas full lines represents theoretical gas transport properties for those membranes coated by protective layer.

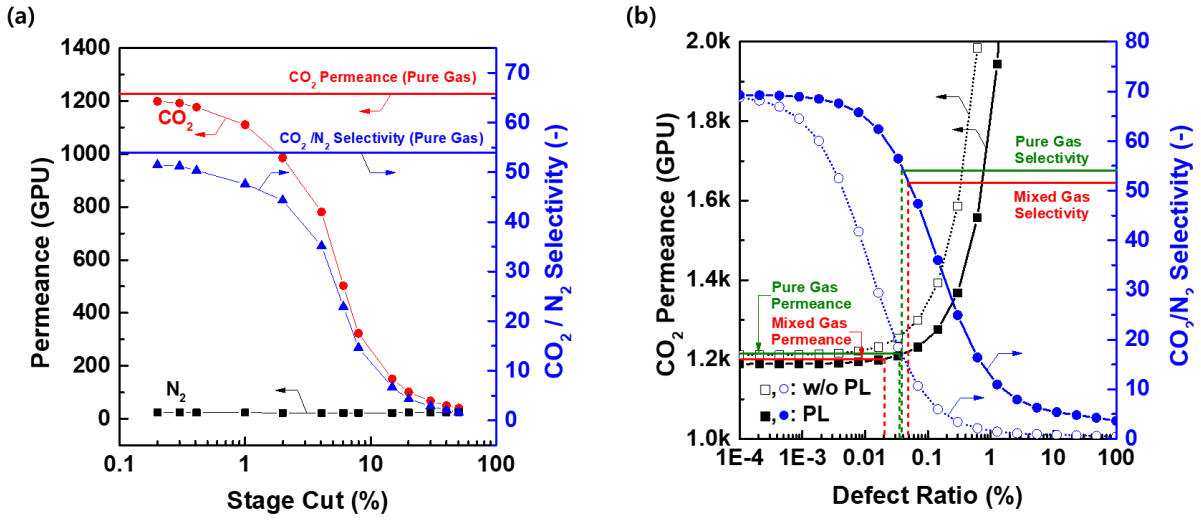

Figure 4.3.4.2 *Coated membranes gas transport properties (a), Defect ratio estimation comparing transport properties with resistance model calculation (b)*

22x34 cm membranes were also prepared using this method and used for plate-and-frame module fabrication, in which the feed gas flows across the membranes within module and permeate gas was designed to be divided into different parts in order to minimize pressure trop across feed and permeate side. Two membranes are placed on each frame (one per side) whose area is around 1080 cm^2, in which 2 cm of glue are applied. Figure 4.3.4.3a-b reports the performance of a single frame membrane module as function of permeate pressure (a) and feed flow rate (b) ; as the permeate pressure drops, CO_2 purity increases because the partial pressure gradient across membrane is increased. In our case, when permeate pressure decreases to 0.03 bar the CO^2 purity rises up to 81% with a 35% increase in CO^2 recovery. We also measured gas purity and recovery as function of feed flow rate, maintaining permeate pressure fixed at 0.2 bar (figure 3.4.4.3 b): purity was 66 % and CO^2 recovery 38 % when feed flow rate was maintained at 0.2 Nm3/h; the CO2 purity was 58% with a CO2 recovery of 60% when the feed flow rate was 0.1 Nm3/h. In bench-scale and lab scale comparision, we observed that permeance for pure CO_2 lab scale was about 1230 GPU, while for single frame module was about 958 GPU. Furthermore, observed selectivity was 53.9 in the case of lab scale experiments and 56.4 for single frame module; these differences can be ascribed to different selective layer thickness, ascribable to coating device efficiency and properties.

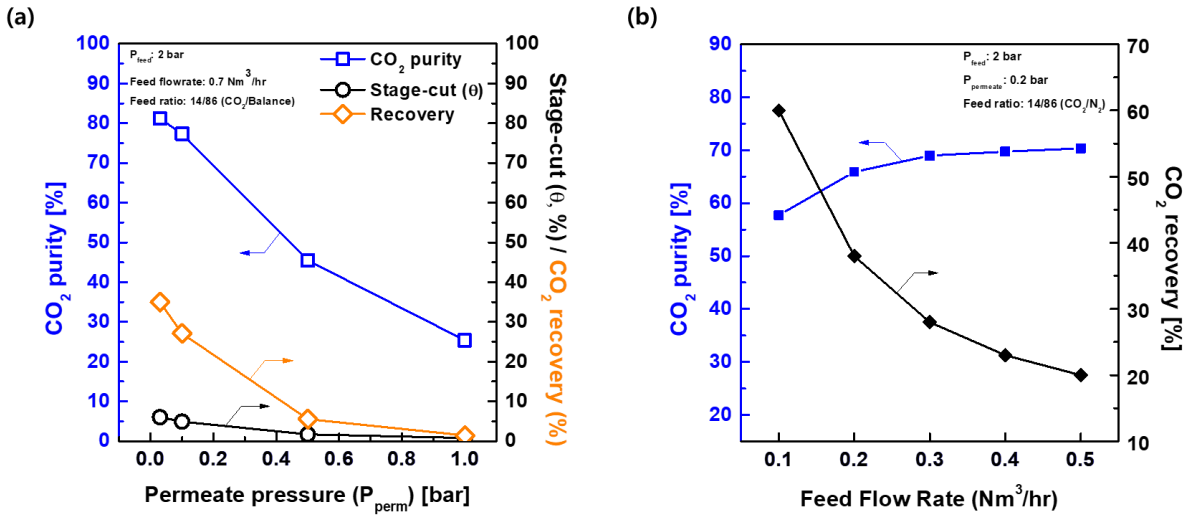

Figure 4.3.4.3 CO_2 purity and recovery as function of permeate pressure (a) and as function of feed flow rate (b)

Starting from single frame module, we were able to fabricate larger size membranes using protective layer coating already discussed in this chapter. The membranes were tested using the following conditions: Feed gas concentration was 14.7 mol % of CO_2 and 18 mol% of O_2 (N_2 balance) and gas feed flow rate was fixed at 30 Nm^3/h. CO_2 purity and recovery increased to 74% and 22% respectively. O_2 concentration was aboutr 7.6%, and our results confirmed that apply protective layer even in large scale membrane module system in order to control defects, is not only possible but represents also a convenient and not expensive way to fabricate high performance membranes for gas separation.

4.4 Experimental part

4.4.1 Materials and chemicals

TeflonTM AF2400 was provided by DuPont and used in order to fabricate protective layer, Galden® HT110 was provided by Solvay Brussel (Belgium) and used as solvent for AF2400. PAN350 membranes were provided by Nanostore (Waltham, MA, USA) and used as substrate membrane. Lab-prepared Graphene oxide (GO) and polymer mixed matrix composite material were used for selective layer preparation. CO_2 permeability of our material is 110 barrer with CO_2/N_2 selectivity of 72.6, considering 1 barrer = 10−10 cm^3(STP) cm/cm^2 s cmHg.

4.4.2 Preparation of TFC membranes and protective layer.

In the case of AF2400 protective layer, an AF2600/ HT110 solution has been prepared using 0.1 wt % of AF2600, stirred at 80 °C for 12 hours. Subsequently solution was casted onto PAN-350 previously coated with selective layer using automatic bar coating machine and dried in vacuum oven in order to remove residual solvent. 7x7 cm membrane sample was prepared for lab scale test and 22x34 cm sample for large scale application test.

4.4.3 Module system and Module fabrication

For large scale tests, plate-and-frame modules were used. Each membrane was 18x30 cm and each frame was designed. For the lab test, module consisted of two membranes whose area was 1080 cm^2 , while for bench scale test 21 membranes for each module were used. In our experiments five membrane modules (56.700 cm^2 area) were connected in parallel.

4.4.3 Gas transport properties measurement.

Lab scale membrane with an effective area of 6.25 cm^2 was tested with an in line high pressure stainless steel membrane holder produced by Merk Millipore (MA, USA) using a mixed gas of 14 mol% CO_2 and 86 mol % N_2 and 2 bar feed pressure. Permeate side was exposed to ambient air and transport properties were measured at 25 °C. For lab scale experiments, membrane holder design expects countercurrent flow between feed and permeate. Gas Transport properties were measured under different stage cuts between 0.2 and 50 % using an Agilent 7890 GC system and two agilent AMD2000 gas flowmeters. Mixed gas permeances were calculated by following equation (1) :

$$Q_A = \left(\frac{273.15}{273.15+T}\right).\left(\frac{1}{p_2 \cdot x_{2a} - p_1 \cdot x_{1A}}\right) \cdot \left(\frac{dV}{dT} \cdot x_{1A}\right) \cdot \frac{P_{atm}}{76} \cdot \frac{1}{A} \cdot 10^6 \qquad (1)$$

where Q_A is the gas permeance of gas A (GPU), T is the temperature (Celsius), p_1 is the permeate pressure (atm), p_2 is the feed pressure (atm), x_{1A} is the mole fraction of gas A in the permeate stream, x_{2A} is the mole fraction of gas A in the feed stream, dV/dT is the volumetric displacement rate in the permeate stream (cm^3/s), *P_{atm} is the atmospheric pressure (atm) and A is the effective membrane area (cm^2). No sweeping gas was used*

in our experiments. Retentate flow was controlled by needle valvle and measured using Agilent ADM2000 gas flowmeter. The permeate stream composition was analyzed by an Agilent 7980 GC system, while Agilent ADM 2000 universal gas flowmeter was used to measure permeate gas stream. Single-frame membrane module was also tested using feed flow rates between 0.1 and 0.5 Nm^3/h, 2 bar feed pressure and 0.2 bar permeate pressure. On this purpose, permeate side was connected to Ulvac DTC-41 vacuum pump and its pressure controlled by DK-Lok needle valve, placed between membrane permeate side and pump. Membrane module was also tested using different permeate pressure, from 0.03 and 1 bar with fixed feed flow rate of 0.7 Nm^3/h and 2 bar pressure. Same composition (14 mol. % CO_2 and 86 mol. % N_2) was used for single membrane module tests, while for bench-scale tests real combustion gas composition of 14.7 mol. % CO_2, 18 mol. % O_2 and balanced N_2 under a feed flow rate of 30 Nm3/hr with a feed pressure of 2 bar (abs.) and a permeate pressure of up to 0.01 bar has been used.

4.5 Chapter conclusions

Defect control is an essential issue concerning all the membranes to be used in gas separation. In this chapter, we introduced a novel, practical and simple approach which allow us to control defect by application of protective layer without great loss of membrane performance. Our method is also supported by mathematical approach which can also be applied to all kind of membranes. Moreover, we demonstrated the possibility to extend our approach to large scale membrane production as well. Membrane efficiency can greatly improved by defect controlling using ultrathin thickness. Membrane with thin selective layer (below 100 nm) can be prepared in large scale without significant decrease of performance, using a protective layer.Our method can easily find application not only for CO_2 capture systems but also for every other type of membrane in which defects represent a crucial aspect.

Chapter 4 references

1. Bhown, A. S.; Freeman, B. C., Analysis and status of post-combustion carbon dioxide capture technologies. *Environ Sci Technol* **2011,** *45* (20), 8624-32.
2. Plaza, M. G.; Pevida, C.; Arenillas, A.; Rubiera, F.; Pis, J. J., CO2 capture by adsorption with nitrogen enriched carbons. *Fuel* **2007,** *86* (14), 2204-2212.
3. Chaffee, A. L.; Knowles, G. P.; Liang, Z.; Zhang, J.; Xiao, P.; Webley, P. A., CO2 capture by adsorption: Materials and process development. *International Journal of Greenhouse Gas Control* **2007,** *1* (1), 11-18.
4. Wang, M.; Lawal, A.; Stephenson, P.; Sidders, J.; Ramshaw, C., Post-combustion CO2 capture with chemical absorption: A state-of-the-art review. *Chemical Engineering Research and Design* **2011,** *89* (9), 1609-1624.
5. Yu, C.-H.; Huang, C.-H.; Tan, C.-S., A Review of CO2 Capture by Absorption and Adsorption. *Aerosol and Air Quality Research* **2012,** *12* (5), 745-769.
6. Hossain, M. M.; de Lasa, H. I., Chemical-looping combustion (CLC) for inherent for CO_2 separations—a review. *Chem Eng Sci* **2008,** *63* (18), 4433-4451.
7. Anders Lyngfelt, B. L., Tobias Mattisson, A fluidized-bed combustion process with inherent CO_2 separation; application of chemical-looping combustion. *Chem Eng Sci* **2001,** *56*, 3101-3113.
8. Tobias Mattisson, A. L., Paul Cho, The use of Iron oxide as an oxygen carrier in chemical-looping combustion of methane with inherent separation of CO_2. *Fuel* **2001,** *80*, 1953-1962.
9. Fu, Q.; Halim, A.; Kim, J.; Scofield, J. M. P.; Gurr, P. A.; Kentish, S. E.; Qiao, G. G., Highly permeable membrane materials for CO2 capture. *Journal of Materials Chemistry A* **2013,** *1* (44), 13769.
10. Budd, P. M.; McKeown, N. B., Highly permeable polymers for gas separation membranes. *Polymer Chemistry* **2010,** *1* (1), 63.
11. Brunetti, A.; Scura, F.; Barbieri, G.; Drioli, E., Membrane technologies for CO2 separation. *Journal of Membrane Science* **2010,** *359* (1-2), 115-125.
12. Linga, P.; Kumar, R.; Englezos, P., The clathrate hydrate process for post and pre-combustion capture of carbon dioxide. *J Hazard Mater* **2007,** *149* (3), 625-9.
13. Duc, N. H.; Chauvy, F.; Herri, J.-M., CO2 capture by hydrate crystallization – A potential solution for gas emission of steelmaking industry. *Energ Convers Manage* **2007,** *48* (4), 1313-1322.
14. Ricaurte, M.; Dicharry, C.; Renaud, X.; Torré, J.-P., Combination of surfactants and organic compounds for boosting CO2 separation from natural gas by clathrate hydrate formation. *Fuel* **2014,** *122*, 206-217.
15. Tuinier, M. J.; van Sint Annaland, M.; Kramer, G. J.; Kuipers, J. A. M., CryogenicCO_2 capture using dynamically operated packed beds. *Chem Eng Sci* **2010,** *65* (1), 114-119.
16. Xu, G.; Liang, F.; Yang, Y.; Hu, Y.; Zhang, K.; Liu, W., An Improved CO2 Separation and Purification System Based on Cryogenic Separation and Distillation Theory. *Energies* **2014,** *7* (5), 3484-3502.
17. Russell L. McGalliard, W. L., Hazel Crest METHOD FOR CRYOGENIC SEPARATION OF CARBON OOXDE FROM HYDROCARBONS. 1980.
18. Zhu, X.; Hua, Y.; Tian, C.; Abney, C. W.; Zhang, P.; Jin, T.; Liu, G.; Browning, K. L.; Sacci, R. L.; Veith, G. M.; Zhou, H. C.; Jin, W.; Dai, S., Accelerating Membrane-based CO2 Separation by Soluble Nanoporous Polymer Networks Produced by Mechanochemical Oxidative Coupling. *Angew Chem Int Ed Engl* **2018,** *57* (11), 2816-2821.
19. Sanders, D. F.; Smith, Z. P.; Guo, R.; Robeson, L. M.; McGrath, J. E.; Paul, D. R.; Freeman, B. D., Energy-efficient polymeric gas separation membranes for a sustainable future: A review. *Polymer* **2013,** *54* (18), 4729-4761.
20. Moghadam, F.; Kamio, E.; Matsuyama, H., High CO 2 separation performance of amino acid ionic liquid-based double network ion gel membranes in low CO 2 concentration gas mixtures under humid conditions. *Journal of Membrane Science* **2017,** *525*, 290-297.
21. Car, A.; Stropnik, C.; Yave, W.; Peinemann, K.-V., Pebax®/polyethylene glycol blend thin film composite membranes for CO2 separation: Performance with mixed gases. *Separation and Purification Technology* **2008,** *62* (1), 110-117.

22. Vinoba, M.; Bhagiyalakshmi, M.; Alqaheem, Y.; Alomair, A. A.; Pérez, A.; Rana, M. S., Recent progress of fillers in mixed matrix membranes for CO 2 separation: A review. *Separation and Purification Technology* **2017,** *188*, 431-450.
23. Tomé, L. C.; Gouveia, A. S. L.; Ab Ranii, M. A.; Lickiss, P. D.; Welton, T.; Marrucho, I. M., Study on Gas Permeation and CO2 Separation through Ionic Liquid-Based Membranes with Siloxane-Functionalized Cations. *Industrial & Engineering Chemistry Research* **2017,** *56* (8), 2229-2239.
24. Hägg, M. B.; Lindbråthen, A.; He, X.; Nodeland, S. G.; Cantero, T., Pilot Demonstration-reporting on CO2 Capture from a Cement Plant Using Hollow Fiber Process. *Energy Procedia* **2017,** *114*, 6150-6165.
25. Merkel, T. C.; Wei, X.; He, Z.; White, L. S.; Wijmans, J. G.; Baker, R. W., Selective Exhaust Gas Recycle with Membranes for CO2 Capture from Natural Gas Combined Cycle Power Plants. *Industrial & Engineering Chemistry Research* **2012,** *52* (3), 1150-1159.
26. Roussanaly, S.; Anantharaman, R.; Lindqvist, K.; Zhai, H.; Rubin, E., Membrane properties required for post-combustion CO 2 capture at coal-fired power plants. *Journal of Membrane Science* **2016,** *511*, 250-264.
27. Merkel, T. C.; Lin, H.; Wei, X.; Baker, R., Power plant post-combustion carbon dioxide capture: An opportunity for membranes. *Journal of Membrane Science* **2010,** *359* (1-2), 126-139.
28. Wang, Y.; Zhao, L.; Otto, A.; Robinius, M.; Stolten, D., A Review of Post-combustion CO2 Capture Technologies from Coal-fired Power Plants. *Energy Procedia* **2017,** *114*, 650-665.
29. Kattula, M.; Ponnuru, K.; Zhu, L.; Jia, W.; Lin, H.; Furlani, E. P., Designing ultrathin film composite membranes: the impact of a gutter layer. *Sci Rep* **2015,** *5*, 15016.
30. Fu, Q.; Wong, E. H. H.; Kim, J.; Scofield, J. M. P.; Gurr, P. A.; Kentish, S. E.; Qiao, G. G., The effect of soft nanoparticles morphologies on thin film composite membrane performance. *J. Mater. Chem. A* **2014,** *2* (42), 17751-17756.
31. Li, P.; Chen, H. Z.; Chung, T.-S., The effects of substrate characteristics and pre-wetting agents on PAN–PDMS composite hollow fiber membranes for CO2/N2 and O2/N2 separation. *Journal of Membrane Science* **2013,** *434*, 18-25.
32. Li, P.; Wang, Z.; Li, W.; Liu, Y.; Wang, J.; Wang, S., High-performance multilayer composite membranes with mussel-inspired polydopamine as a versatile molecular bridge for CO2 separation. *ACS Appl Mater Interfaces* **2015,** *7* (28), 15481-93.
33. Halim, A.; Fu, Q.; Yong, Q.; Gurr, P. A.; Kentish, S. E.; Qiao, G. G., Soft polymeric nanoparticle additives for next generation gas separation membranes. *Journal of Materials Chemistry A* **2014,** *2* (14), 4999.
34. Liang, C. Z.; Chung, T. S., Ultrahigh Flux Composite Hollow Fiber Membrane via Highly Crosslinked PDMS for Recovery of Hydrocarbons: Propane and Propene. *Macromol Rapid Commun* **2018,** *39* (5).
35. TRIPODI, J. M. S. H. a. M. K., COMPOSITE HOLLOW FIBER MEMBRANES FOR GAS SEPARATION: THE RESISTANCE MODEL APPROACH. *Journal of Membrane Science* **1981,** *8*, 233-246.
36. K. Kimmerle, T. H. a. H. S., Analysis of gas permeation through composite membranes. *Journal of Membrane Science* **1991,** *61*, 1-17.
37. S.K. Karode, S. S. K., Analysis of transport through thin film composite membranes using an improved Wheatstone bridge resistance model. *Journal of Membrane Science* **1997,** *127*, 131-140.
38. I. PINNAU, J. G. W., I. BLUME, T. KURODA and K.-V. PEINEMANN, GAS PERMEATION THROUGH COMPOSITE MEMBRANES. *Journal of Membrane Science* **1988,** *37*, 81-88.
39. S.K. Karode, V. S. P., S.S. Kulkarni, An improved model incorporating constriction resistance in transport through thin film composite membranes. *Journal of Membrane Science* **1996,** *114*, 157-170.
40. Gaohong He, X. H., Renxian Xu, Baolin Zhu, An improved resistance model for gas permeation in composite membranes. *Journal of Membrane Science* **1996,** *118*, 1-7.
41. Ashworth, A. J., Relation between gas permselectivity and permeability in a bilayer composite membrane. *Journal of Membrane Science* **1992,** *71*, 169-173.

General Conclusions and future perspectives

In the last decade, enhancement in life standards, growth of population especially in highly industrialized areas, lowering resources amount new needs and demands require to be fulfilled, mostly about those aspects concerning mankind fundamental needs such as water purification, environmental caring or food industry. Membrane technology represents one of election ways to carry those expectations out because of its outstanding features, raised up since their first introduction into the world market in the last century, in which synthetic polymers demonstrated their capability and great potential. In this stack, material tailoring probably represents one of most appealing and fascinating issue owing great potential in terms of material design. The creation of materials which perfectly fit to specific needs can be done in several ways; one of most promising is represented by the use of coating, main theme in this thesis work : the coating offers several customization chances overcoming one big problem which often occurs, represented by the loss of original properties. In chapters 2,3,4 three different application on that purpose are reported:

- ***Chapter 2***

  In chapter 2 the creation of PVDF-graphene Thin Film Composite membrane has been realized by coating hydrophobic polymer with graphene layer. In order to enhance adhesion between polymer and graphene, first step was to functionalize the polymer by chemical treatment, using a synthetic approach consisting into two phases: Basic treatment which introduces polymerizable double bonds onto polymer chain, followed by radical co-polymerization with suitable monomer containing aromatic ring and polymerizable bond either, in order to ease the adhesion between the polymer and graphene layer. On functionalized polymer, powder and membranes either, spectroscopic and morphological analysis were performed in order to investigate composition and properties, before association with graphene. All the analysis confirmed that:

  - Co-polymerization occurs and polymer was functionalized

  - The average pore size is in the range of microfiltration

  Graphene was synthetized using Chemical Vapor Deposition (CVD) method, a technique in which a metal (usually Cu or Ni) in the presence of hydrocarbon like methane or ethylene, at high temperatures (above 1000 °C) catalyzes the break of C-H bonds and formation of C-C bonds. In order to estimate graphene defects and eventually check multilayer areas, samples have been analyzed using optical microscope before the PVDF-f-GM creation. Composite membrane fabrication was

achieved by coating with freshly synthetized graphene layer using laminating machine, followed by catalyst removal process using suitable iron salts solutions. All membranes were prepared without using additives or pore forming agents such as PEG, PVP, LiCl and tested. Results showed that if no pore forming agents are used, membranes prepared using pristine PVDF possess low pore size and therefore can't work properly in DCMD operation in which MF-range pore size is required. On the other hand, functionalization leads to formation of membranes with correct pore size which fit well for MD processes. Three different membranes were tested: pristine PVDF, PVDF-f which has good water flux and high salt rejection (up to 99.9) and PVDF-f-GM in which the presence of graphene causes decrement in water flux but better rejection and better durability.

- ***Chapter 3***

  In Chapter 3 is reported an efficient and practical approach for the synthesis of a particular polymerizable surfactant class with high antimicrobial and antifouling activity: AATEABs, a class of molecule formed by three main parts: polymerizable part, alkyl chain called "linker" (with variable length) and final ammonium salt part which confers the antibacterial activity as know in literature. Our synthetic approach expects 2 step process: esterification reaction between bromo-alcohol and acryloyl chloride, followed by quaternization reaction with triethylamine which leads to formation of AATEABs with chain length of C_6, C_9, C_{11} and C_{12}. Since the biological activity can change depending on alkyl chain length, the synthetic approach was extended to other AATEABs bearing C_2 and C_3 alkyl chain length, using a reaction scheme which was partially revised, consisting in three steps: reaction of bromoalkanols with Et_2NH, followed by esterification with acryloyl chloride and finally quaternization with EtBr. In a second moment, we focused our attention on process optimization, which allows to fabricate AATEABs avoiding the use of prohibitive conditions, working under air and starting from cheap and easily available chemicals. Furthermore, AATEABs were obtained with high degree of purity and yield. AATEABs biological activity was tested against Gram+/- and yeast-strains and resulted to be particularly high for AATEABs bearing C11 (AUTEAB) and C12 (ADTEAB) chain length. AATEABs resulted therefore to be promising candidates as polymerizable coating materials for commercial membranes, which can be used whenever antifouling properties are needed. The proposed synthetic approach is simple and efficient and can easily be applied to large scale operations as well.

Chapter 4

In chapter 4, our attention was focused on the creation and of TFC membranes and the possibility to

control their defects by coating, to be used for CO_2/N_2 separation. It is well known that one common problem to commercialize functional and efficient CO_2/N_2 separation membrane, is related to presence of defect which can increase as long as coating thickness decreases. However thin selective layer is fundamental in order to get best separation performance since thin selective layer means higher CO_2 permeance. In this work we analyzed the relation between number of defects and transportation properties and introduce a novel method which permits preparation of TFC membrane for gas separation with low amount of defects, very important in order to achieve optimal gas separation. This can be reached by protective layer whose thickness plays a primary role in process effectiveness and that can be demonstrated by mathematical approach. It is confirmed that thinner selective layer greatly enhances separation performances for every kind of membrane.The method discussed in chapter 4, was applied to creation of membrane modules tested in a pilot test facility and resulted to be really effective in the case of extremely thin coating, even under 100 nm.

Indeed, due membrane excellent and outstanding properties and new outcoming materials, membrane technology-based operations, from their inception to last years. are becoming one of most dominant technologies used either for single operation like fruit juice or water treatment, up to the advanced ones like gasses storage and their separation for space technology. Yet, one of most advanced although partially unexplored use of membranes is represented by their association to nanomaterials (NMs). In fact, though novel NMs are everyday freshly created, a lot of knowledges and investigations are still needed in order to achieve the best interaction between plastics and nanomaterials, one problems which sometimes represent a limitation on their application. Therefore, the potential of NMs nowadays probably represents one of most appealing topic of study and research which needs to be developed more.